MACHINE LEARNING-BASED ClASSIFICATION AND REDUCTION OF MOTION ARTIFACT NOISE IN ECG SIGNALS FOR WEARABLE VITAL SIGN MONITORING DEVICES

by

Ali Asgharzad Hamidi

Submitted in partial fulfilment of the requirements
for the degree of Doctor of Philosophy

at

Dalhousie University
Halifax, Nova Scotia
May 2024

TABLE OF CONTENTS

LIST OF TABLES

LIST OF FIGURES

ABSTRACT

Wearable vital signs monitoring devices, while widely adopted, face challenges in clinical diagnosis due to artifact noises. This thesis introduces a novel application of machine learning—specifically, the K-Nearest Neighbor (KNN) model—to recognize artifacts in ECG signals using 3-axis accelerometer data.

The proposed fine KNN model, leveraging wavelet scattering coefficients, effectively classifies accelerometer samples likely to contain artifact noises in ECG signals, achieving a remarkable positive predictive value of 94.7%. To enhance accuracy and reliability, a robust technique is proposed, recognizing artifacts using wavelet scattering coefficients from both accelerometer and ECG signals. The KNN model achieves a test accuracy of 98.8%, making it suitable for integration into wearable ECG monitoring devices.

Following artifact noise identification, a two-stage technique reduces noise levels and reconstructs the signal. Wavelet denoising preserves crucial signal information, and a denoising autoencoder enhances Signal-to-Noise Ratio (SNR) and reduces Root Mean Square Error (RMSE).

Importantly, the proposed models can be implemented in wearable ECG monitoring devices without additional sensors. This opens possibilities for applications in various vital signs monitoring scenarios, such as photoplethysmography (PPG), electroencephalography (EEG), or other monitoring devices. The research significantly contributes to advancing noise reduction techniques in wearable health monitoring, ensuring accurate vital sign measurements for improved clinical applications.

LIST OF ABBREVIATIONS USED

AE	Autoencoder
AI	Artificial Intelligence
AUC	Area Under the Curve
AV	Atrioventricular
BIOR	Biorthogonal
BW	Bandwidth
CPR	Cardiopulmonary resuscitation
DAE	Denoising Autoencoder
DB	Daubechies
ECG	Electrocardiogram
EEG	Electroencephalogram
EMD	Empirical Mode Decomposition
EMG	Electromyography
FDR	False Discovery Rate
FNR	False Negative Rate
FIR	Finite Impulse Response
FCN	Fully Convolutional Neural Network
HAR	Human Activity Recognition
ICA	Independent Component Analysis
IQR	Interquartile Range
KNN	K-Nearest Neighbors
ML	Machine Learning
MATLAB	Matrix Laboratory
MA	Motion Artifact
PPG	Photoplethysmography
PPV	Positive Predictive Value
PSD	Power Spectral Density
PCA	Principal Component Analysis

ROC	Receiver Operating Characteristic
RMS	Root Mean Square
RMSE	Root Mean Square Error
SNR	Signal-to-Noise Ratio
SVD	Singular Value Decomposition
SA	Sinoatrial
STD	Standard Deviation
SGD	Stochastic Gradient Descent
SYM	Symlet
TPR	True Positive Rate

ACKNOWLEDGEMENTS

CHAPTER 1 INTRODUCTION

An Electrocardiogram (ECG) serves as a crucial record, depicting the electrical potentials generated by the heart during its depolarization and repolarization phases, primarily driven by the movement of Na+ and K+ ions in the blood. Typically, the ECG signal exhibits amplitudes in the range of 2 mV and necessitates a recording bandwidth spanning from 0.1 to 120 Hz [2]. Utilizing a non-invasive technique, electrodes are strategically placed on the patient's skin to acquire the ECG, offering valuable insights into the cardiac health of the individual [1] .

The ECG signal, along with heart rate monitoring, plays a pivotal role in assessing cardiac well-being. Variations in heart rate, rhythm, or alterations in the morphological pattern of the ECG signal can be indicative of cardiac arrhythmias. The detection and diagnosis of such conditions hinge upon the careful analysis of recorded ECG waveforms. Critical information about the nature of heart-related diseases can be gleaned from the amplitude and duration of the P-QRS-T-U waves.

However, the clinical acquisition of ECG signals is not without challenges, as various types of artifacts can infiltrate the recording process. Among these, power line interference, external electromagnetic field interference, noise stemming from random body movements and respirational activities, electrode contact noise, electromyography (EMG) noise, and instrumentation noise are of primary concern. These artifacts pose a threat to signal quality, compromise frequency resolution, and significantly impact the morphology of ECG signals, thereby distorting crucial information.

To ensure the accuracy and reliability of diagnostic information, it becomes imperative to address and minimize these disturbances in the ECG signal. Strategies for noise reduction and signal enhancement are essential for preserving the integrity of the recorded data, facilitating more accurate diagnoses, and ultimately improving patient outcomes. As advancements in signal processing techniques continue, the field of ECG analysis is poised to benefit from enhanced methodologies that mitigate the impact of artifacts, providing healthcare professionals with clearer insights into cardiac health.

ECG Morphology

The ECG waveform of a healthy individual exhibits distinct components, each representing specific electrical events in the cardiac cycle. In Fig. 1.1, common labels are employed, aligning with established medical ECG terminology to describe these components. Here is the details of each component:

P Wave:

The P wave in the ECG corresponds to the electrical impulse's conduction from the sinoatrial (SA) node towards the atrioventricular (AV) node. As this electrical activity propagates from the right to the left atrium, the atria undergo depolarization, signifying their contraction. The result is the characteristic P wave in the ECG [2] .
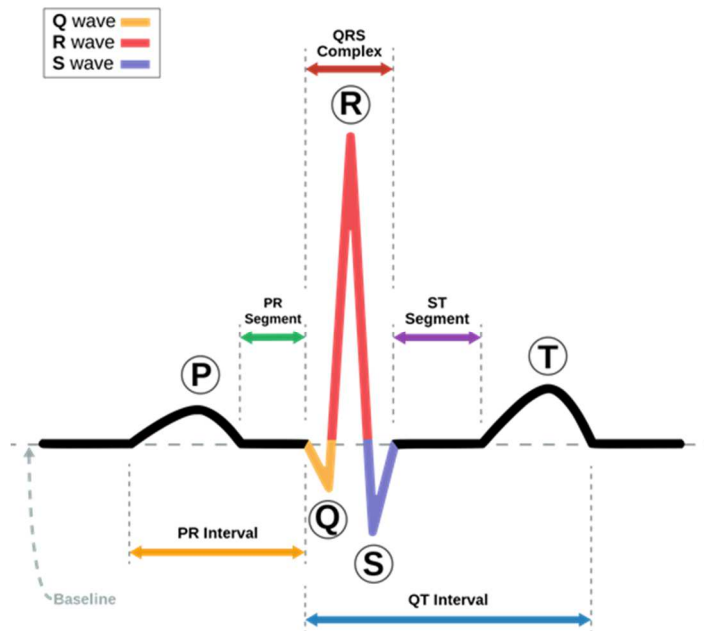
Figure 2-1. Normal ECG QRS Complex (Wikipedia).

QRS Complex:

The QRS complex is a prominent feature in the ECG waveform, consisting of three sequential waves denoted as Q, R, and S. This complex is a direct outcome of the rapid depolarization of both ventricles. Notably, the ventricular muscles possess a larger mass compared to the atrial muscles, leading to a substantially larger amplitude in the QRS complex compared to the P wave.

ST Segment and T Wave:

Beyond the P wave and QRS complex, the ECG waveform further encompasses the ST segment and T wave. The ST segment represents the interval between ventricular depolarization and repolarization. The T wave, on the other hand, signifies the repolarization of the ventricles. Together, these components provide crucial insights into the electrical activity of the heart, aiding in the diagnosis of various cardiac conditions.

U Wave:

In some cases, an additional component known as the U wave may be observed, although it is less conspicuous. The U wave is believed to represent the delayed repolarization of the Purkinje fibers in the heart, contributing additional information to the comprehensive assessment of cardiac function.

The systematic understanding of these ECG components is essential for medical professionals in diagnosing cardiac abnormalities. By recognizing the distinctive patterns associated with each wave and segment, clinicians can gain valuable insights into the health and functioning of the heart, facilitating timely interventions and patient care.

Artifacts in ECG

Removing motion artifacts from ECG signals poses a significant challenge due to several inherent complexities. These artifacts, characterized by a broad frequency spectrum, often overlap with the frequency components of the ECG signal itself. Consequently, devising effective filtering methods becomes challenging, as any attempt to eliminate motion artifacts risks inadvertently removing vital ECG signal information.

A notable difficulty arises from the transient nature of motion artifacts—they manifest for brief durations, making their identification and isolation a formidable task. The transient nature implies that conventional filtering techniques may struggle to distinguish between the motion artifacts and the ECG signal, leading to potential loss of relevant data.

Complicating matters further is the diverse range of movements that can induce motion artifacts. Since different types of motion generate distinct artifacts, devising a universal noise removal method applicable to all scenarios becomes a formidable task. The challenge lies in accommodating the variability in motion-induced artifacts without compromising the fidelity of the ECG signal.

While it might be tempting to employ signal-wide filtering to address motion artifacts, such an approach carries the risk of losing crucial information embedded in the signal. Filtering the entire signal may inadvertently discard elements vital for medical diagnostic purposes, especially when dealing with artifacts that resemble large-amplitude waveforms, occasionally mistaken for QRS complexes.

Attempting to filter the entire signal encounters limitations related to the wide-ranging frequency of motion artifacts. Existing denoising methods, which typically focus on specific frequency ranges, may fall short in addressing the diverse frequency characteristics of motion artifacts. Their adaptability to various frequency noises might not be sufficient, particularly when faced with the complex and variable nature of motion-induced disturbances [3].

Motion artifacts in electrocardiogram (ECG) signals share characteristics with baseline wander, but pose a more challenging issue due to considerable spectral overlap with the PQRST complex.

The prevalence of motion-related disturbances in ECG recordings is notable in the 0.1 to 10 Hz frequency range, encompassing various activities such as breathing, minor body movements, and muscle contractions [[5],[6]]. These disturbances introduce challenges in accurate signal analysis and interpretation, particularly in clinical settings where patients may exhibit involuntary movements affecting the ECG signal.

While the majority of motion artifacts are concentrated in the 1 to 10 Hz range, it is worth noting that instances of artifact noise above 10 Hz can occur in specific scenarios. For

example, during intense or rapid movements, the frequency of motion artifact noise may extend beyond 10 Hz. However, in general, this higher frequency range is considered less significant compared to the lower frequencies [[5],[6]].

The severity of artifact noises can vary, and for certain situations, frequencies up to 100 Hz may be encountered, contingent on the nature and intensity of the movement [[5],[6]]. Understanding the frequency characteristics of motion artifacts is crucial for the development of effective signal processing techniques aimed at mitigating their impact on ECG signals.

It is important to note that the 1-10 Hz range predominantly occurs in clinical scenarios where patients exhibit minimal or no rapid body movements [[5],[6]]. Recognizing these frequency patterns assists in tailoring signal processing methods to address specific challenges associated with motion artifacts in different clinical contexts, ultimately contributing to the improvement of ECG signal quality and diagnostic accuracy.

1.1   MOTIVATIONS AND OBJECTIVES

Cardiovascular diseases stand as a leading cause of global mortality, impacting approximately 550 million individuals worldwide[7]. This alarming statistic underscores the critical need for effective diagnostic tools, and vital sign monitoring devices play a pivotal role in the identification and management of heart-related conditions. Among these vital signs, Electrocardiography (ECG) signals reign supreme as the most widely employed diagnostic tool in cardiology [8]. ECG signals are instrumental in both diagnosing and monitoring patients with cardiac disorders, providing crucial insights into the electrical activity of the heart.

However, the utility of ECG monitoring devices faces a significant challenge—artifact noise. Artifact noise in ECG signals is often a result of various factors such as parkinsonian muscle tremors, dry electrode gel, loose leads, wandering baselines, arterial pulse tapping, CPR compression, muscle tremors, and neuromodulation [9]. These artifacts, distinct from

cardiac electrical activity, can introduce distortions that compromise the accuracy of medical diagnoses. Notably, wearable ECG monitoring devices, while revolutionizing healthcare, are particularly susceptible to artifact noise, making it imperative to capture ECG signals in stable clinical environments.

The impact of artifact noise on wearable devices is further exacerbated by the unavoidable nature of these disturbances. Movement of electrodes on the skin, stemming from body activity or patient movement, results in impedance variations and motion artifacts. This poses a significant challenge for wearable devices used in high-activity scenarios, as artifact noise may lead to the loss of critical information and signal degradation.

Efforts to address noisy ECG signals have evolved over time, with various methodologies employed for detection and denoising. Statistical analysis, time-domain and frequency-domain filters, wavelet thresholding, Empirical Mode Decomposition (EMD), Independent Component Analysis (ICA), and diverse denoising approaches have been explored [[29], [32], [74] , [81]]. While these methods are effective against general noise, the persistent challenge lies in addressing artifact noise specifically, which remains a primary obstacle in leveraging wearable ECG devices for medical diagnosis.

In response to this challenge, innovative approaches are being explored. Recognizing that artifact noise often coincides with heightened body activity, leveraging 3-axis accelerometers alongside ECG signals presents a promising avenue. Human Activity Recognition (HAR) systems, a subset of machine learning applications, have demonstrated efficacy in identifying high body activity situations using accelerometer signals [[29], [32]]. This integration allows for a comprehensive understanding of artifact noise, enabling more accurate medical diagnoses. The widespread availability of accelerometers in both vital sign monitoring devices and smartphones further enhances the feasibility and accessibility of this approach.

Addressing artifact noise in wearable ECG monitoring devices is a crucial step toward enhancing the reliability and accuracy of medical diagnoses. The integration of machine learning applications, particularly HAR systems, and the strategic use of accelerometers offer a promising solution to identify and mitigate artifact noise, paving the way for improved signal quality and diagnostic outcomes in the realm of cardiovascular health.

The primary goal of this research is to identify samples containing artifact noises through the application of a novel methodology. To achieve this, a K-nearest neighbors (KNN) classification method is employed, leveraging extracted features from both ECG and 3-axis accelerometer signals.

To address the denoising aspect, a robust algorithm is proposed, incorporating a Bior wavelet filter and a denoising autoencoder model. This combined approach proves effective in mitigating the impact of artifact noise on ECG signals, resulting in a cleaner representation of the initially noisy training dataset. The denoising process is crucial for obtaining accurate and reliable information from ECG signals, especially in clinical applications where signal fidelity is paramount.

The denoising algorithm is designed to adapt to the intricacies of real-world scenarios, where artifacts can significantly affect signal quality. The utilization of a Bior wavelet filter ensures that relevant frequency components are retained, while the denoising autoencoder model further refines the denoising process by learning intricate patterns from the contaminated signals.

Furthermore, the denoising algorithm operates in tandem with the sampling frequency, ensuring that the denoised signals align seamlessly with the original data. This synchronization is vital for preserving the temporal relationships within the signals and maintaining the integrity of the clinical information they convey.

In conjunction with denoising, features essential for subsequent classification tasks are extracted using wavelet scattering transform. This multi-scale feature extraction method enhances the discriminative power of the features, enabling the classification model to better capture and differentiate between subtle variations in the signals.

In summary, this research encompasses a comprehensive approach that not only identifies artifact noises in ECG and accelerometer signals but also addresses the denoising challenge through a sophisticated algorithm. The proposed methodology aims to elevate the performance of clinical practices by ensuring accurate signal representation, paving the way for improved diagnostic capabilities and further advancements in healthcare signal processing.

1.1.1 Previous Works

The removal of motion artifacts from ECG signals poses substantial challenges, several factors contribute to the complexity of this task:

- Broad Frequency Spectrum: Motion artifacts span a wide frequency range, overlapping with the frequency spectrum of ECG signals. This spectral overlap complicates the filtering process, as it becomes challenging to remove motion artifacts without unintentionally attenuating the ECG signal itself.
- Transient Nature: Motion artifacts are often short-lived, occurring for brief periods. Identifying and eliminating these artifacts without causing a loss of ECG signal content is intricate due to their transient nature.
- Diverse Causes: Motion artifacts can result from various types of movements, further complicating the development of a universal noise removal method that effectively addresses all motion artifact scenarios.
- Signal Integrity Concerns: Applying filters to entire ECG signals may lead to the loss of crucial diagnostic information. Preserving signal integrity is crucial for accurate medical interpretations.
- Waveform Similarity: Motion artifacts manifest as high-amplitude waveforms, occasionally resembling QRS complexes. This similarity can lead to misinterpretation, making it inadvisable to utilize such samples for medical diagnostic purposes.

To address these challenges, the following methods have been employed for eliminating noise in ECG signals:

Filtering

The application of band-pass filters to eliminate motion artifact-related frequency components. However, using a wide-range band-pass filter may result in the loss of vital signal information [10][11]].

Adaptive Filtering

Real-time adaptation to noise characteristics using filters that track both frequency and amplitude. Adaptability may be insufficient when dealing with diverse frequency noises [[13], [14]].

Statistical Methods

Utilizing statistical techniques to detect and eliminate motion artifacts by modeling both the ECG signal and the artifacts. Challenges arise due to variations in motion artifacts based on movement types.

The detection of noisy samples in ECG signal has been a subject of extensive research, employing various techniques for signal processing and analysis. Initial attempts involved statistical analysis based on extracted features, such as RR intervals and QRS peaks[10]. Time-domain and frequency-domain filters, as well as wavelet thresholding techniques, have also been utilized to identify and mitigate noisy ECG signals [[11], [13]]. More advanced decomposition techniques, including EMD and ICA, have been explored for their effectiveness in detecting and managing noisy ECG signals [[11], [13]].

Previous studies have addressed the challenge of denoising ECG signals using diverse approaches, ranging from weighted averages [[17],[18]] and adaptive filtering [19] to techniques like independent component analysis [20] and EMD [[20], [24]]. While these methods have proven useful against general noise, the specific concern in medical diagnosis using wearable ECG devices often lies in artifact noise.

Artifact noises are inevitable in wearable ECG monitoring devices and can significantly impact the identification of a representative ECG signal. Continuous filtering of the signal may lead to the loss of important information, especially when dealing with high-magnitude artifacts caused by intense physical activity. Conventional low-pass filtering or exponential smoothening techniques may fall short in effectively handling such artifacts.

Numerous prior studies have focused on mitigating noise in ECG signals. While filter-based methods are common, they may be impractical for effectively eliminating a broad spectrum of frequency components associated with artifact noise. Motion artifacts exhibit similarities with baseline wander but pose greater challenges due to substantial spectral overlap with the PQRST complex. Predominantly, these artifacts manifest within the 1 to 10 Hz range. In ECG recordings, disturbances associated with motion are observed across

9

the 0.1 to 10 Hz frequency spectrum, covering activities like breathing, minor body movements, and muscle contractions. While artifact noise can exceed 10 Hz in specific situations, the frequency range of 1-10 Hz is predominant in clinical scenarios without rapid body movements [[4],[5]].

The application of machine learning classification for detecting motion artifacts in ECG signals brings forth numerous advantages over traditional methods. By combining the strengths of conventional signal processing techniques with the capabilities of machine learning, a more robust and efficient system for artifact detection can be achieved. The following points elaborate on the key benefits of this synergistic approach:

- Automatic Feature Learning:
  Machine learning models excel in autonomously identifying relevant features from ECG data. This reduces the reliance on manual feature engineering, a process often time-consuming and requiring domain expertise. Unlike traditional methods, machine learning models can capture intricate data patterns comprehensively.
- Flexibility and Adaptability:
  Machine learning models showcase high flexibility and adaptability to various types of motion artifacts. Their ability to discern complex patterns and adjust to variations in artifact characteristics makes them more resilient compared to rigidly designed traditional algorithms.
- Generalization:
  Machine learning models effectively generalize to novel, unseen motion artifacts after being trained on a diverse dataset. Traditional methods may struggle with generalization, especially when confronted with artifacts significantly differing from those encountered during their design.
- Scalability:
  Machine learning approaches are inherently scalable, accommodating extensive datasets encompassing a wide array of motion artifacts. This scalability enhances model performance and accuracy by ensuring a comprehensive representation of artifact variability.
- Continuous Improvement:
  Machine learning models can be regularly updated and fine-tuned with new data, ensuring ongoing enhancement as more artifact samples become available. In contrast, traditional methods might necessitate a complete redesign for significant changes.
- Integration with Other Tasks:

Machine learning models seamlessly integrate into larger systems and pipelines for automated ECG analysis. This enables effortless incorporation into clinical workflows, facilitating a holistic approach to medical signal processing.

- Reduced Human Effort:
  Once trained, machine learning models can autonomously detect motion artifacts in real-time without constant human intervention. This not only enhances efficiency but also contributes to cost-effectiveness in clinical settings.
- Interpretability (in some cases):
  While machine learning models are sometimes perceived as "black boxes" certain algorithms, such as decision trees and linear models, offer interpretability. This interpretability can be crucial in medical applications, allowing clinicians to understand the rationale behind specific classification decisions.

The fusion of machine learning with traditional signal processing techniques presents a comprehensive and efficient approach to motion artifact detection in ECG signals, offering a range of benefits from automatic feature learning to continuous improvement and seamless integration into clinical workflows.

Human activity recognition (HAR) systems, which represent a specialized subset of machine learning applications, leverage signals not only from accelerometers but also from gyroscopes, magnetometers, and even cameras [[29], [32]]. This multimodal input enables HAR systems to recognize and categorize a wide range of high-intensity body activities, providing a contextual understanding of the user's movements and activities. In the context of ECG signal analysis, the utilization of accelerometer data in conjunction with machine learning techniques enhances the capacity to distinguish between genuine cardiac signals and artifacts induced by motion or physical activity. In this research, the focus on human HAR aligns with prior studies in the field [[29], [30], [31], [32]]. A pertinent strategy for evaluating my results involves a comparative analysis with established HAR works. HAR typically involves the classification of human activities based on body movement, with these movements generating artifact noise in ECG signal due to impedance variations between the skin and electrodes. Notably, some earlier works in HAR employed balanced labels and extensive datasets [[45],[46]], while others integrated gyroscope, accelerometer, and magnetometer data to enhance test accuracy for their models [[47], [49]]. It is essential

to highlight that the proposed model does not rely on such additional sensor data, as many ECG monitoring wearable devices lack gyroscope or magnetometer sensors.

While motion artifacts are well-studied in signals like EEG, there is a noticeable gap in the detection of motion artifacts in ECG signals within clinical environments. A notable exception is a study [61] that proposed a model achieving an impressive accuracy of 96.87% in classifying artifacts. However, this study segmented ECG signals into 5-second intervals, a limitation for clinical cardiac diagnosis, as artifacts may occur in smaller segments. This research aims to address this gap by exploring novel ML methods specifically tailored for the detection of motion artifacts in ECG signals, ensuring applicability to real-world clinical scenarios where precise diagnosis is paramount.

Table 2-1. Some of related works' comparison.

Work	Methodology	Data Type
[45]	KNN	Accelerometer
[46]	Decision Tree KNN/QDA	Accelerometer
[49]	MLWP	Accelerometer + Gyroscope + Magnetometer
[47]	Logistic Regression	Accelerometer + Gyroscope
[48]	Deep Learning, Belief Network	Accelerometer + Gyroscope
This work [Chapter 1]	Fine KNN using scattering features	Accelerometer

The advantage of incorporating accelerometers lies in their widespread availability, found in most wearable monitoring devices and smartphones. Recognizing artifact noises through this approach enables a more accurate medical diagnosis by identifying specific segments of the signal affected by noise. Machine learning applications, particularly those tailored for healthcare wearable devices, offer promising solutions, automatically learning and improving signal quality [[29], [32]].

To tackle the challenge of identifying artifact noises in ECG signals, an innovative approach integrates 3-axis accelerometer data with ECG signals. This strategy is particularly effective in addressing artifact noises that frequently emerge during episodes of intense physical activity. The integration of 3-axis accelerometer data into the ECG signal processing framework allows for a more comprehensive understanding of physiological responses during periods of heightened physical exertion.

In summary, the search for effective methods to remove noise from ECG signals involves a wide range of techniques. Recent advancements, including the use of machine learning and sensor fusion, offer solutions for accurately identifying and reducing artifact noises. This approach shows great potential for enhancing the reliability of wearable ECG monitoring devices for medical diagnosis. One approach to address the challenge of identifying artifact noises involves integrating 3-axis accelerometer data with ECG signals. This method proves particularly effective in managing noise during intense physical activity. Integrating accelerometer data into the ECG signal processing framework provides a deeper understanding of physiological responses during periods of high activity.

Table 2-2. Some of related works' comparison

Work	RMSE	SNR Improvement (%)	Method
[24]	0.037	6.49	WT filtering + DNN
[72]	0.0189	12.57	Disentangled Autoencoder
[73]	0.063	9.55	FCN-based DAE
This Work	0.0058	12.64	WT Bior filtering + DAE

After identifying artifact noises, one approach to tackle the issue of motion artifact removal is by using a denoising autoencoder. This technique employs unsupervised learning and optimization principles to generate a compact representation of the clean ECG signal while efficiently removing noise.

Table 1-2 provides a comprehensive comparison between my research and previous studies with related objectives. In the work presented by [24], a denoising autoencoder coupled with a wavelet transform was utilized, incorporating a scale-adaptive thresholding technique to address noise in signal data. This effort resulted in a notable enhancement of the SNR, improving from 21.56 dB to 22.96 dB. Similarly, in [72], a disentangled autoencoder was employed to eliminate noise from ECG signals, and its performance was compared with a fully convolutional neural network (FCN). Their methodology yielded a substantial average SNR improvement of 12.57%. Another study, [73], introduced a denoising autoencoder based on an FCN for noise reduction in ECG signals, achieving a commendable SNR improvement ratio of 9.55%. It is crucial to highlight that these prior investigations primarily targeted specific noise types within predefined frequency ranges.

In summary, this introduction highlights the significance of ECG signals in diagnosing cardiovascular health, emphasizing the need to address artifact noise that compromises signal quality. ECG signals, obtained through non-invasive methods, are essential for detecting cardiac arrhythmias and other conditions. However, various types of noise, including power line interference, body movements, and electromagnetic interference, can distort these signals, posing challenges for accurate diagnosis. To mitigate these issues, advanced denoising techniques and machine learning methods are explored. This research proposes a novel methodology incorporating K-nearest neighbors (KNN) classification, wavelet filtering, and denoising autoencoders, aiming to enhance the reliability of ECG signals for clinical applications by effectively identifying and removing artifact noise. The integration of accelerometer data further supports the identification of high-activity periods, improving the accuracy of noise detection and contributing to more reliable diagnostic outcomes in wearable ECG monitoring devices.

1.2   ORGANIZATION OF THE DISSERTATION

The thesis comprises five chapters, each contributing to the understanding and improvement of artifact noise detection and reduction in ECG signals. The subsequent chapters are outlined as follows:

Chapter 2:

This chapter introduces a novel approach for ECG artifact noise detection. ECG signals are acquired following a dedicated protocol, and artifact noise is systematically analyzed within the captured signals. A fine KNN classification method is proposed, utilizing features extracted from 3-axis accelerometer signals using wavelet scattering transform to train the model. The methodology is extensively discussed, accompanied by the

presentation of results, and a comprehensive review of previous works related to HAR is provided.

Chapter 3:

Building upon the model proposed in Chapter 2, this chapter presents a more robust method for artifact noise detection. Features are extracted using the wavelet scattering transform from both ECG and accelerometer signals. The proposed model demonstrates higher accuracy in recognizing artifact noise samples within the ECG signal. The results are thoroughly discussed and compared to previous works, showcasing the improved accuracy achieved by the model.

Chapter 4:

This chapter introduces a comprehensive two-step approach to artifact noise reduction. Initially, artifact noise is identified utilizing the methods proposed in Chapters 2 and 3. Following the recognition of ECG samples with artifacts, a Bior wavelet denoising method is proposed to mitigate high-amplitude noise within the classified samples. Subsequently, a Denoising Autoencoder (DAE) is employed to reconstruct the signal and further reduce motion artifact noise. Results are discussed in detail, comparing the outcomes with clean ECG signals. Power density spectrum and other signal features are considered to evaluate the efficacy of the reconstructed signal, and a comparison with previous works demonstrates the high accuracy of the proposed method.

Chapter 5:

The final chapter summarizes the key findings of the dissertation and provides a conclusion. Additionally, potential research directions for future work are outlined, opening avenues for further exploration and advancements in the field of ECG artifact noise detection and reduction. This comprehensive conclusion helps contextualize the significance of the research conducted and encourages ongoing investigations in related areas.

CHAPTER 2   A NEW APPROACH FOR ECG ARTIFACT DETECTION USING FINE-KNN CLASSIFICATION AND WAVELET SCATTERING FEATURES IN VITAL HEALTH APPLICATIONS

2.1   INTRODUCTION

This chapter is focused on the extraction of features from accelerometer signals using the wavelet scattering transform, Figure 2-1. Subsequently, leveraging a KNN classifier to train the proposed model, aiming to identify artifacts in ECG signals that share the same timestamp. This novel application involves the utilization of the KNN classification method within a machine learning framework to effectively detect artifact noises in ECG signals based on my curated dataset.

Figure 2-1. Block diagram of proposed method.
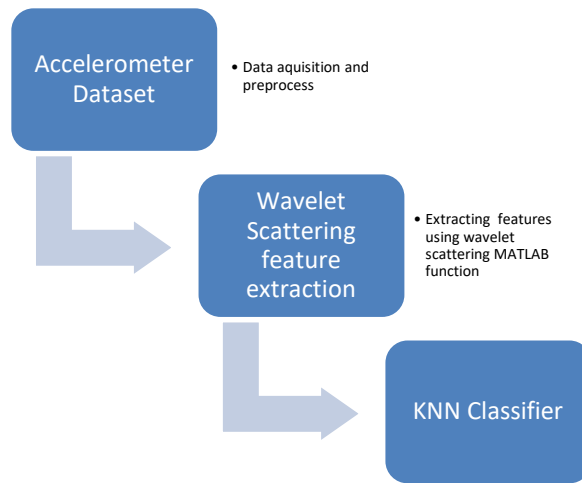
The approach, which employs wavelet scattering transform for feature extraction, demonstrates promising results in enhancing the robustness of feature representation. The KNN classifier is then instrumental in leveraging the learned patterns to discern and categorize artifacts in ECG signals. Importantly, the methodology explored in this chapter is not limited solely to ECG signal analysis. It has the potential for broader applications in

vital sign monitoring, extending to other domains such as photoplethysmography (PPG) and electroencephalogram (EEG) monitoring devices.

The utilization of the wavelet scattering transform for feature extraction adds a layer of sophistication to my approach, allowing me to capture intricate details across different scales in the accelerometer signals. Additionally, the combination of principal component analysis (PCA) and the KNN machine learning methods contributes to the training and refinement of my model, further enhancing its accuracy and adaptability to diverse datasets.

This chapter lays the foundation for a versatile and effective methodology that can be applied not only to artifact detection in ECG signals but also to a spectrum of vital sign monitoring applications. The incorporation of advanced signal processing techniques and machine learning methods demonstrates the potential for widespread applicability and impact in the realm of healthcare and beyond.

This chapter is structured as follows:

- Data Acquisition Method and Protocols:

Section 2.2 provides a detailed description of the methods and protocols employed for data acquisition. It outlines the procedures followed to collect the necessary data for the study.

- Signal Analysis:

In Section 2.3, the analysis of the acquired signals is presented. This involves a comprehensive examination of the characteristics, patterns, and key features inherent in the collected data.

- Wavelet Scattering Transform as Feature Extraction:

Section 2.4 delves into the wavelet scattering transform, elucidating its role as a feature extraction method. The discussion covers the principles and advantages of employing wavelet scattering to enhance the representation of signals.

- Machine Learning Classification Model:

Section 2.5 elaborates on the construction of the machine learning classification model. It encompasses explanations of the KNN classifier and PCA methods, detailing how these components contribute to the model's architecture.

- Model Training and Test Results:

In Section 2.6, the focus shifts to the training of the model and the subsequent examination of test results. This section includes a comparative analysis with previous works, offering insights into the model's performance and its advancements over existing approaches.

2.2 DATA ACQUISITION METHOD AND PROTOCOLS

The provided dataset comprises labeled raw accelerometry data obtained from a MAX ECG monitoring device during various activities, including walking, driving, stair climbing, sitting, and clapping, recorded from a healthy 48-year-old male participant. The MAX ECG monitor device was strategically placed on the chest to collect the data, while the MoveSense Android application facilitated the capture, clock synchronization, and storage of data in CSV files.

The dataset is annotated with activity types, where each label corresponds to a specific activity: 1 for walking, 2 for descending/ascending stairs, 4 for driving, 77 for clapping, and 99 for non-study activities, including sitting. The dataset includes five columns: labels, timestamps (t) indicating relative time, and X, Y, and Z accelerometer signals.

To enhance the dataset's signal quality, a 5th order moving average filter from the MATLAB Clean Data toolbox was applied to smooth the acceleration components, because this type of filter provides a balanced approach to noise reductio. A 5th order moving average filter effectively reduces high-frequency noise, which is common in acceleration data from sensors due to vibrations and rapid movements. By averaging five consecutive data points, the filter smooths out short-term fluctuations, resulting in a cleaner signal. Higher-order moving average filters can over-smooth the data, potentially removing relevant signal variations and leading to a loss of important information. By using a 5th

18

order filter, MATLAB ensures that the signal is smoothed enough to reduce noise but not so much that it eliminates useful signal details [85]. The data collection protocol involved a sequence of activities, such as driving for 10 km, followed by a stop and clapping for 5 minutes. The participant was instructed to clap three times at the beginning and end of each activity to facilitate accurate segmentation and identification of start and stop times.

The walking component of the dataset involved traversing 1.7 km on level ground, descending and ascending stairs, lasting for a total of 18 minutes. The participant mimicked free-living activity by walking at a usual pace along a predefined course. Additionally, data corresponding to a few seconds before/after activities, sitting, and standing were included and labeled as "99."

The primary objective of capturing this dataset was to investigate the impact of each activity on the signal and identify potential noises in the ECG signal. ECG signals corresponding to each activity were analyzed to identify artifact noises, with the label "77-clapping" specifically indicating the presence of such noise. The clapping activity, characterized by extensive body movements, resulted in significant artifact noises in the ECG signal.

A time-domain plot of the accelerometer signals, along with labels, is presented in Figure 2-2 Notably, extreme signal fluctuations are observed in samples labeled as "77." The detection and classification of labels with a high probability of containing artifact noises enable the targeted filtering of those specific parts of the signal.
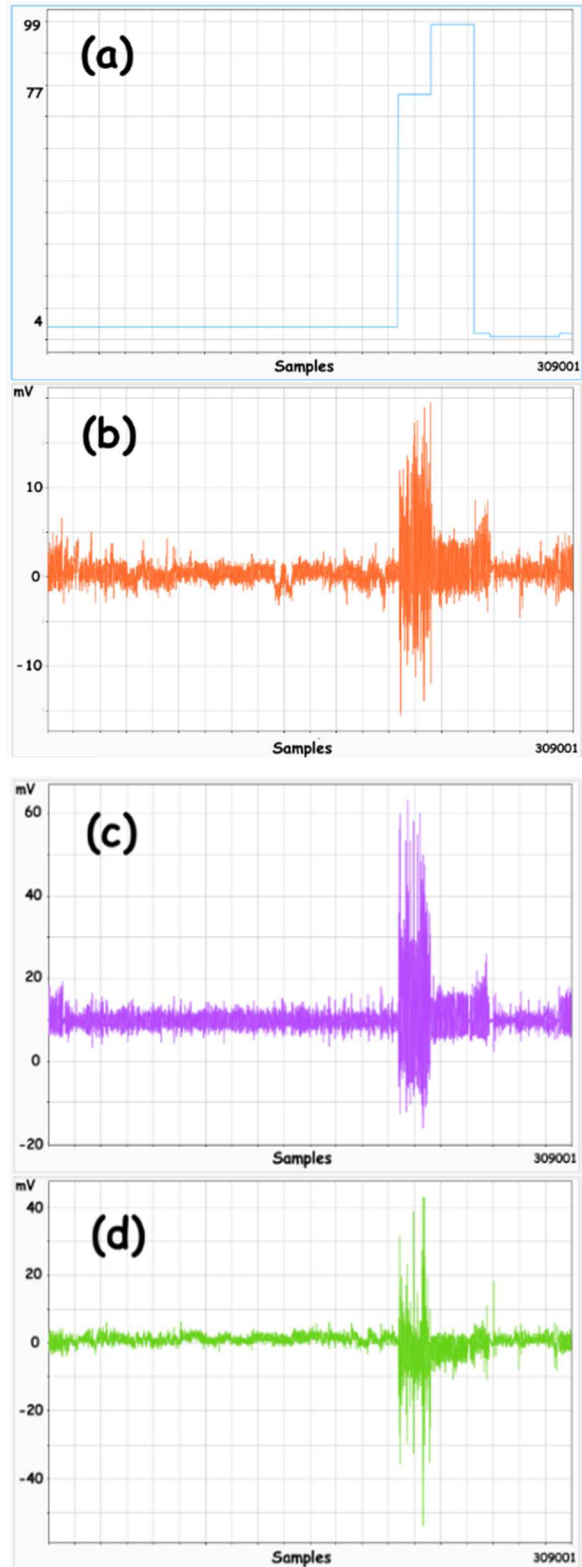
Figure 2-2. (a) Dataset labels, time-domain plot of (b) X, (c) Y, and (d) Z accelerometer signals (dataset)

20

The dataset encompasses X, Y, and Z signals from the accelerometer sensor with a sampling frequency of 104 Hz, ECG signals sampled at 125 Hz, and corresponding timestamps. MATLAB Data Clean Toolbox was utilized for retiming the dataset file and data cleaning. The dataset consists of a total of 309,000 samples, providing a comprehensive resource for studying the interplay between various activities and their effects on both accelerometer and ECG signals.

Table 2-1. Number of samples including 3 signals (X, Y, Z) in Phisyonet dataset [87].

Label	#Samples
1	319,080
2	118,098
3	110,118
4	385,611
77	52,824
99	311,664
Total	1,609,059

The capturing protocol used in this work is similar to the Physionet dataset [87], which allowed me to use both datasets to train a Fine-KNN classification model. The Physionet dataset comprises labeled raw accelerometry data obtained during various activities such as walking, stair climbing, and driving, involving 32 healthy adults equipped with four different accelerometer devices positioned on the left wrist, left hip, left ankle, and right ankle. The participants, consisting of 13 men and 19 women aged between 23 and 52 years, with 31 of them being right-handed, wore 3-axial ActiGraph GT3X+ devices for data collection, synchronized externally using ActiLife software [87]. Activities were labeled accordingly (1=walking; 2=descending stairs; 3=ascending stairs; 4=driving; 77=clapping; 99=non-study activity) [87]. The study protocol comprised a walking pathway (approx. 0.66 miles) followed by a driving trail (approx. 12.8 miles), with data retrieval immediately

after each participant's session. The walking segment included intervals of walking on level ground, descending stairs, and ascending stairs, lasting between 9.0 and 13.5 minutes each, during which participants were instructed to walk at their usual pace along a predefined course to simulate free-living activity [87].

This step was pivotal in confirming the adequacy of the captured dataset before constructing my proposed model. As depicted in Table 2-1, the Physionet dataset encompassed 1,609,059 samples of 3-axis accelerometer signals, which were utilized to train a simple Fine-KNN model employing time-domain features through cross-validation with 5 folds, with 25% of the dataset allocated as test data. Labels 2 and 3 were merged as label 2 for model training using the Physionet dataset. Furthermore, I applied Principal Component Analysis (PCA) to reduce dimensionality, retaining 95% of the variance. Table 2-2 displays the test accuracy results for both datasets, demonstrating comparable outcomes.

The congruent test accuracy results for both datasets, as evidenced in Table 2-2, affirmed the sufficiency and comparability of the captured dataset with the Physionet dataset. This validation constituted a crucial prerequisite before advancing to the development of my proposed model, ensuring the robustness and reliability of the foundational data.

Table 2-2. Dataset comparison using my captured accelerometer dataset and Physionet dataset [87].

Method	Dataset	Test Accuracy (%)
Fine-KNN with PCA (95%)	Physionet[87]	90.1
Fine-KNN with PCA (95%)	Captured Dataset	89.4

2.3 SIGNAL ANALYSIS

To streamline the processes of feature extraction and model training using classification learner the accelerometer and ECG datasets were strategically partitioned into 20 distinct CSV files. Each CSV file corresponds to samples associated with a specific label, effectively organizing the data for enhanced analysis and modeling. The rationale behind

dividing the dataset into multiple CSV files lies in the requirement of the MATLAB Classification Learner toolbox [82], which necessitates input datasets in the form of timetables. This decision was driven by the aim to simplify the structure of input data, making it more compatible with the tool's functionalities. By segregating data into individual files based on labels, the input becomes more coherent and conducive to efficient analysis, feature extraction, and model training.
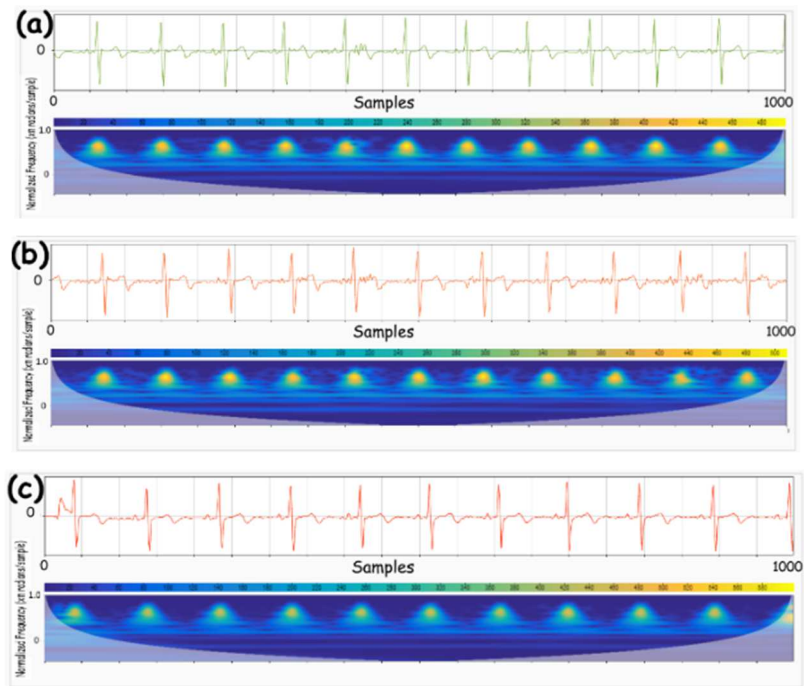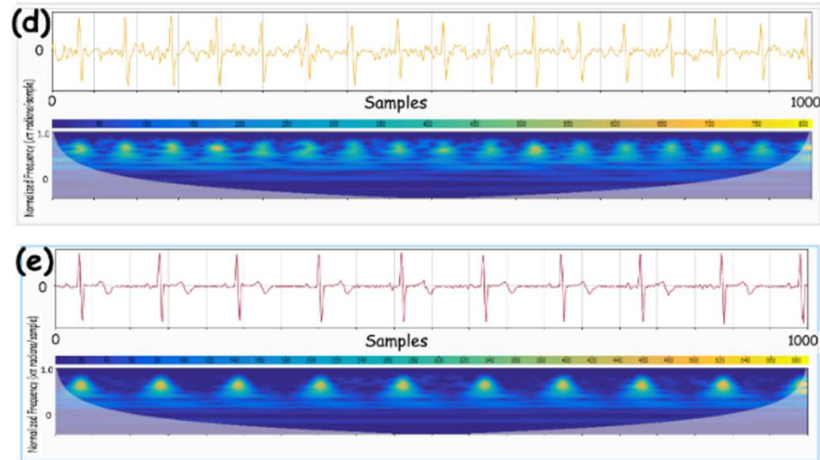
Figure 2-3. Time-domain ECG signal and related scalogram of captured dataset for (a) "1". (b) "2" (c) "4" (d) "77" and (e) "99" labels. (window of 1000 samples).

Figure 2-3 (d) illustrates both the time-domain and scalogram plots of 1000 ECG samples, each containing artifact noise. The ECG signal is notably distorted, evident in both its time-domain representation and the frequency-domain scalogram plot. The frequency-domain plot reveals a substantial number of components, highlighting the complexity introduced by the artifact noise.

Specifically, in the samples labeled as "77" (as presented in Fig 2.3.d), the artifact noise is prominently observed. The ECG signal in these instances appears significantly distorted, and the frequency-domain scalogram plot exhibits a multitude of components indicative of the introduced artifacts. The identification of these artifacts in the samples labeled as "77" underscores the presence of signal abnormalities within this subset of the ECG data. The comprehensive analysis of both time and frequency domains through the scalogram plot allows for a detailed examination of the impact of artifact noise on the ECG signal. These findings not only confirm the presence of artifacts but also emphasize the importance of addressing and mitigating these abnormalities, particularly in samples labeled as ""77," to ensure the reliability and accuracy of subsequent signal processing and classification tasks.

In this comprehensive analysis, a total of 109 time-domain and frequency-domain features were meticulously extracted from the datasets captured by the 3-axis accelerometer and ECG signals. This detailed feature extraction process aimed to showcase the manifestation of artifact noise within samples labeled as "77" and concurrently investigate the statistical

attributes associated with these particular instances. The suite of individual features for each dataset encompasses a diverse range of statistical attributes, including Root Mean Square (RMS), standard deviation (STD), maximum and minimum range values, peak amplitude, band power, kurtosis, skewness, and interquartile range (IQR).

Each of these statistical attributes plays a pivotal role in providing insights into various aspects of signal characteristics. By leveraging these features, the ability to conduct a nuanced analysis of the samples labeled as "77" is gained, specifically focusing on their inherent artifact noise. The interquartile range, a statistical attribute calculated for the captured signals, emerges as a particularly insightful metric. IQR is an excellent measure for representing the variability within the dataset, aiding in the identification of distinctive patterns and characteristics [86]. Higher values of IQR, observed in an accelerometer signal, signify rapid body activities captured by the 3-axis accelerometer. These elevated IQR values correlate with a heightened likelihood of encountering ECG artifact noises [86]. Therefore, the inclusion of IQR in feature set enhances the discriminative power of the analysis, allowing for a more nuanced interpretation of the interplay between accelerometer signals and the presence of artifact noise in ECG samples labeled as "77."

Table 2-3 presents the IQR values for the samples. Notably, the accelerometer signals labeled as "77" exhibit IQR values ranging from 2.5987 to 15.7992. The highest IQR value is observed in these samples, indicating high-intensity movement and the presence of significant artifacts. This elevated IQR indicates a significant spread of data points, emphasizing the need for a detailed analysis of these particular samples. In addition to IQR, another crucial statistical feature considered is the standard deviation, which gauges the dispersion of data concerning the mean. STD provides insights into the magnitude and variability of signal oscillation. A low STD suggests that the signal is closely centered around the mean, while a high STD implies a more widely distributed signal. This variability is indicative of the signal's magnitude of change. Analyzing the accelerometer dataset, high STD values are found to be associated with rapid changes in signals, often resulting from swift posture adjustments. Samples labeled as "77" consistently exhibit the highest STD values, indicating increased variability and abrupt changes in the signals. This insight is crucial in understanding the nature of the movement and identifying potential

artifact noise in these specific samples. By considering both IQR and STD, these statistical attributes offer a comprehensive view of the signal characteristics. These features not only emphasize the distinctive characteristics of samples labeled as "77" but also offer valuable insights into the presence of artifact noise [3]. Hence, it aids in labeling samples containing artifact noise. The analysis identifies artifact noise in the label "77" using time-domain features extracted from the signal.

Table 2-3.Statistical performance comparison of 3-Axis accelerometer signal among different time-domain features.

Labels	1	2	4	77	99
X RMS	0.9728	1.2845	0.8446	2.8253	1.3075
Y RMS	9.2477	10.0313	9.84	14.5224	10.0667
Z RMS	1.4255	1.3402	1.4762	3.8397	1.5964
ECG RMS	333.6022	309.7283	302.6719	418.2551	327.2388
X STD	0.6712	1.2593	0.7764	2.6593	1.112
Y STD	0.8695	2.293	1.0915	9.5646	2.1962
Z STD	1.1501	1.234	0.9481	3.6073	1.5641
ECG STD	328.1553	303.882	296.6482	413.8744	321.6916
Y Min	2.2685	3.7712	3.2687	-16.2311	3.9866
Z Min	-7.9349	-10.7418	-4.1493	-53.8763	-10.7585
Y Max	16.937	26.0468	19.3538	63.2876	20.713
Z Max	18.3799	11.2251	6.3173	43.0053	4.1828
X IQR	0.6461	1.699	0.777	2.5987	1.5602
Y IQR	0.8471	2.43	1.2084	15.7992	2.9552
Z IQR	1.1917	1.3663	1.2682	2.8332	1.5458
ECG IQR	106	85	73	177	87

2.4 WAVELET SCATTERING TRANSFORM AS FEATURE EXTRACTION

The wavelet scattering transform can be regarded as an equivalent deep convolutional network, structured through a cascade of wavelets, modulus nonlinearities, and lowpass filters. This configuration allows the extraction of low-variance features from real-valued time series with minimal setup, making it particularly advantageous for applications in machine learning and deep learning [33]. The notable advantage of wavelet scattering resides in its capability to generate signal representations that demonstrate not only translation or shift-invariance but also stability against time-warping deformations [33].

Utilizing the wavelet scattering transform for the extraction of features from ECG or accelerometer signals significantly enhances the accuracy of a trained model. Several factors contribute to the effectiveness of this approach:

Multiresolution Analysis

Wavelet scattering excels in capturing information at multiple resolutions. In the case of ECG and accelerometer data, which often contain features at different scales, the multiresolution analysis empowers the model to effectively capture and represent relevant information across various frequency bands. This comprehensive analysis contributes to a more nuanced understanding of the signal's characteristics.

Translation Invariance:

Wavelet scattering is renowned for its translation-invariant properties. This means that small shifts in the input signal do not significantly impact the representation. In scenarios involving accelerometer and ECG signals, where precise alignment of features may vary, the translation-invariant nature of wavelet scattering ensures that the model focuses on essential information regardless of slight temporal shifts.

Preservation of Signal Characteristics:

Wavelet scattering captures both amplitude and phase information. The preservation of these signal characteristics is essential for maintaining the integrity of the original signal while extracting relevant features. In ECG and accelerometer signals, where both

amplitude and phase information play a vital role, this attribute significantly contributes to the improved performance of the model.

Non-Redundancy:

Wavelet scattering provides a non-redundant representation of the signal, emphasizing unique features without unnecessary duplication. This non-redundancy enhances the efficiency of the feature set, preventing the model from being overwhelmed by redundant or irrelevant information. The focus on essential features improves the model's ability to generalize to new data and enhances its overall performance.

The coeffication of wavelet scattering transform for feature extraction offers a holistic approach to signal analysis, particularly in the context of ECG and accelerometer data. Its ability to handle multiresolution information, maintain translation invariance, preserve signal characteristics, and provide a non-redundant representation collectively contributes to the increased accuracy and robustness of models trained on such features.

The processing of data in the wavelet scattering transform occurs in stages, and each stage involves three fundamental operations, as illustrated in Figure 2-4 This multi-stage processing is a key characteristic of the transform and contributes to its effectiveness in capturing complex signal structures. The cascade of wavelets enables the decomposition of the signal into various frequency components, providing a multi-scale representation that is crucial for discerning patterns at different levels of detail.

Convolution (Wavelets) — Nonlinearity (Modulus) — Averaging (Scaling Function)
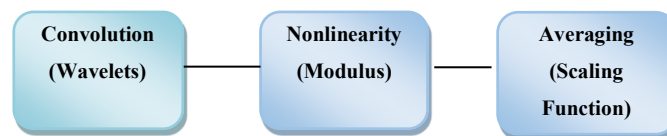
Figure 2-4. Three main operations of wavelet transform stages.

In the context of the wavelet scattering framework, Figure 2-5 (a) visually represents Morlet (Gabor) wavelet filter banks, illustrating the deployment of two distinct banks. The parameters Q_1 and Q_2, set at 8 and 1 respectively, play a pivotal role in defining the

characteristics of the wavelet filters. Specifically, $\lambda=2^{(k/Q)}$ for $k \in Z$, where Q^{-1} corresponds to the bandwidth of ψ, contributes to the adaptability of the wavelet filters across different scales and frequencies. The choice of Morlet (Gabor) wavelet filters, characterized by their complex sinusoidal shape, enhances the network's ability to capture both temporal and frequency-related features. The use of two banks further allows for a more comprehensive analysis of the signal, accommodating variations in different frequency bands. This multi-scale and multi-frequency analysis is particularly advantageous in scenarios where signals may exhibit diverse patterns across varying temporal and amplitude scales.
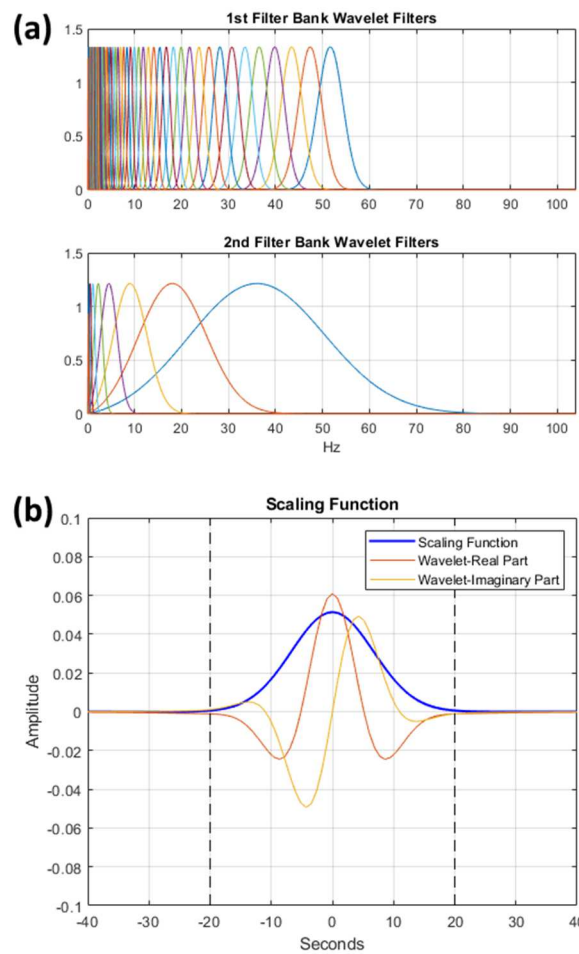
Figure 2-5.Scaling function- coarsest-scale wavelet first filter bank with invariance scale of 40 seconds (a) Filter banks (b) Scaling Function.

The invariance scale, Morlet wavelet filter banks, and the flexibility introduced by parameter choices in the wavelet scattering decomposition collectively contribute to the effectiveness of this approach in capturing intricate details within accelerometer signals. The adaptability to translations, coupled with the ability to discern changes in duration and amplitude, positions wavelet scattering as a robust technique in the realm of signal processing and feature extraction for accelerometer data.

The specific configuration employed in the wavelet scattering framework in this work, involves the use of two complex-valued 1-D Morlet filter banks. These filter banks exhibit an invariance scale of 40 and operate with a sampling frequency of 104. The choice of an invariance scale of 40 was determined through experimentation, considering its ability to preserve the most pertinent signal information for my classification model. Additionally, a frequency resolution per octave was set for the first and second filter banks, denoted as Q1=8 and Q2=1, respectively. Q2 indicates the quality of the low-pass filter in the first-order wavelet filter bank. Higher Q2 values enhance frequency localization but may lead to increased time spreading. Conversely, Q1 indicates the quality of the high-pass filter in the second-order wavelet filter bank. Lower Q1 values prioritize frequency localization, potentially resulting in increased time spreading.

In an example involving ECG signals, MATLAB suggested specific values of 8 and 1 for Q2 and Q1, respectively. A Q2 value of 8 provides adequate frequency localization while minimizing time spreading, thereby facilitating the capture of relevant features in the signal. On the other hand, a Q1 value of 1 was recommended to prioritize frequency localization over time spreading, enabling the detection of fine-scale variations in the high-frequency components of the signal.

It is worth emphasizing that the adaptability of the invariance scale parameters was explored, and the selection of 40 demonstrated superior performance in preserving essential signal characteristics for my specific classification task.This parameter tuning contributes to the overall effectiveness of the wavelet scattering function in extracting discriminative features, making it a valuable asset in signal processing applications where accurate representation and classification are paramount.

2.4.1 Wavelet Scattering in MATLAB

A wavelet scattering network offers a powerful means to extract low-variance features from real-valued time series and image data for application in machine learning and deep learning contexts, requiring minimal configuration. These features exhibit insensitivity to translations within a user-defined invariance scale and maintain continuity with respect to deformations. In the case of 2-D data, such features also demonstrate insensitivity to rotations. The scattering network employs predefined wavelet and scaling filters to achieve these characteristics.

The foundation for this mathematical framework was laid by Mallat in collaboration with Bruna and Andén, marking a pioneering effort in the study of convolutional neural architectures [[34], [37]]. Subsequently, Andén and Lostanlen contributed by developing efficient algorithms for the wavelet scattering of 1-D signals [[36], [38]], while Oyallon extended this work to encompass 2-D scattering with the development of efficient algorithms[38]. The collaborative efforts of Andén, Lostanlen, and Oyallon have significantly shaped the ScatNet [40] and Kymatio [41] software, essential tools for computing scattering transforms. Mallat and his peers identified three key properties inherent in deep learning architectures for extracting meaningful features from data, namely:

- Multiscale contractions
- Linearization of hierarchical symmetries
- Sparse representations

Remarkably, the wavelet scattering network embodies all these properties. Wavelet transforms effectively linearize small deformations, such as dilations, by segregating variations across different scales. Furthermore, for many natural signals, the wavelet transform inherently yields sparse representations. The scattering transform, when coupled with other features of the scattering network, generates data representations that minimize intra-class differences while preserving discriminability across different classes. An essential distinction between the scattering transform and deep learning networks lies in the fact that the filters are predefined, rather than being learned. This a priori definition of

filters imparts a unique advantage to the scattering transform—since it doesn't necessitate learning filter responses, it can be successfully applied in situations where training data is scarce. This characteristic makes the scattering transform a valuable tool in scenarios where traditional deep learning networks may face limitations due to insufficient training data availability. To perform feature extraction on data using MATLAB, I leverage the waveletScattering function for time series and waveletScattering2 for image data. Configuring the network involves setting parameters such as the invariance scale size, the number of filter banks, and the number of wavelets per octave in each filter bank. For waveletScattering2, an additional parameter is the number of rotations per wavelet. To obtain features from time series, I employ the waveletScattering object functions scatteringTransform or featureMatrix.

The process of the scattering transform unfolds iteratively. Initially, the data undergoes convolution with the scaling function to yield zeroth-order scattering coefficients. The subsequent steps involve:

1. Applying the wavelet transform to the input data with each wavelet filter in the first filter bank.
2. Computing the modulus of each filtered output, resulting in nodes known as the scalogram, U[1].
3. Averaging each modulus with the scaling filter to produce the first-order scattering coefficients, S[1].

This process repeats at every node, and the scatteringTransform function returns both the scattering and scalogram coefficients. Meanwhile, the featureMatrix function provides the scattering features. These outputs are easily consumable by various learning algorithms. The Wavelet Scattering Transform is a mathematical operation that encompasses a series of convolutions and modulus operations on an input signal using a set of wavelet filters. The resulting coefficients effectively capture the energy of the input signal across different scales and time-shifts. Leveraging the hierarchical structure of wavelet scattering, this method excels in feature extraction, particularly in scenarios involving noisy data, as it provides a robust and discriminative representation of signal characteristics. In applications like healthcare, where accurate analysis of signals, such as ECG data, is critical, the

Wavelet Scattering Transform proves to be a valuable tool for enhancing the performance of learning algorithms.

2.4.2 Number of Coefficients

The determination of the number of scattering coefficients in the waveletScattering method is influenced by various parameters, including SignalLength, InvarianceScale, and SamplingFrequency. The computation of scattering coefficients is closely tied to the characteristics of the wavelet filter banks, including their number, quality factors (Q_1 and Q_2), and the chosen invariance scale, all in conjunction with the length of the signal. The calculation of scattering coefficients follows a two-step process:

1. The zeroth-order scattering coefficients result from convolving the signal with a wavelet filter bank at the finest scale. The number of zeroth-order coefficients corresponds to the number of wavelet filters in the filter banks, and in this example, there are 2 filter banks (one with $Q_1=8$ and one with $Q_2=1$).
2. The 1st-order scattering coefficients are derived by convolving the zeroth-order coefficients with a wavelet filter bank at the next larger scale. The number of 1st-order coefficients is the product of the number of wavelet filters in the filter bank and the number of zeroth-order coefficients.

2.4.3 Scattering Path

The Wavelet Scattering Transform allows for multiple orders of scattering coefficients, capturing the time-frequency structure of the input signal at different scales and time-shifts. The number of coefficients at each order is determined by the length of the input signal X1, the invariance scale, and the sampling rate, among other factors. In this case, the InvarianceScale is set to 40 seconds, indicating the maximum time-shift between coefficients at different orders. The number of coefficients at each order is determined by dividing the length of the input signal by the invariance scale and downsampling at each

layer. The resulting XS1 matrix is of size 261 × 36, where 261 is the number of paths through the scattering tree, and 36 is the number of coefficientts at each scale. The featureMatrix function is then used to compute the scattering coefficients for the input signal X1, resulting in a matrix XS1 with dimensions 261 × 36. Each row corresponds to a unique scattering path, and each column corresponds to a different scattering coefficient. The number of paths is determined by the number of unique scattering paths computed by the wavelet scattering transform network.

The number of paths is calculated as the total number of possible combinations of wavelet coefficients across all scales and windows. In this example, with 2 layers and an invariance scale of 40 seconds, the calculation is $\text{NumofLayers}^{(\text{NumofLayers}-2)} \times \text{Coeffs@eachScale} \times (\text{SignalLength} / \text{Invariance Scale})$, resulting in 8208 paths. However, not all of these paths are unique due to symmetries of the wavelet filters [84]. MATLAB uses a process of pruning and symmetry reduction to eliminate redundant paths, resulting in a final number of 261 unique paths.

2.5   MACHINE LEARNING CLASSIFICATION MODEL

2.5.1 KNN Classifier

K-Nearest Neighbor (KNN), is a versatile supervised machine learning algorithm used for both classification and regression tasks. It is particularly effective for imbalanced datasets, making it a suitable choice as a classifier in such scenarios. In my specific dataset, characterized by its imbalanced nature, it is advised against down-sampling or up-sampling to avoid compromising time series features.

The parameter "K" in KNN represents the number of neighbors considered when predicting or classifying a new unknown variable. The algorithm seeks to identify the closest neighbors around an unknown datapoint to determine its class. The distance from all points in the proximity of the unknown data is calculated, and those with the shortest distances are filtered out. The success of classification and prediction hinges on selecting an appropriate value for K.

Determining the optimal value for K involves testing the model's accuracy across different K values (Table 2-4). It is a common practice to choose an odd value for K to avoid situations where elements from both groups are equal. Larger K values may lead to underfitting, causing the model to struggle with learning from the training data, while smaller K values may result in overfitting, where the model captures noise along with the training data.

KNN is a non-parametric supervised classifier that compares data with the entire dataset. After transforming data points into mathematical vectors, the algorithm calculates the distance between vectors to find the probability of similarity to the test data. Classification is then based on the points that share the highest probabilities. Three different distance functions—Euclidean, Minkowski, and Hamming—can be employed in this process. In this context, the Euclidean distance function is utilized, representing the shortest distance between two points regardless of dimensions, and it is the most commonly used method in KNN.
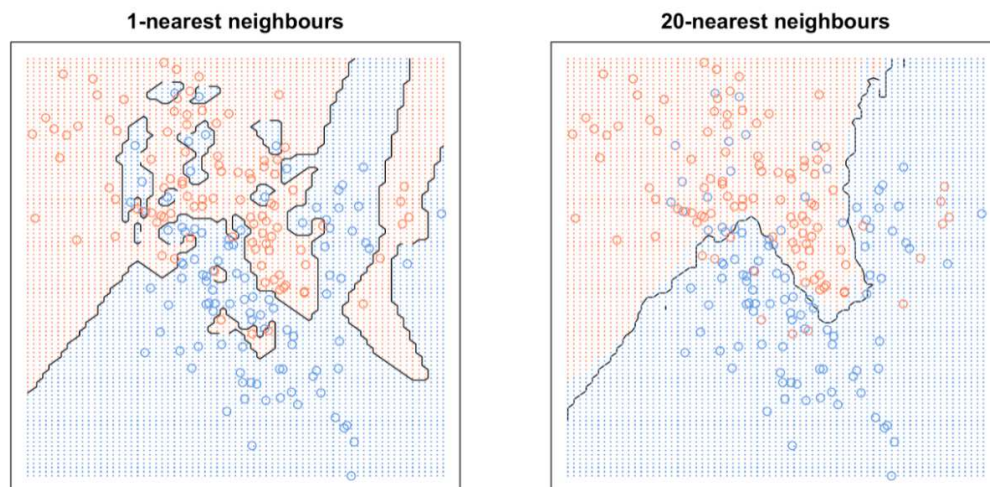
Figure 2-6. K=1 and K=20 Nearest neighbors.

KNN is advantageous in handling non-linear data, making it suitable for scenarios where the relationship between the dependent and independent variables is not a straight line [76]. It excels in scenarios where it is necessary to identify the K nearest neighbors of the test data, providing a small number of training samples close to the test samples. In comparison

to simpler algorithms like linear regression, KNN's ability to work well with non-linear data is a notable strength.

The Fine-KNN variant, employed in this work, takes advantage of the simplicity of KNN by considering only one neighbor for data point distinction. To determine the optimal value of "K" for the KNN classifier, various nearest neighbors methods were employed to train the proposed model. The test accuracy results were compared, and it was found that the best value for "K" is 1, indicating fine KNN.

Table 2-4.Comparison of different trained Nearest Neighbors methods to find best number of K.

Classifier Type	Model Flexibility	Test Accuracy (%)
Fine KNN	Finely detailed distinctions between classes, K = 1	94.7
Medium KNN	Medium distictions between classes. K=10	94.4
Coarse KNN	Coarse distinctions between classes. K=100	93
Cosine KNN	Medium distinctions between classes, using a Cosine distance metric. K =10	89.3
Cubic KNN	Medium distinctions between classes, using c cubic distance metric. K=10.	94.2
Weighted KNN	Medium distinctions between classes, using a distance weight. K=100.	94.5

The Euclidean distance function plays a pivotal role in the Fine-KNN classifier, quantifying the dissimilarity between data points in the feature space. Moreover, the Euclidean distance function employed by the Fine-KNN classifier is well-suited for accelerometer signals. Its capability to measure the distance between points in a

multidimensional space allows for the effective capture of similarities and differences in signal patterns [76]. This is crucial when dealing with accelerometer data that may exhibit nuanced variations influenced by factors such as motion intensity, orientation, and environmental conditions.

The choice of Fine-KNN for accelerometer signal classification aligns with the unique requirements of the dataset. Accelerometer signals, being inherently dynamic and subject to diverse environmental conditions, benefit from the simplicity and adaptability of the Fine-KNN classifier. It excels in scenarios where a single nearest neighbor provides sufficient discriminatory information, making it particularly suitable for applications where precision in signal classification is paramount.

2.5.2 PCA (Principal Component Analysis)

To enhance the accuracy of the KNN classifier, employing dimensionality reduction techniques such as PCA becomes a valuable strategy. The application of PCA is particularly advantageous when employed before KNN, as it contributes to the meaningful adjustment of the distance metric used in the classification process. In this study, PCA is implemented with the objective of capturing 95% of the variance within the dataset. Large datasets often pose challenges in terms of interpretation, prompting the utilization of PCA to alleviate this issue by reducing dimensionality. This not only increases interpretability but also mitigates information loss. PCA achieves this by generating new uncorrelated variables that successively maximize variance. The core functionality of PCA lies in its ability to transform a large dataset with interrelated variables into a new set of variables known as principal components. These components are uncorrelated and are arranged in descending order of component variance. The coefficient matrix, denoted as Coeff, is pivotal in this process. Each column of Coeff contains coefficients for a specific principal component.

The mathematical formulation Coeff=PCA(X) signifies the computation of principal component coefficients or loadings for an n-by-p data matrix X, where rows correspond to observations and columns to variables. By default, PCA centers the data and employs the

37

singular value decomposition (SVD) algorithm. The overarching goal of PCA is to reduce the dimensionality of a dataset, consisting of numerous interrelated variables, while preserving as much variation as possible. This transformation results in a set of principal variables that are uncorrelated, enhancing interpretability without sacrificing critical information present in the dataset.

This technique is particularly beneficial in circumventing the dimensionality curse associated with large datasets, where memory and CPU resources are constrained. Notably, MATLAB provides a built-in PCA option within the Classification Learner Tool [82[, simplifying the implementation of PCA in conjunction with classification tasks and facilitating efficient management of large datasets. As such, the combination of PCA and KNN serves as a robust methodology for improving the accuracy of classification algorithms, especially in scenarios involving complex, high-dimensional data.

Moreover, PCA serves as a versatile tool in the realm of data analysis, offering benefits beyond dimensionality reduction. PCA not only diminishes noise in the data but also plays a pivotal role in feature selection and the generation of independent, uncorrelated features [43].

One of the primary advantages of PCA is its noise reduction capabilities. PCA identifies the principal components of the data, which are new variables that are linear combinations of the original variables. These principal components are ordered by their importance, with the first component explaining the maximum variance in the data, followed by the second component, and so on. The principal components extracted by PCA are orthogonal to each other, meaning they are uncorrelated. As a result, redundant or noisy information present in the original high-dimensional data tends to be spread across multiple components. By selecting only the most important components, PCA effectively filters out the noise present in the less significant components. By reducing the dimensionality of the data while preserving its essential structure, PCA enhances the signal-to-noise ratio. The signal, which represents the meaningful information in the data, is retained in the reduced-dimensional space, while the noise, which represents irrelevant or random variations, is diminished. By identifying and eliminating noise components in the dataset, PCA allows for a cleaner and more focused representation of the underlying patterns [43]. In the context of training

model on accelerometer dataset, where noise may be prevalent due to various environmental factors, PCA becomes instrumental in enhancing the signal-to-noise ratio.

In addition to noise reduction, PCA assists in feature selection to some extent. It achieves this by highlighting the principal components that contribute the most to the variance in the data. This selective emphasis on crucial features not only simplifies the dataset but also aids in creating a more efficient representation for model training [43]. Feature selection is particularly valuable when dealing with high-dimensional datasets, as it helps focus on the most relevant information. Feature selection process in MATLAB is explained in Appendix C.

Furthermore, PCA generates independent and uncorrelated features, providing a unique advantage in model training. This independence ensures that the selected features are not redundant, offering a diverse set of information for the model to learn from [43]. The absence of correlation among features can contribute to better model interpretability and generalization.

An additional noteworthy benefit of PCA is its ability to mitigate overfitting. Overfitting occurs when a model learns noise in the training data, resulting in poor generalization to new, unseen data. By retaining only essential features and discarding noise, PCA helps in creating a more parsimonious model that is less prone to overfitting [43]. This, in turn, contributes to enhanced model performance and reliability.

Considering these advantages, PCA emerges as a judicious choice for training accelerometer dataset. Its multifaceted impact, ranging from noise reduction to feature selection and addressing overfitting concerns, aligns well with the challenges often encountered in accelerometer data analysis. Integrating PCA into the preprocessing pipeline can significantly contribute to the robustness and effectiveness of models trained on accelerometer datasets.

2.6 MODEL TRAINING AND TEST RESULTS

The wavelet scattering network is characterized by its ability to manifest multiscale contractions, linearize hierarchical symmetries, and provide sparse representations. These properties collectively contribute to the creation of data representations that minimize intra-class differences while preserving discriminability across different classes. One notable advantage of the wavelet scattering transform is its independence from the need to learn filter responses. This characteristic proves invaluable, especially in scenarios where training data may be limited[42]. By utilizing predefined wavelet filters, the function computes the scalogram and subsequently applies an averaging filter to facilitate feature extraction.

As previously mentioned, the dataset has been partitioned into individual samples corresponding to each label, resulting in 15 matrices across 5 labels and 3 signals. The utilization of 1-D wavelet scattering transform has proven effective in extracting reliable features from the raw signals captured by a 3-axis accelerometer. This transformative process involves essential operations such as convolution, nonlinearity, and averaging (low-pass filtering) to generate a wavelet scattering transform for a given time series input signal. As it explained in Appendix A, convolution in wavelet scattering transform helps by capturing different frequency components present in the ECG signal, including those affected by motion artifact noise. Nonlinearity introduces nonlinearities into the transformed signal, enabling the model to capture complex patterns and variations. For each signal, the wavelet scattering function set, characterized by an invariance scale of 40 seconds, dissects each block of the signal into distinct scattering windows. Table 2-5 provides an overview of the number of samples and their corresponding scattering coefficients. The MATLAB DSP toolbox's "numCoefficients" function is employed to calculate the number of scattering coefficients for each matrix, each window has 261 scattering paths. Calculation of scattering paths is explained in Appendix C. Following feature extraction, a timetable is constructed with 15 cells, each containing the extracted features for an individual matrix. This timetable serves as the training dataset input for the Classification Learner tool.

Table 2-5. Number of samples and corresponding windows for each signal (X, Y, and Z).

Label	Number of samples for each signal	Number of windows
1	36462	36
2	52530	52
4	133488	131
77	54384	54
99	31827	32

The Fine KNN model was trained utilizing the raw dataset from a 3-axis accelerometer, with wavelet scattering coefficients serving as essential features, as previously outlined.

In preparation for model training, all wavelet scattering coefficients were seamlessly integrated into the Classification Learner Toolbox as a timetable in CSV format. The dataset was then strategically partitioned into distinct training and test sets, a crucial step to assess the model's performance on unseen data. The utilization of the Classification Learner Toolbox's internal option for PCA further enhanced the model's training process. PCA, configured to retain 95% of the variance, played a pivotal role in reducing the dimensionality of the training dataset. This reduction not only streamlined computational efficiency but also ensured that the model could discern the most impactful features in the dataset, thereby optimizing its predictive capabilities[43].

The PCA process facilitated the creation of new uncorrelated variables, with each variable capturing maximized variance successively. This transformation contributes to the model's ability to focus on the most relevant information during training. By selectively retaining features that contribute significantly to the dataset's variance, PCA aids in mitigating the risk of overfitting while preserving the essential characteristics of the data.

During the testing phase, 25% of the captured dataset was designated as test data. This partitioning strategy allows for a robust evaluation of the model's generalization performance, ensuring its efficacy in making accurate predictions on new and unseen instances. The incorporation of rigorous testing procedures underscores the model's

reliability and its potential for real-world applications where performance on diverse datasets is paramount.

In a wavelet scattering network, the features extracted encompass a combination of information from all layers, not solely relying on the output of the final convolution layer. This architectural design allows for a holistic representation of the input signal, capturing nuanced details across different hierarchical levels. One noteworthy characteristic of the scattering coefficients is the variation in energy levels across layers—typically, the energy decreases as the layer level ascends. It has been observed that the first two layers contain a substantial portion, around 99%, of the total energy in the scattering coefficients [44]. The first layer of the scattering network captures low-frequency components of the signal, which tend to contain a significant portion of the ECG signal's energy. These components often represent the overall trend or global structure of the signal. The second layer of the scattering network combines information from the first layer in a hierarchical manner, leading to the extraction of higher-level abstractions or more complex patterns. These abstractions may still capture a substantial amount of energy due to their relevance to the ECG signal's structure.

As it is explained in Appendix A, to achieve wavelet decomposition within the scattering network, Gabor wavelets are employed. Gabor wavelets are well-suited for this purpose due to their ability to effectively capture both temporal and frequency characteristics of signals. The decomposition process involves the utilization of a low-pass filter (ϕ), which, in the context of wavelet scattering, is often implemented as a Gaussian function. This filter plays a critical role in identifying and retaining essential features while suppressing unwanted noise, contributing to the network's robustness in handling various signal complexities.

The use of Gabor wavelets in conjunction with the Gaussian low-pass filter not only facilitates efficient wavelet decomposition but also ensures that the resulting features are informative and discriminative. The scattering network's ability to consider multiple layers and the concentration of energy in the initial layers make it well-suited for applications where a comprehensive understanding of signal characteristics is paramount. The wavelet scattering network's feature extraction mechanism, employing Gabor wavelets and a

42

Gaussian low-pass filter, offers a versatile and powerful approach for signal analysis. The consideration of energy distribution across layers enhances the network's ability to discern important signal patterns, making it a valuable tool in various domains, including image and signal processing.

In this chapter, a robust KNN model designed for classification is introduced, incorporating a reliable evaluation strategy involving 5-fold cross-validation. The model is carefully configured with a choice of 1 neighbor and utilizes the Euclidean distance metric, showcasing its effectiveness in capturing local patterns in the feature space. Impressively, this proposed KNN model achieves a commendable test accuracy of 94.7%, attesting to its robust performance.

Figure 2-7. Test confusion matrix of the trained/tested KNN model with wavelet scattering coefficients(a) TPR (true positive rate) vs FNR (false negative rate) (b) PPV (positive predictive value) vs FDR (false discovery rate).

In Figure 2-7, I delve into the performance of the model by presenting a comprehensive test confusion matrix. Notably, the "4" label emerges as the best-predicted class, boasting the largest number of accurately classified samples. The True Positive Rate (TPR), representing the proportion of correctly classified observations per true class, is particularly noteworthy for label 77, achieving an impressive 91.2%. On the flip side, the False Negative Rate (FNR) is minimized, with the highest occurrence at 2.9% when classifying as 99 labels.

Figure 2-7 (b) provides a visual representation that underscores the model's prowess in accurately predicting the "4" class while shedding light on challenges encountered in predicting the "2" class. This class experiences the highest False Discovery Rate (FDR), highlighting areas for potential improvement in the model's predictive capabilities.

The 94.7% test classification accuracy attained with the proposed approach underscores its efficacy in handling the inherent complexities of the dataset. Notably, the model leverages raw signals from a 3-axis accelerometer, acknowledging the imbalanced nature of the dataset. To further enhance the model's ability to discern intricate patterns, wavelet

scattering coefficients have been employed as features during the training phase. This innovative feature extraction technique contributes significantly to the success of the classification model by providing a more comprehensive representation of the underlying signal structures.

The combination of this innovative feature extraction method and the robust KNN algorithm positions my approach as a promising solution for effective classification tasks. This is particularly true when confronted with challenging and imbalanced datasets, demonstrating the adaptability and performance of the proposed methodology in real-world scenarios.
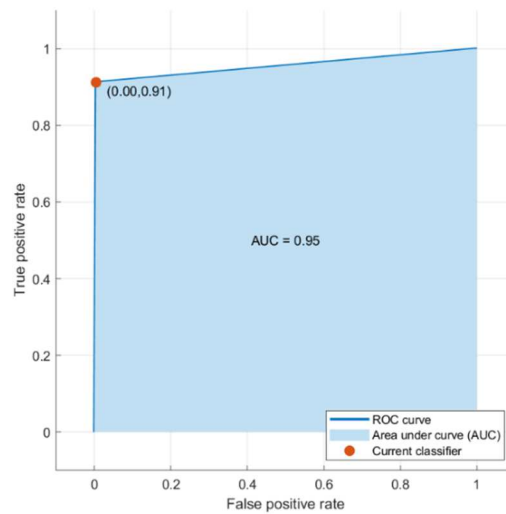
Figure 2-8. Test ROC curve of label 77

The Receiver Operating Characteristic (ROC) curve serves as a graphical representation of the trade-off between TPR and FPR across various classification score thresholds. By plotting TPR against FPR, the ROC curve provides valuable insights into the performance of a classifier under different conditions. The AUC "Area under the ROC Curve" is a numerical metric derived from the ROC curve and reflects the integral of TPR values concerning FPR, spanning from FPR=0 to FPR=1.

45

A higher AUC value signifies superior overall classification quality, with the AUC range falling between 0 and 1. A value of 1 indicates perfect classification, while a value of 0.5 suggests performance equivalent to random chance. The AUC value is a valuable quantitative measure, offering a comprehensive assessment of a classifier's ability to discriminate between classes. In the context of Figure 2-8, which portrays the ROC curve for the label "77," the accompanying AUC value of 0.95 attests to the classifier's strong discriminatory performance. This high AUC suggests that the classifier exhibits robust sensitivity (true positive identification) while effectively minimizing false positive identifications.

Understanding and analyzing ROC curves and their associated AUC values are fundamental steps in evaluating and fine-tuning classification models. Researchers and practitioners leverage these metrics to gauge the efficacy of their classifiers, enabling informed decisions on model selection and parameter tuning to achieve optimal performance in diverse applications. In essence, the ROC curve and AUC serve as crucial tools in the assessment and refinement of classification models, contributing to the ongoing advancements in machine learning and data-driven decision-making.

2.7 SUMMARY

In this chapter, a novel approach to machine learning is introduced, showcasing the application of a KNN model for the classification of extracted wavelet scattering coefficients derived from a 3-axis accelerometer signal. The primary objective is to leverage this model to detect artifact noises present in associated ECG signals. The underlying premise involves considering human body activity as a key factor in recognizing artifacts within ECG signals.

To accomplish this, a well-established supervised machine learning technique, the KNN classifier was employed. The performance of this approach is thoroughly evaluated by testing its ability to classify both human activity and artifacts in 3-axis accelerometer signals, utilizing the wavelet scattering coefficients obtained from the captured dataset.

The results of the trained model are promising, demonstrating a high-test accuracy of 94.7% and a positive predictive value (PPV) of 93% specifically for samples labeled with artifact noises (denoted as "77"). This noteworthy performance suggests the potential utility of the proposed model as an effective artifact recognition technique, particularly in the context of vital sign monitoring devices such as those used for EEG, PPG, and ECG signals.

CHAPTER 3   ROBUST ECG ARTIFACT NOISE CLASSIFICATION METHOD USING WAVELET SCATTERING FEATURES IN VITAL HEALTH APPLICATIONS

3.1   INTRODUCTION

In Chapter 1, a novel approach was introduced for the classification of ECG samples that include artifacts, leveraging 3-AXIS accelerometer signals synchronized with ECG data obtained from a wearable device. Building upon this foundation, Chapter 2 presented an advancement aimed at enhancing the classification accuracy. This was achieved by proposing a method that utilizes features extracted not only from the 3-axis accelerometer signals but also from the accompanying ECG signal to train the classifier.

Figure 3-1. Block diagram of proposed model
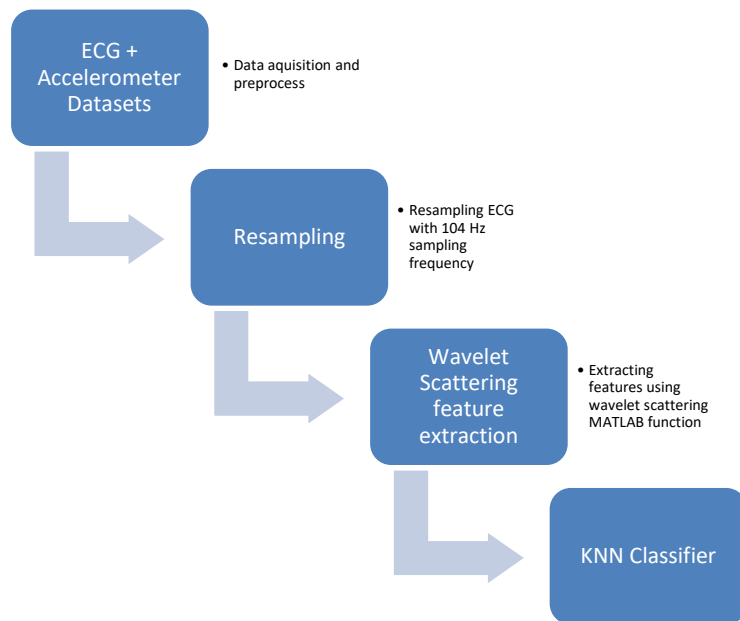
The primary objective of this chapter is to address the challenges posed by artifact— containing ECG samples through a more comprehensive feature extraction strategy. By incorporating information from both the ECG and accelerometer signals, the proposed

method aims to capture a broader range of relevant noise characteristics, thus contributing to the refinement of the classification model.

As demonstrated in Figure 3-1, a machine learning approach is introduced to train a model capable of recognizing artifact noises within ECG and accelerometer signals. The chosen machine learning technique for this task is the KNN classification method. This method is employed to train the model using features extracted from both the ECG and accelerometer signals.

A crucial aspect of the feature extraction process is the use of the wavelet scattering transform. This technique allows for the extraction of robust features by capturing information at multiple scales and providing a more resilient representation of the signal, especially in the presence of artifacts. The sampling frequency is carefully matched to ensure the compatibility of the signals before the application of the wavelet scattering transform. This chapter not only builds upon the groundwork laid in Chapter 1 but also introduces a new dimension to the classification approach. The incorporation of features from both ECG and accelerometer signals, coupled with the application of the KNN classification method and wavelet scattering transform, reflects a comprehensive and innovative strategy aimed at improving the accuracy of classifying ECG samples containing artifacts.

This chapter is structured to provide a comprehensive exploration of the research conducted. Each section is carefully designed to contribute to the reader's understanding of the study's methodology, challenges, and outcomes. The chapter unfolds as follows:

Data Acquisition Method, Protocols and Frequency Matching

Section 2.2 outlines the data acquisition process, encompassing the methods and protocols employed. It delves into the procedures undertaken to collect essential data for the study. Furthermore, this section provides an in-depth description of the frequency matching

process applied to ECG and accelerometer signals. Ensuring both signals share the same sampling frequency is a crucial step in the feature extraction process.

Signal Analysis

The analysis of acquired signals is presented in Section 2.3.This involves a meticulous examination of signal characteristics, patterns, and key features inherent in the collected data. The section provides insights into the nature of the signals under investigation.

Feature Extraction, Model Training and Test Results

In Section 2.4, the focus shifts to the training of the model and the subsequent examination of test results. This section includes a comparative analysis with previous works, offering valuable insights into the model's performance and highlighting advancements over existing approaches.

By meticulously organizing the chapter in this sequential manner, the reader is systematically guided through the various stages of the research, from the exploration of previous works to the final evaluation of the machine learning classification model. This structured narrative enhances comprehension and facilitates a cohesive understanding of the research journey.

3.2   DATA ACQUISITION METHOD AND PROTOCOLS

The acquired datasets, consisting of ECG and accelerometer data, are utilized as detailed in Section 2.1, employing the same data cleaning process facilitated by the Data Clean MATLAB tool. The captured dataset encompasses signals from the accelerometer sensor along the X, Y, and Z axes, each sampled at a frequency of 104 Hz. Simultaneously, the associated ECG signal is recorded at a sampling frequency of 125 Hz, complete with

corresponding timestamps for temporal alignment. The accelerometer dataset is composed of 309,000 samples for each of the X, Y, and Z signals, while the ECG dataset comprises 371,394 samples, as depicted in Figure 3-2.
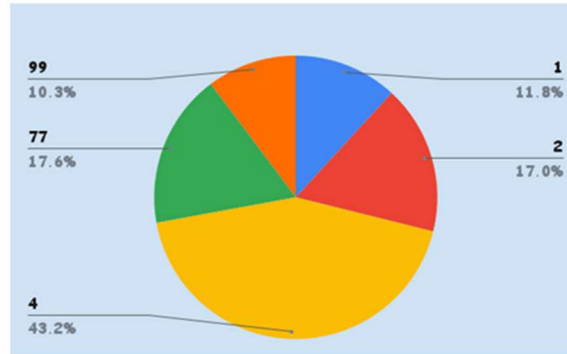
Figure 3-2. My captured dataset label distribution.

The use of consistent data cleaning procedures ensures the quality and reliability of the datasets, addressing potential artifacts or inconsistencies that may arise during data capture. The timestamps accompanying the ECG signal facilitate temporal synchronization with the accelerometer data, allowing for meaningful correlation and joint analysis of physiological and movement-related information.

The careful selection of sampling frequencies plays a pivotal role in accurately capturing the dynamics of accelerometer signals and ECG signals, both essential components for comprehensive health and activity monitoring. In this context, a deliberate choice was made to set the sampling frequency at 104 Hz for accelerometer signals and 125 Hz for ECG signals.

Commercial wearable devices often impose constraints on sampling frequencies and other parameters due to technological and resource limitations. In this scenario, the highest available sampling frequency for the accelerometer was 104 Hz, while 125 Hz emerged as the closest match for the ECG signal. This matching process was facilitated through a mobile application, allowing simultaneous capture of both signals with the aim of achieving easier frequency alignment during subsequent analysis.

By aligning the sampling frequencies, the chosen approach facilitates seamless frequency matching during subsequent stages of signal processing. This alignment is crucial for the extraction of relevant features and patterns, as it allows for a more accurate representation of the interplay between physical movements and cardiac events. This, in turn, enhances the interpretability of the data, providing a more nuanced understanding of health and activity dynamics.The considerable number of samples in both the accelerometer and ECG datasets provides a rich source of information for comprehensive analysis.

3.3   SIGNAL ANALYSIS

In Section 2.3, a comprehensive exploration was undertaken, presenting a visual and statistical examination of the impact of artifact noise on both ECG and Accelerometer signals. The analysis highlighted the deleterious effects on the the QRS complex usually contains frequencies between 8 to 50 Hz [5], although abnormal ventricular conduction complex of the ECG signal [5], illustrating the need for robust methodologies in handling such noise in signal processing.

To facilitate subsequent stages of feature extraction and model training, a strategic approach was implemented in preprocessing the accelerometer and ECG datasets. This involved partitioning the datasets into 20 distinct CSV files, each containing samples associated with a specific label. The rationale behind this segmentation was twofold: firstly, it streamlined the input data structure for compatibility with the MATLAB Classification Learner toolbox; secondly, it addressed the toolbox's preference for timetables as input datasets.

An additional preprocessing step involved resampling the ECG signal at a frequency of 104 Hz, employing the resampling tools available in the Digital Signal Processing (DSP) module of MATLAB, as elaborated in Appendix E. The resampled ECG signals were subsequently merged with accelerometer signals, creating a cohesive dataset for further analysis. The antialiasing low-pass filter employed in MATLAB is implemented as a finite

impulse response (FIR) filter [53]. FIR filters are chosen for their advantageous linear phase response and are commonly crafted using methodologies such as windowing or frequency-sampling techniques [53].

Utilizing a combination of up-sampling, antialiasing filtering, and down-sampling, this methodology allows for the alteration of the input signal's sampling rate while concurrently minimizing aliasing effects and preserving the essential characteristics of the signal [53]. By strategically manipulating the sampling rate through these sequential steps, the approach effectively mitigates the potential introduction of unwanted artifacts, ensuring the fidelity of the signal representation.

Furthermore, the linear phase response inherent in FIR filters is instrumental in maintaining the temporal relationships within the signal, a crucial aspect in applications where the timing of events is of paramount importance. This preservation of temporal coherence is vital, particularly in fields such as digital signal processing, communications, and audio processing, where the accurate representation of signal dynamics is imperative for successful analysis and interpretation.

In practical terms, the efficacy of this antialiasing technique extends to scenarios where signal processing involves diverse frequency components. By dynamically adjusting the filter cut-off frequency based on the signal's characteristics, the approach accommodates variations in the input signal, making it versatile for a wide range of applications.

Figure 3-3 illustrates a time-domain plot of the captured ECG signal, offering insights into the signal's characteristics. Notably, artifact noise becomes evident in samples labeled as "77," as highlighted in Figure 3-3(c) and Figure 3-3(d) The presence of artifacts is visually apparent as the ECG signal appears distorted, and the frequency-domain scalogram plot reveals a multitude of components.

In particular, Figure 3-3(d) presents a scalogram diagram of the captured ECG signal, with artifacts distinctly marked by red circles. These artifacts are specifically observed in samples labeled as "77," indicating a correlation between this label and the occurrence of

signal abnormalities. The scalogram's visual representation offers a comprehensive view of the signal's frequency components and the impact of artifacts.
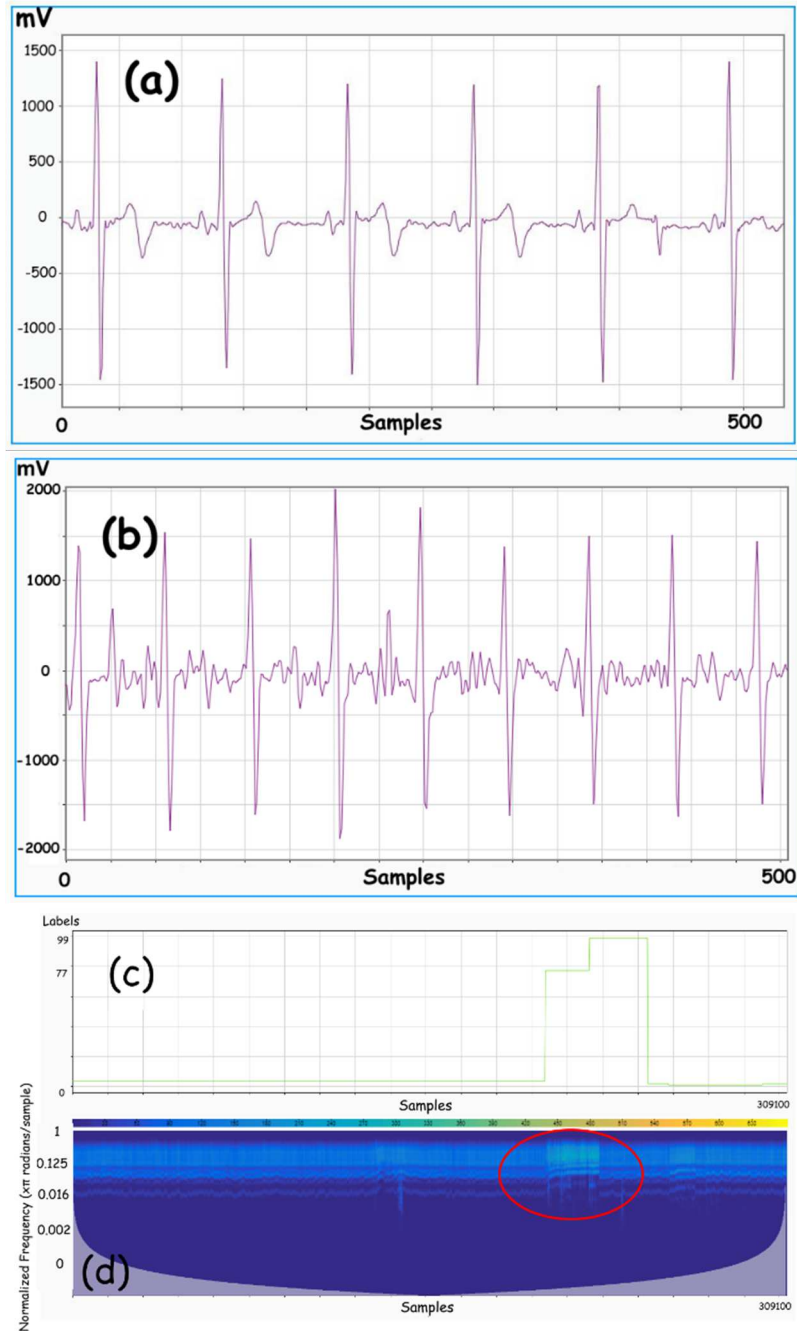

Figure 3-3.Time-domain plot of ECG signal (a) with no artifacts. (b)with artifacts and window length of 500 samples (label 77). (c) Captured dataset labels, (d) Scalogram of captured ECG signal. Artifacts are marked in red.

54

To delve deeper into the artifacts, Figure 3-3(b) provides a time-domain plot specifically focusing on 500 samples from the ECG signal labeled as "77." Both Figure 3-3(d) and Figure 3-3(b) consistently depict the distortion in the ECG signal, emphasizing the significant number of components evident in the frequency-domain scalogram plot.

These collective findings strongly suggest the presence of artifacts and signal abnormalities within the ECG data associated with the "77" label. Understanding and addressing these artifacts are critical for accurate signal analysis and subsequent classification tasks, such as those involving the use of classifiers like the K-nearest algorithm. By employing techniques like wavelet scattering transform for feature extraction, it becomes possible to enhance the robustness of feature sets, making the classification process more effective, especially in the presence of artifacts. The combination of detailed visual analysis and advanced signal processing methods contributes to a comprehensive approach in handling artifacts and ensuring the reliability of ECG data analysis.

Table 3-1 provides a comprehensive overview of the attributes associated with both clean signals, labeled as "4," and noisy signals, labeled as "77." Notably, the highest peak value is observed in the segment labeled "77," indicative of artifact noise that introduces significant amplitude signal fluctuations.

Kurtosis, a statistical measure of the distribution's tail and peak, reveals interesting insights into the nature of the signals. The Noisy ECG exhibits the lowest kurtosis value (8.8788), a metric that characterizes the degree of signal deviation from a Gaussian distribution. Artifact noise can introduce irregular and spurious peaks or distort the signal's shape, causing deviations from the expected kurtosis of a Clean ECG signal. Unusual kurtosis values may point to the presence of outliers or non-normal data points attributed to noise. Distinct patterns in kurtosis values may offer clues about the specific type of artifact noise; for instance, muscle movement artifacts could manifest as sharp, non-Gaussian peaks, while baseline drift might result in a flatter distribution with low kurtosis.

Table 3-1. An overview to characteristics of clean, noisy, filter output and final reconstructed ECG signals.

Parameter	Clean ECG (label 4)	Noisy ECG (label 77)
Mean(µV)	-59.8197	-60.4043
Peak Value (µV)	1586	2024
RMS (µV)	306.2112	441.8252
STD (µV)	298.7792	437.7131
Median (µV)	-56	-64
Shape Factor	2.0316	1.7799
Kurtosis	15.5691	8.8788
Clearance Factor	15.6746	11.8628
Band-Power 0.45 –10 Hz (%)	15.83	21.31

The clearance factor, which measures the separation between the QRS complex and the signal baseline, provides additional insights. A high clearance factor indicates well-separated QRS complexes, whereas a low clearance factor suggests poor separation. Artifact noise often compromises QRS complex visibility by introducing high-frequency components that obscure the baseline, thereby reducing the clearance factor.

As highlighted in Section 2.1, artifact noise predominantly occurs within the 0.45-10 Hz bandwidth. The "Band-power" value in Table 3-1 signifies the percentage of signal power within this frequency range relative to the total signal power spanning from 0 to 62.5 Hz (Nyquist frequency). As expected, the presence of artifact noise is reflected in an increased band-power (0.45-10 Hz) from 15.83% in the clean signal to 21.31% in the noisy signal. It is important to note that the occurrence of artifact noise can vary across different frequency ranges, contingent on the speed of body movement.

In conclusion, the detailed analysis of these attributes provides valuable insights into the characteristics of clean and noisy ECG signals, aiding in the identification and understanding of artifact noise and its impact on signal features. Such insights are crucial for developing effective signal processing and classification strategies, particularly in applications where accurate signal interpretation is essential.

3.4 FEATURE EXTRACTION, MODEL TRAINING AND TEST RESULTS

In this dedicated section, my attention pivots towards the intricate process of feature extraction from both ECG and Accelerometer 3-axis signals. This pivotal step serves as a foundation for subsequent model training and the examination of test results. Notably, the dual consideration of ECG and Accelerometer signals enriches the feature set, allowing for a more comprehensive understanding of physiological and motion-related aspects.

The feature extraction process is a critical precursor to model training, as it involves distilling meaningful information from raw signals. For ECG signals, it entails capturing essential cardiac characteristics, while accelerometer 3-axis signals contribute valuable insights into body movements and orientations. The fusion of these distinctive features aims to create a holistic representation of the underlying physiological and physical dynamics.

As the model undergoes training with the enriched feature set, the subsequent examination of test results becomes a crucial evaluation phase. This involves assessing the model's performance metrics, such as accuracy, precision, and recall, to gauge its efficacy in accurately classifying and recognizing patterns within the signals. The interpretation of these results provides valuable insights into the model's reliability and effectiveness in real-world scenarios.

Furthermore, this section incorporates a comparative analysis with existing works in the field. By benchmarking this model against previous approaches, I gain a deeper understanding of its strengths and potential areas for improvement. Comparative studies offer valuable benchmarks, shedding light on the advancements achieved over prior methodologies and establishing the model's standing within the broader research landscape.

The insights derived from the comparative analysis not only validate the model's performance but also contribute to the ongoing refinement of signal processing techniques. By identifying areas where my approach excels or diverges from earlier methods, I pave the way for continuous innovation and optimization in the realm of physiological signal analysis. This section serves as a comprehensive exploration of feature extraction from ECG and Accelerometer signals, encompassing the nuanced intricacies of model training and the meticulous evaluation of test results. The inclusion of a comparative analysis elevates the discussion, providing a holistic perspective on the model's performance and its contributions to the evolving landscape of signal processing in healthcare and motion analysis.

3.4.1 Feature Extraction

As it explained in Appendix A and Section 2.4, a noteworthy advantage of the scattering transform is its independence from learning filter responses, making it particularly applicable in scenarios where training data may be limited. This feature distinguishes wavelet scattering from some other feature extraction methods that heavily rely on extensive training datasets [[16]- [18]].

In my specific implementation, I have adopted a wavelet scattering framework that incorporates two complex-valued 1-D Morlet filter banks. The selection of specific parameters, such as an invariance scale of 40 and a sampling frequency of 104, has been

the result of consideration. The rationale behind this choice is deeply rooted in the need to strike a balance between capturing essential signal characteristics and avoiding unnecessary features that could compromise accuracy.

In the process of experimentation, it was observed that MATLAB imposes limitations on using smaller invariance scale numbers (Appendix B). A smaller scale can lead to the omission of certain signal characteristics, impacting the overall representation (Appendix A, B and Section 2.4). On the other hand, opting for a larger invariance scale introduces unnecessary features in the signal, potentially lowering classification accuracy.

Figures 3-4 (a) and 3-4 (b) visually depict the Gabor wavelets integral to my approach, along with their corresponding low-pass filter. Furthermore, Figure 3-4 (b) illustrates that the coarsest-scale wavelet consistently adheres to the invariance scale determined by the time window of the low-pass filter.

By employing the Wavelet Scattering function and carefully selecting appropriate wavelet filters, I ensure the effective extraction of relevant features. This process allows me to capture essential information from the data, forming a robust foundation for training my classification model. The integration of wavelet scattering in my approach not only enhances feature extraction but also contributes to the creation of a classification model capable of discerning intricate patterns in the presence of artifacts or noise within the signal data.

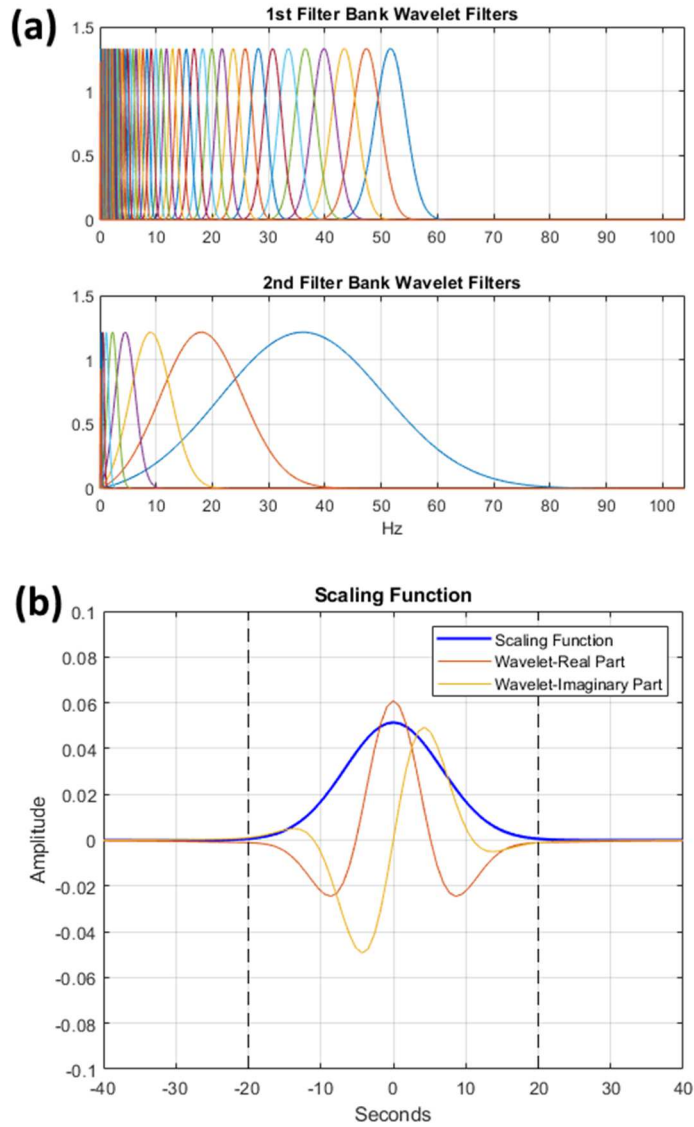**Figure 3-4. (a) Filter banks and (b) Scaling function- coarsest-scale wavelet first filter bank with invariance scale of 40 seconds.**

Table 3-2 presents a detailed overview of the captured dataset, delineating the number of samples and windows. Each window, a fundamental unit of analysis, comprises 261 scattering paths. These paths contribute collectively to the holistic feature representation of the data.

Table 3-2. Number of samples and corresponding windows for each signal (Accelerometer and ECG).

Label	Number of samples for each signal	Number of windows
1	36462	36
2	52530	52
4	133488	131
77	54384	54
99	31827	32

3.4.2 Results and Discussions

The fine KNN model underwent training utilizing wavelet scattering coefficients extracted from the 3-axis accelerometer and ECG raw datasets, as detailed in Section 2.5 and Appendix C. The Classification Learner toolbox in MATLAB [82] was employed for importing all scattering coefficients. Subsequently, the dataset was split into training (75%) and testing (25%) subsets to facilitate model training and evaluation. By importing the scattering coefficients into the Classification Learner as a table, effective data manipulation within the toolbox was ensured.

In practical applications, the proposed model aims to classify labels and identify ECG artifacts within vital sign monitoring systems. The model is adept at efficiently processing and analyzing data collected over short time spans. Its application is particularly valuable for detecting and filtering out or removing artifact noises present in vital sign monitoring systems, thereby enhancing the accuracy and reliability of recorded data for medical diagnosis.

While ECG signals are typically captured in stable clinical environments for enhanced diagnostic accuracy, existing works often focus on classifying noisy and clean ECG signals rather than specifically detecting motion artifacts in ECG signals [[56], [57]]. For instance, in [59], a balanced dataset (50:50) comprising acceptable (clean) and unacceptable (noisy) ECG signals was used with a convolutional neural network (CNN) for classification. Their deep learning model successfully screened 88% of noisy signals. Another approach proposed in [60] involved a robust technique based on signal decomposition on mixed codebooks. This method addressed the challenge of extracting ECG waves and identifying

61

various ECG noises, achieving a classification accuracy of 97.19%. However, it is worth noting that this technique was not specifically designed for detecting or classifying artifact noises.

In a different study [61], a model was proposed to classify artifacts with an impressive accuracy of 96.87% using a KNN classifier. However, this model segmented ECG signals into 5-second intervals, which may be less suitable for clinical diagnosis purposes, as artifacts can manifest in smaller segments. The adaptability and versatility of the proposed method in addressing artifacts in various vital signals, along with its potential for real-time application, position it as a valuable contribution to the field of signal processing and medical diagnostics.

In this research, the proposed KNN model takes a distinctive approach, incorporating a robust methodology for evaluation. The model leverages a 5-fold cross-validation strategy, considering 1 nearest neighbor and utilizing the Euclidean distance metric. Impressively, this model achieves a commendable test accuracy of 98.8%. Figure 3-6 presents the test confusion matrix, offering insights into the model's performance across various classes.

It is noteworthy that the class labeled "4" attains the highest prediction accuracy. This outcome may be attributed to the class having the largest number of samples, indicating a potential challenge in dealing with imbalanced datasets. To delve deeper into the model's performance metrics, the TPR is examined, representing the proportion of correctly classified observations per true class. Simultaneously, the FNR indicates the proportion of incorrectly classified observations per true class.
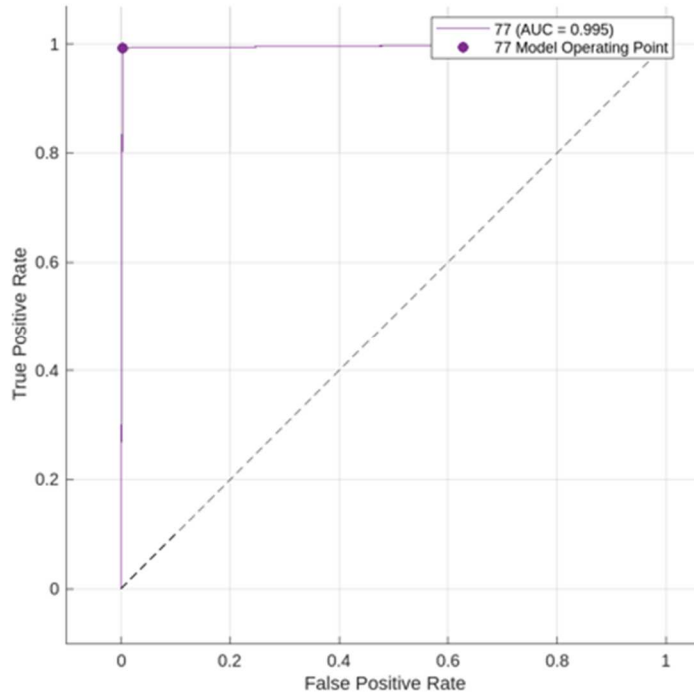
Figure 3-5. Test ROC curve of label 77.

This comprehensive evaluation of the proposed KNN model sheds light on its strengths and weaknesses across various classes, providing valuable insights for refining and optimizing the model's performance in future iterations. The consideration of class-specific metrics offers a nuanced understanding of the model's behavior, allowing for targeted improvements and ensuring its effectiveness across diverse scenarios.

ROC is a valuable graphical representation that contrasts the TPR against the FPR at various classification score thresholds. This visualization serves as a crucial tool for assessing the effectiveness of a classifier in distinguishing between different classes. An additional metric derived from the ROC curve is the AUC, which offers a quantitative measure of the classifier's overall performance.

The AUC values range from 0 to 1, where higher values signify superior classification performance. In the context of Figure 3-5, which depicts the ROC curve specifically for the "77" label, the calculated AUC value is an impressive 0.995. This high AUC value is indicative of excellent classification performance, particularly for labels associated with

artifact noises (77). The model, therefore, demonstrates a remarkable ability to discriminate instances of the "77" label from other classes.

For the class labeled "77," the TPR impressively reaches 99.3%, underscoring the model's proficiency in correctly identifying instances within this category. Conversely, the highest false negative rate (2.9%) is observed for the class labeled "99." Figure 3-6(b) further elucidates the prediction performance across different classes, revealing nuances in the model's predictive accuracy.

Surprisingly, despite the overall high accuracy, the class labeled "4" exhibits the poorest prediction values. Additionally, the class labeled "2" stands out with the highest FDR, highlighting areas for potential improvement in the model's precision within this particular class.

The significance of a high AUC value lies in the model's capacity to effectively balance sensitivity and specificity, crucial in scenarios where accurate classification amidst noise or artifacts is essential. The robust performance observed in the ROC curve and the corresponding AUC value suggests that the model exhibits a high level of precision in distinguishing instances of the "77" label, thus contributing to its overall efficacy in handling artifact noises.

It is worth noting that while the AUC is a valuable summary metric, examining the ROC curve itself can provide additional insights into the trade-offs between sensitivity and specificity at different decision thresholds. This comprehensive evaluation ensures a nuanced understanding of the classifier's behavior, facilitating informed decisions in the context of the specific application or dataset under consideration.

Figure 3-6. Test confusion matrix of the trained/tested KNN model with wavelet scattering coefficients(a) TPR (true positive rate) vs FNR (false negative rate) (b) PPV (positive predictive value) vs FDR (false discovery rate).

The proposed methodology has demonstrated remarkable success, achieving a test classification accuracy of 98.8%. This exceptional result underscores the effectiveness of my approach in handling the complexities of the input data. My method primarily harnessed raw signals obtained from accelerometers and ECG measurements as the input dataset. However, this initial dataset posed a challenge due to an inherent imbalance in the distribution of classes.

To overcome this class distribution imbalance, a critical preprocessing step involved the extraction of wavelet scattering coefficients as features from the accelerometer signals. This step not only addressed the class distribution issue but also enriched the dataset with discriminative features capable of capturing nuanced patterns, particularly in the presence of artifact noise in ECG signals.

The utilization of wavelet scattering coefficients as features for model training proved to be a pivotal decision. This feature extraction technique excels in preserving important signal characteristics while mitigating the impact of noise and artifacts. The resultant high classification accuracy achieved in this study serves as a testament to the robustness and efficacy of my approach in accurately classifying ECG artifact noise.

Furthermore, it is noteworthy to highlight the adaptability of the proposed method to handle diverse challenges in signal processing. The raw signals from accelerometers and ECG, although initially presenting an imbalance, were successfully transformed into a feature-rich dataset that significantly improved the model's ability to discern subtle variations and accurately classify instances of artifact noise in ECG signals.

In conclusion, the comprehensive integration of raw signal utilization, wavelet scattering feature extraction, and a strategic approach to addressing class distribution imbalances has proven to be a winning combination. The achieved high classification accuracy not only affirms the success of the proposed methodology but also positions it as a promising solution for robust signal processing applications, particularly in scenarios where accurate classification of ECG artifact noise is paramount.

3.5 SUMMARY

In this chapter, a novel machine learning approach design is introduced for the detection of artifact noises in ECG signals. The employed methodology leverages a KNN machine learning model trained with wavelet scattering coefficients extracted from both accelerometer and ECG signals. This innovative approach was chosen to enhance the model's ability to discern subtle patterns indicative of artifacts in complex physiological data.

The evaluation of the trained model yielded highly promising results, demonstrating a remarkable test accuracy of 98.8%. Notably, PPV for samples specifically labeled with artifact noises (denoted as "77") reached an impressive 98.6%. These compelling outcomes suggest the potential efficacy of the proposed model as an advanced artifact recognition technique.

The success of this model opens up exciting possibilities for its application in vital sign monitoring devices, including EEG, PPG, and ECG devices. Integrating this model into such devices holds the promise of significantly improving their functionality by effectively filtering out unwanted artifact noises. This enhancement is anticipated to elevate the accuracy and reliability of vital sign measurements, which is crucial for ensuring the precision of diagnostic and monitoring tools in healthcare settings.

In conclusion, the introduced machine learning approach represents a significant step forward in artifact noise detection within physiological signals. Its successful implementation and impressive performance metrics position it as a promising tool for improving the accuracy and reliability of vital sign monitoring devices, with broader applications in the realm of healthcare technology.

CHAPTER 4   A ROBUST TWO-STEP APPROACH TO ECG ARTIFACT NOISE REDUCTION

4.1 INTRODUCTION

In this chapter, a comprehensive two-step denoising approach is introduced to address motion artifact noise in ECG signals. Beyond noise reduction, the chapter delves into the realm of ECG signal compression, aiming to not only cut costs but also significantly enhance the efficiency of signal processing. The primary objective is to showcase the superiority of integrating denoising and compression techniques within the context of clinical practice, thereby achieving both improved denoising performance and enhanced compression capabilities.

Figure 4-1. Integration Diagram of Proposed System (using Wavelet signal denoiser + DAE)
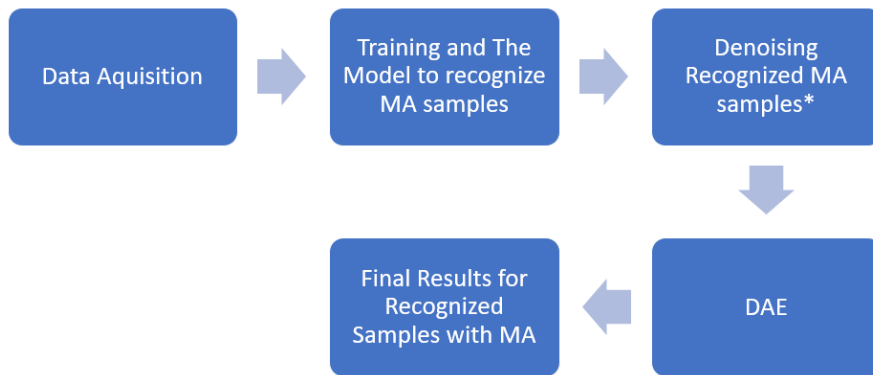
As it demonstrated in Figure 4-1, building on the foundation laid in Chapter 3, where a robust ML classification algorithm was developed to identify ECG samples affected by artifact noise, this chapter focuses on a novel denoising algorithm. The proposed algorithm leverages the power of a DAE architecture to effectively compress ECG signals. By employing a synergistic denoising strategy that combines a Bior wavelet filter with the advanced capabilities of a denoising autoencoder model, the algorithm becomes adept at classifying and denoising ECG signals contaminated by artifact noise.

The incorporation of a Bior wavelet filter adds an additional layer of sophistication to the denoising process, enabling the extraction of pertinent features across different scales in the ECG signal. The denoising autoencoder model complements this by learning intricate

patterns and representations inherent in the signal, enhancing the algorithm's ability to discern and mitigate artifact-induced noise.

The denoising process is pivotal for the subsequent steps in ECG signal analysis. By effectively classifying and denoising ECG signals contaminated by artifact noise, the algorithm ensures a cleaner representation of the initially noisy training dataset. This cleaner representation not only facilitates more accurate analysis and diagnosis in clinical settings but also contributes to the creation of a robust foundation for downstream applications, such as real-time monitoring and predictive modeling.

This chapter introduces a sophisticated two-step denoising approach, emphasizing the integration of motion artifact noise reduction and ECG signal compression. Through the utilization of a Denoising Autoencoder architecture and a Bior wavelet filter, the proposed denoising algorithm demonstrates its efficacy in enhancing signal quality, thereby advancing the capabilities of clinical ECG signal processing.

This chapter is thoughtfully organized to offer a thorough exploration of the conducted research. The progression unfolds in a structured manner, delving into various key aspects of the study.

Theoretical Basis of Method:

Section 4.2, delves into the theoretical foundations that underpin the proposed methodology. This includes a detailed explanation of the employment of the wavelet bior denoiser (4.2.1) and the denoising autoencoder (4.2.2). The combination of these two methods serves as a two-stage process designed to effectively eliminate artifact noise in ECG signals, ensuring a high-performance outcome. This section provides a comprehensive understanding of the methodologies employed and their synergistic application to enhance signal quality.

Data Preparation:

Section 4.3 focuses on the critical phase of data preparation. The acquired signals undergo a meticulous analysis, involving an in-depth examination of signal characteristics and the identification of key features inherent in the collected data. This section not only sheds light on the nature of the signals under investigation but also offers a detailed analysis of

noise behavior within the signal. Understanding these nuances is pivotal for subsequent stages in the research.

Training the Model:

In Section 4.4, the narrative shifts towards the training of the model, a pivotal stage in the research journey. The subsequent examination of test results in 4.1.1 provides valuable insights into the model's efficacy. This section includes a comparative analysis with previous works, establishing a benchmark for the model's performance. By highlighting advancements over existing approaches, the novel contributions of this research is showcased, offering a deeper understanding of the model's capabilities.

Throughout these sections, the chapter aims to provide a comprehensive and detailed account of the research methodology, from its theoretical underpinnings to the practical implementation and evaluation. The meticulous structure ensures clarity and coherence, allowing readers to navigate through the intricacies of the research process with a clear understanding of each stage's significance.

4.2   THEORETICAL BASIS OF METHOD

The ECG waveform serves as a graphical representation of the intricate depolarization and repolarization processes within the heart. The His-Purkinje system, known for its remarkable conduction velocity of 2-4 m/sec, plays a pivotal role in the rapid transmission of electrical impulses through the ventricles, resulting in the swift movement of the QRS complex on an ECG and the formation of a QRS loop on a vectorcardiogram [62]. Responsible for the expeditious electric conduction in the ventricles, the His-Purkinje System (HPS) coordinates the contraction of ventricles, ensuring efficient cardiac pump function by relaying electrical impulses from the atrioventricular node to the muscle cells [64].

In contrast, the atria exhibit a slower conduction velocity, typically ranging from 0.5 to 1 m/sec. The activation propagation through the atria gives rise to the P-wave on the ECG or the P-loop on the vectorcardiogram. Repolarization, occurring at a much slower rate, contributes to the formation of the slow-deflecting T-wave (or T-loop) [64]. The varied speeds of wavefront propagation throughout the cardiac cycle correspond to different frequency components present in the ECG waves. T-wave content is concentrated within frequencies from zero (DC) to 10 Hz, P-wave content exhibits frequencies ranging from 5 to 30 Hz, and the QRS complex typically encompasses frequencies between 8 to 50 Hz, with abnormal ventricular conduction possibly reaching frequencies above 70 Hz, resulting in notches on the QRS complex [63].

For accurate cardiac vascular disease diagnosis, medical experts require clean and complete QRS complexes[64]. This necessity underscores the challenge posed by the presence of artifact noise in wearable ECG monitoring devices, which renders the acquired signals unsuitable for medical purposes. To address this, I propose a robust method for recognizing and classifying artifact noises. Electrode motion artifacts, often induced by skin stretching altering the skin's impedance, resemble baseline wander in their signal characteristics. These artifacts, prevalent in the frequency range of 1 to 10 Hz, manifest as large-amplitude waveforms sometimes mistaken for QRS complexes in the ECG [5].

Attempting to remove these noises from the original signal involves reconstructing the signal, as traditional filters are ineffective due to the wide-ranging frequency spectrum and high amplitude of artifacts. However, my results indicate that reconstruction is not a foolproof solution. The substantial noise introduces signal corruption and distortion, making it challenging or impossible to achieve successful reconstruction. This highlights the complexity and importance of addressing artifact noise in ECG signals for accurate and reliable medical diagnosis.

4.2.1 Wavelet Bior Denoiser

The application of Biorthogonal (Bior) wavelet filters, a subset of wavelet filters, presents a powerful approach for mitigating artifact noise in ECG signals through wavelet denoising

techniques. Within the realm of wavelet families, biorthogonal wavelets stand out due to their distinctive characteristics, featuring one scaling function (father wavelet) and one wavelet function (mother wavelet). Unlike other wavelet families such as Daubechies (db) or Symlet (sym) wavelets, Bior wavelets demonstrate remarkable proficiency in temporal localization, rendering them highly effective in capturing short-duration features or transient events within the signal with exceptional accuracy [26].

In the context of ECG signals, preserving the sharp, short-duration features, such as the QRS complex, is pivotal for accurate diagnosis. While Bior wavelets exhibit remarkable time localization capabilities, they display relatively poorer frequency localization compared to other wavelet families. This characteristic can present challenges in precisely distinguishing between various frequency components within the signal, particularly when addressing noise that is concentrated within specific frequency bands [26].

The wide frequency support of Bior wavelets, coupled with their proficiency in capturing fine temporal details of ECG waveforms, makes them well-suited for preserving diagnostic features [26]. MATLAB, a widely used computational tool, offers a dedicated wavelet signal denoiser that leverages the strengths of Bior wavelets for mitigating motion artifact noise in ECG signals.

The denoising process involves decomposing the ECG signal into a series of wavelet coefficients, each corresponding to different frequencies and time scales. This decomposition is facilitated by the wavelet transform, a mathematical technique that serves as the foundation for the denoising procedure. The MATLAB wavelet signal denoiser employs a judicious thresholding step, eliminating noise coefficients while retaining those crucial for representing the ECG signal [84]. The denoised ECG signal is then reconstructed based on the retained wavelet coefficients.

The efficacy of the MATLAB wavelet signal denoiser, especially in reducing noise in ECG signals, has been substantiated in a study featured in the journal "Computers in Cardiology" [65]. In this study [65], the authors examined algorithms designed to filter white Gaussian noise and 50 Hz power line noise from ECG signals. Utilizing various wavelets, they investigated the impact and efficacy of these wavelet selections on the filtering procedure.

Notably, this denoiser surpassed traditional band-pass filters in effectively eliminating motion artifact noise from ECG signals.

Specifically, the Bior 1.1 wavelet filter, a representative of biorthogonal wavelet filters, demonstrates its effectiveness in noise removal across a broad spectrum of frequencies. Implementing a seven-level decomposition scheme, Bior 1.1 breaks down the signal into seven distinct levels of detail. Throughout this process, the lowpass coefficients of the initial level of detail are retained, while the high-pass coefficients are discarded. This iterative filtration process enhances the adaptability of Bior 1.1 in handling signals with diverse frequency components, making it a valuable tool for comprehensive noise removal in ECG signals [84].
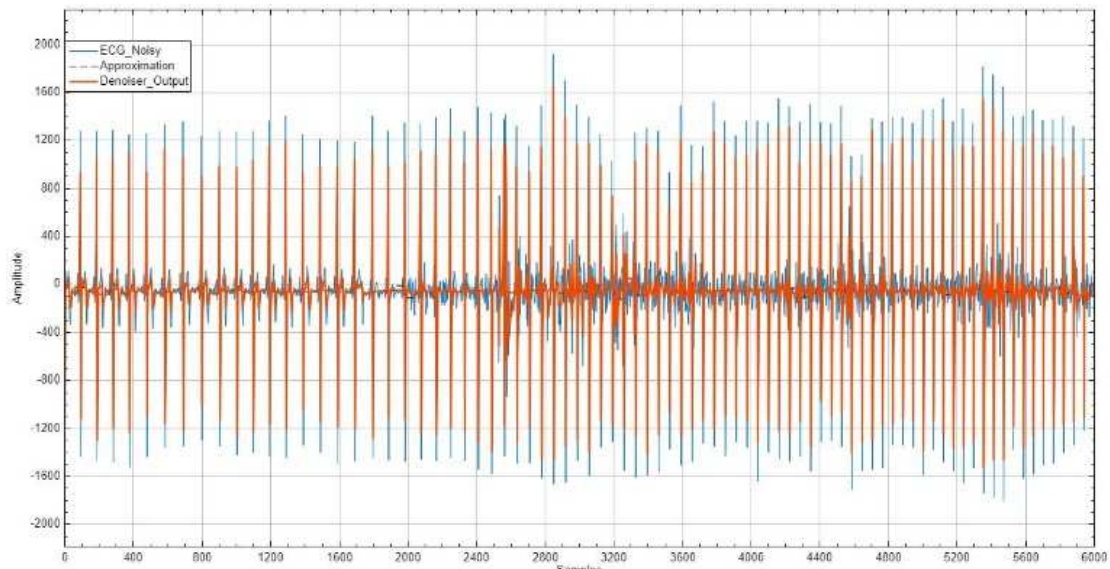
Figure 4-2. Original ECG signal with artifact noise (blue) vs denoised signal using wavelet signal denoiser (red) – 6000 samples.
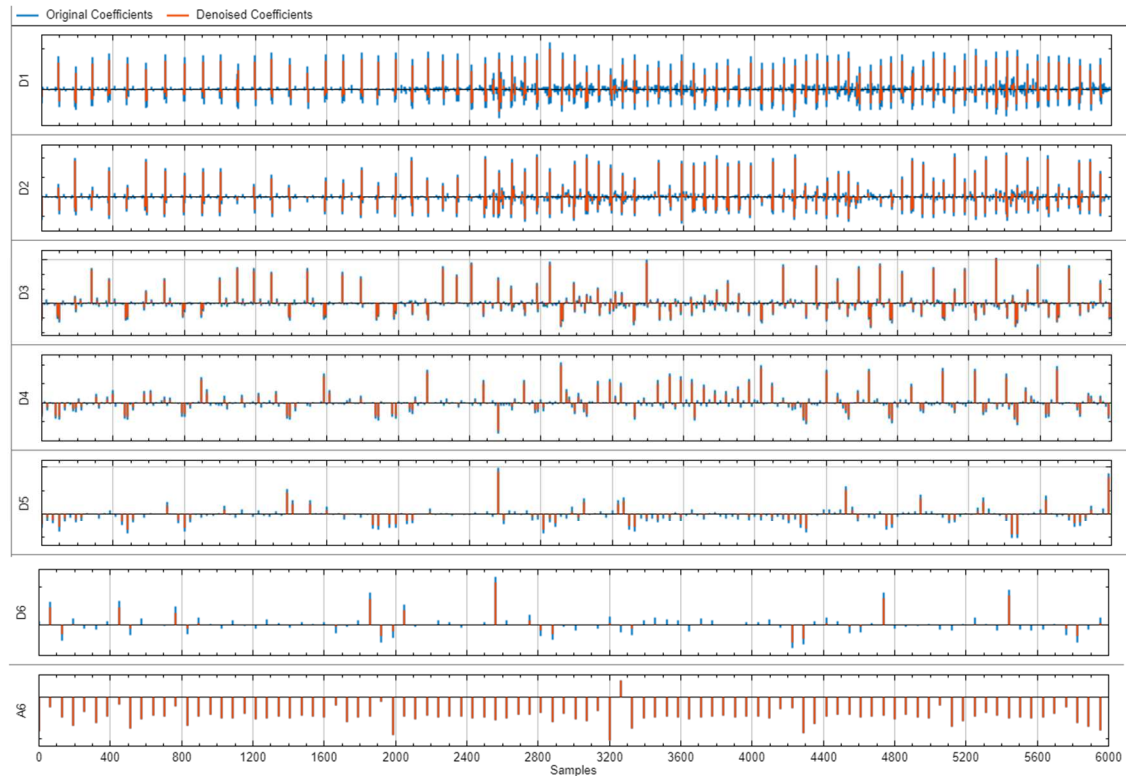
Figure 4-3. Coefficients extracted using MATLAB wavelet signal denoiser (Original vs Denoised ECG signals).

The demonstrated efficacy of the Bior 1.1 wavelet filter in mitigating a spectrum of noise types, including baseline wander, muscle noise, and power line interference, highlights its robust suitability for comprehensive noise reduction in ECG signals [26]. Employing the Bior 1.1 filter and the universal threshold denoising method in MATLAB, with specific parameter configurations (level = 6, soft threshold rule, and Q-value = 0.05), the ECG signal underwent a processing phase. The results, depicted in Figures 4-2 and 4-3, showcase the original and denoised signals alongside the extracted coefficients. The choice of a decomposition level of 6 is pivotal, as it enables the signal to be decomposed into six distinct levels, facilitating a comprehensive multi-resolution analysis. This analysis, conducted to capture details at various scales, strikes a delicate balance between preserving relevant signal information and removing noise. The careful consideration of this parameter is crucial, as excessively large values risk distorting the signal shape, emphasizing the importance of finding an optimal decomposition level. Soft thresholding,

a key component of the denoising method, plays a vital role in shaping the denoised signal. This technique tends to produce smoother results by aggressively shrinking smaller coefficients more than their larger counterparts. Its suitability for signals with sparse representations makes it an apt choice for ECG signals, where preserving the integrity of the signal's essential features is paramount. The Q-value, another significant parameter in this denoising process, exercises control over the threshold value and holds a crucial role in distinguishing signal from noise. A lower Q-value corresponds to a higher threshold, leading to a more assertive removal of noise. This dynamic interplay between the Q-value and thresholding contributes to the precision of the denoising process.

In the quest for an optimal balance between effective noise reduction and the preservation of vital ECG signal features, the chosen characteristics, including the specific filter, level of decomposition, soft thresholding, and Q-value, collectively form a tailored approach. This approach ensures that the denoising process achieves its goal of enhancing signal clarity while mitigating the impact on crucial ECG signal characteristics.

The primary objective of this processing was to effectively reduce noise levels, particularly those characterized by high amplitudes, while simultaneously minimizing any potential loss of information within the ECG signal. The next step involves the reconstruction of the signal using a DAE to address any alterations that may have occurred during the initial filtering phase.

Within the MATLAB wavelet signal denoiser, I benefit from the flexibility to fine-tune parameters, tailoring the noise reduction process to meet specific requirements. For instance, should the goal be to further eliminate noise, adjustments such as increasing the number of decomposition levels or raising the threshold value can be explored. However, it is crucial to note that as these parameters are elevated, there is a simultaneous reduction in the level of detail present in the signal, as highlighted in previous studies [26].

4.2.2 Denoising Autoencoder

Autoencoders

Autoencoders represent a specific class of neural networks widely employed in unsupervised learning tasks, with a notable application being denoising. Unsupervised learning, synonymous with unsupervised machine learning, involves machine learning algorithms analyzing and clustering unlabeled datasets. This process enables the discovery of concealed patterns or data groupings without the need for human intervention. In the denoising context, autoencoders play a crucial role by learning to reconstruct clean versions of noisy input data through the acquisition of a compressed representation of the underlying structure.

MATLAB serves as a convenient environment for the implementation and training of autoencoders, facilitating the exploration of various architectures and training strategies. The theoretical foundation of autoencoders for denoising is grounded in the principles of dimensionality reduction and reconstruction. The fundamental concept involves training an autoencoder to encode and decode data with the primary goal of minimizing the disparity between the original input and the reconstructed output. This process empowers the autoencoder to discern the essential features of the data while effectively filtering out undesirable noise.

Here is a high-level overview of the autoencoder denoising process in MATLAB:

Data Preparation:

As a preliminary step, prepare a dataset containing pairs of clean input data and their corresponding noisy versions. These paired instances serve as the training set for the autoencoder.

Network Architecture:

Define the architecture of the autoencoder within MATLAB [83], specifying the number and sizes of layers. Typically, an autoencoder comprises an encoder and a decoder, with one or more hidden layers facilitating the compression of input data and subsequent reconstruction.

Training:

Initiate the training phase by utilizing the noisy input data as both input and target output. The training objective is to minimize the disparity between the input and output, necessitating the adjustment of network weights and biases through optimization algorithms like stochastic gradient descent (SGD).

Noise Removal:

Once trained, the autoencoder transforms into a valuable tool for denoising new input data. The noisy data is fed into the trained autoencoder, which encodes it into a compressed representation before decoding to yield the denoised output.

The crux of the denoising capability lies in the autoencoder's ability to extract meaningful features from noisy input during training. The minimization of reconstruction error ensures effective noise filtration, resulting in the production of a clean version of the input. While autoencoders, with well-designed architectures and training strategies, exhibit effectiveness in denoising tasks, their performance hinges on factors such as the quality and diversity of training data, as well as network architecture and hyperparameters. Hence, a degree of experimentation and tuning is often requisite to attain the desired denoising performance.

Denoising Autoencoders

Motion artifacts pose a significant challenge in the analysis of ECG signals due to their wide frequency spectrum, often overlapping with the frequency range of the ECG signal itself. Filtering out motion artifacts without inadvertently removing crucial components of the ECG signal is a complex task. These artifacts manifest as large-amplitude waveforms, occasionally resembling QRS complexes, making it challenging to utilize such samples for accurate medical diagnostics.

In addressing motion artifacts, one commonly used approach involves Denoising Autoencoders (DAEs), which are neural network-based denoising techniques. However, DAEs are typically chosen for their time-domain denoising capabilities rather than their frequency localization characteristics. Unlike wavelet-based methods, DAEs do not

inherently possess the ability to precisely identify and isolate noise in specific frequency bands (Appendix D).

Wavelet-based methods, renowned for their dual-domain analysis in both time and frequency, offer a contrasting advantage. This becomes particularly crucial when dealing with ECG signals contaminated with artifact noise exhibiting specific frequency characteristics. Wavelets effectively isolate and attenuate noise components within defined frequency bands while preserving essential ECG features.

In contrast, DAEs focus on learning data-driven representations of signals in the time-domain, often lacking the precision required for isolating noise in specific frequency bands. However, this characteristic aligns with the challenge presented by motion artifacts, which have a widespread frequency spectrum.

DAEs are commonly employed for general noise reduction and feature preservation, prioritizing broader applications over precise frequency localization. Within the realm of signal processing and image restoration, autoencoders, in general, have gained significant popularity. A notable contribution is the denoising autoencoder introduced by Vincent et al. [27], which intentionally introduces noise into the initial input data. This unique approach enhances the model's resilience by minimizing the discrepancy between output and input data.

The DAE stands out as an optimal choice for the reconstruction and denoising of ECG signals contaminated with motion artifact noises, owing to several key attributes:

Non-linearity Handling:

DAEs excel in capturing non-linear relationships within data. Given the inherent complexity of ECG signals and their propensity to exhibit non-linear patterns, the application of a DAE becomes particularly effective. This capability allows the model to adeptly capture and model intricate features present in the signals.

Feature Learning:

One of the notable advantages of DAEs is their ability to autonomously learn relevant features from input data during the training process. In the context of ECG signals with motion artifacts, which may display diverse and complex patterns, this feature learning capability proves invaluable. The model automatically identifies and adapts to the intricate features within the data.

Robust to Noise:

The primary objective of a DAE is to reconstruct input signals from their corrupted versions, inherently rendering them robust to noise. By learning to reconstruct signals despite the presence of motion artifact noises, DAEs effectively contribute to the denoising of ECG signals, ensuring the preservation of essential information.

Adaptability:

DAEs exhibit a high degree of adaptability to variations in input data, enabling them to handle different levels and types of noise. This adaptability is particularly critical when working with real-world ECG signals, which may exhibit diverse noise characteristics. The model's ability to adapt ensures robust performance across varying signal conditions.

Reduced Dimensionality:

The latent representation learned by DAEs not only captures essential information but also discards noise. This reduction in dimensionality facilitates a more focused representation of the signal, thereby aiding in the effective removal of noise. The model can distill the crucial aspects of the signal while minimizing the impact of unwanted artifacts.

Training on Noisy Data:

DAEs follow a training paradigm involving noisy input and clean target pairs. This approach is instrumental in teaching the model to distinguish between signal and noise. By exposing the DAE to a variety of noisy input scenarios during training, the network

develops a robust understanding of noise patterns, enabling it to generalize well to denoise unseen signals effectively.

In conclusion, the Denoising Autoencoder emerges as a powerful tool for ECG signal denoising, leveraging its capacity to handle non-linearities, learn intricate features, and exhibit robustness to noise. These attributes make DAEs well-suited for real-world applications, where ECG signals often exhibit complex patterns and may be affected by various types of noise, such as motion artifacts.

4.3 DATA PREPARATION

The data acquisition and preparation process followed the methodology detailed in Section 3.2. ECG signals were acquired using the MAX ECG monitoring device, and subsequent preprocessing steps were applied to ensure data quality. After preprocessing, the dataset was organized and segmented into distinct CSV files based on the corresponding labels assigned to each signal.

Specifically, 6000 samples were selected for analysis, encompassing two main categories: clean signals labeled as '4' and signals with artifacts labeled as '77.' This deliberate selection allowed for a focused investigation into the variations present in the signals concerning bandpower, time-domain features, frequency-domain characteristics, and other relevant signal attributes.

The choice of these specific labels facilitates a targeted exploration of signal differences, providing insights into how the presence of artifacts impacts various signal properties. This detailed analysis is essential for understanding the effects of artifacts on ECG signals and aids in devising effective signal processing and classification strategies.

Moreover, the segmentation of the dataset into clean and artifact-laden signals enables a comparative study, shedding light on the distinctive features associated with each signal type. Such an approach is crucial for developing robust algorithms and classifiers capable of accurately distinguishing between normal and artifact-affected ECG signals.

This well-defined dataset, organized by labels, not only streamlines the analytical process but also serves as a valuable resource for future studies and benchmarking. The systematic

exploration of bandpower, time-domain, and frequency-domain characteristics across these carefully selected samples contributes to a comprehensive understanding of the signal properties, laying the foundation for informed decision-making in signal processing tasks.

4.4 TRAINING THE MODEL

Motion artifacts present challenges in ECG signal processing due to their similarity to baseline wander, but mitigating these artifacts is a more complex task. The spectral content of motion artifacts significantly overlaps with that of the PQRST complex, posing a considerable challenge for effective removal. Typically manifesting in the frequency range of 1 to 10 Hz, motion-related disturbances in ECG recordings often arise from activities such as breathing, minor body movements, and muscle contractions [[70],[71]].

While most motion artifacts are found within the 0.1 to 10 Hz range, there are exceptions, particularly during vigorous or rapid movements, where the noise may extend beyond 10 Hz. However, this higher-frequency noise is generally considered less substantial compared to the lower frequency range. Notably, in my observations, artifact noises in the specific case have been identified reaching up to 100 Hz in frequency, highlighting the importance of understanding and characterizing the nature of the movement [[70],[71]].

To address the challenge of motion artifact removal, I employed a denoising autoencoder implemented in MATLAB. This denoising technique utilizes the principles of unsupervised learning and optimization to acquire a condensed representation of the clean ECG signal while effectively eliminating noise. During the training phase, the denoising autoencoder aims to minimize the loss function, a task typically achieved through gradient-based optimization methods. To facilitate the training process, MATLAB provides built-in functions such as 'trainAutoencoder' or 'trainNetwork,' which handle the intricacies of backpropagation and parameter updates, streamlining the implementation and training of DAEs in MATLAB [83].

The denoising autoencoder was trained on a workstation using MATLAB R2022. This robust training environment ensures the efficient processing and optimization required for

achieving precise reconstruction of ECG signals, free from motion artifacts. The successful implementation of denoising autoencoders in MATLAB serves as a valuable tool in enhancing the quality of ECG data, especially when confronted with challenges posed by motion artifacts.

Training a DAE involves a series of computational steps, primarily centered around the backpropagation of gradients and the subsequent adjustment of model parameters using optimization techniques such as gradient descent. This iterative process refines the weights and biases of the DAE by considering the gradients of the loss function with respect to these parameters. The overarching goal is to iteratively update the model's parameters to converge towards values that minimize the loss function, thereby enhancing the denoising performance of the autoencoder.

Gradient descent, a widely employed optimization method in DAE training and various other neural network models, plays a pivotal role in this process. It systematically adjusts the model's parameters, fine-tuning them to reach optimal values that lead to improved denoising capabilities.

In the specific context of the proposed Denoising Autoencoder, I've chosen the 'satlin' transfer function for the encoder and 'purelin' for the decoder. These transfer functions define how the input information is transformed at each layer of the autoencoder. Additionally, L2 weight regularization with a factor of 0.01 is incorporated to prevent overfitting, and sparsity regularization with a coefficient of 4 is applied to encourage sparsity in the network.

Moreover, a sparsity ratio of 0.1 is set to control the level of sparsity within the hidden layers of the autoencoder. The architecture of the DAE comprises 75 hidden layers, a design choice that can influence the model's capacity to learn complex representations of the input data. The training process is executed over a maximum of 500 epochs, allowing the model to learn and adapt over multiple iterations.

The selection of the 'satlin' transfer function for the encoder in the DAE is a strategic choice aimed at introducing saturation and enabling the network to learn intricate non-linear relationships within the data. This function proves effective in capturing complex patterns present in the input signal, thereby enhancing the model's capability to represent the

underlying structure of ECG data. On the other hand, the 'purelin' transfer function is judiciously chosen for the decoder due to its linear nature, ensuring that the decoder's output is a direct linear transformation of the hidden layer. This characteristic facilitates the reconstruction of the denoised signal.

To prevent overfitting, L2 weight regularization is applied, penalizing large weight values. The chosen regularization factor of 0.01 strikes a delicate balance between encouraging the network to learn meaningful features and preventing it from fitting noise present in the training data. This parameter choice aligns with recommendations from MATLAB. Sparsity regularization further contributes to the DAE's effectiveness by encouraging the learning of sparse representations. With a coefficient of 4, the emphasis is placed on having a small number of active neurons in the hidden layers. This promotes a more compact and efficient representation of the input signal, as suggested by MATLAB. Additionally, a sparsity ratio of 0.1, as recommended by MATLAB, sets the target level of sparsity within the hidden layers, aiding in controlling the activation of neurons and promoting a sparse representation [83].

The decision to incorporate 75 hidden layers in the DAE architecture is deliberate, aiming to enhance the model's capacity to learn intricate representations of the input data. A deeper network allows for more hierarchical and abstract feature learning, capturing complex patterns within the ECG signal. The chosen range of hidden layers, spanning from 25 to 100, was explored to determine the value yielding optimal performance.

In terms of training parameters, the DAE undergoes training for a maximum of 500 epochs, providing sufficient iterations for the model to adapt and learn from the input data. Notably, peak performance is achieved at epoch 56, indicating that the DAE effectively denoises the input data.

It is noteworthy that during training, the performance of the DAE is assessed using a performance metric, and in this case, the peak training performance reached 32.5748 at epoch 56. This metric serves as a quantitative measure of how well the DAE is denoising the input data, with higher values indicating better performance. The epoch at which the peak performance is achieved provides insights into the convergence and effectiveness of the training process.

83

The training of a Denoising Autoencoder involves a thoughtful selection of parameters, transfer functions, and regularization techniques to optimize denoising performance. The iterative nature of the process, driven by gradient descent, allows the model to adapt and improve its ability to reconstruct clean data from noisy inputs. The specific choices made in the proposed DAE, such as the transfer functions and regularization parameters, contribute to its unique characteristics and denoising capabilities.

4.4.1 Results and Discussions

Table 4-1 offers a comprehensive overview of attributes associated with various stages of ECG signal processing, including the clean signal (labeled as 4), the noisy counterpart (labeled as 77), the output after applying wavelet denoising, and the ultimately reconstructed ECG signal. This tabulated data serves as a valuable resource for conducting direct comparisons, enabling a lucid evaluation of the impact and efficacy of both the wavelet filtering (denoising) and DAE stages on the signal. In Table 4-1, "Clean ECG" represents the parameters for label 4 samples. "Noisy ECG" represents the label 77 classified samples using the proposed methods in Chapters 2 and 3. "Filter Output" represents the output characteristics for label 77 classified samples applied to the proposed Bior wavelet denoiser in this chapter. The "Reconstructed" column represents the final results for classified noisy ECG samples after applying the proposed DAE. Finally, "Reconstructed Raw ECG" represents the final results for applying all samples of the captured raw ECG signal to the denoiser. This comparison shows how the results could differ without classifying the artifact noise and without applying the proposed models from Chapters 2 and 3.

Notably, the "77" labeled segment in the Table 4-1 exhibits the highest peak value, indicative of artifact noise and notable amplitude signal fluctuations. The kurtosis value, a statistical measure of the shape of the signal distribution, is found to be lowest in the Noisy ECG segment (8.8788). This reduction in kurtosis suggests the presence of irregular and

spurious peaks introduced by artifact noise, leading to deviations from the expected distribution of a clean ECG signal.

As demonstrated in Table 4-1, the kurtosis value for the reconstructed raw ECG is 10.8192, which is smaller than that of the clean signal, indicating the presence of outliers or non-normally distributed data points. The bandpower in the 0.45 – 10 Hz range for the reconstructed raw ECG is 20.08%, which is close to the 21.31% for the noisy signal. Additionally, other parameters in Table 4-1 indicate distortion and the presence of artifact noise in the reconstructed raw ECG signal.

Artifact noise in ECG signals can manifest as irregular peaks or distortions, resulting in non-Gaussian behavior in the data distribution. Unusual kurtosis values may signify the presence of outliers or non-normally distributed data points, often attributed to the influence of noise. Different types of artifact noise may exhibit distinct patterns in kurtosis. For instance, muscle movement artifacts may introduce sharp, non-Gaussian peaks, while baseline drift could lead to a flatter distribution with low kurtosis.

The clearance factor, measuring the separation between the QRS complex and the baseline of the ECG signal, is a vital parameter. A high clearance factor indicates a well-separated QRS complex, while a low clearance factor suggests poor separation. Artifact noise can impede this separation, as it introduces high-frequency components to the ECG signal, obscuring the QRS complex.

Samples with artifact noises were classified in Chapters 2 and 3, and these classified samples were then applied to the denoising method proposed in this chapter. Additionally, the raw dataset was applied to the trained Denoising Autoencoder (DAE), and the results are demonstrated in Table 4-1. The column "Reconstructed raw ECG" shows the results for the proposed DAE using the whole raw ECG signal samples without classifying the artifact noise. The column "Reconstructed" shows the final results for the proposed system where classified ECG samples with artifact noise were applied to the proposed model. Comparing these two columns shows that classifying artifact noises using 3-axis accelerometer and ECG signals before applying the denoising method significantly enhances the denoising performance of the DAE. Below is a detailed explanation of the rationale behind my approach and its potential impact on the results:

Rationale for Classifying Artifact Noise Before Using DAE

Targeted Denoising:

By classifying and isolating the artifact noise first, I ensured that the DAE specifically targets the noisy segments of the signal. This approach allows the DAE to focus its learning and reconstruction capabilities on the parts of the signal that need the most attention, rather than applying a generalized denoising process to the entire signal.

Signal Preservation:

Applying the DAE to the entire signal, including the clean segments, could potentially distort the already clean parts of the ECG. By classifying the noise first, the clean sections of the signal are preserved in their original state, ensuring that the integrity of the true ECG signal is maintained.

Improved DAE Performance:

The DAE can be more effectively trained when it is provided with examples that are specifically noisy. The learning process becomes more efficient as the autoencoder learns to differentiate between noise patterns and true signal patterns. This targeted training can lead to better reconstruction performance compared to a generalized approach.

Reduced Computational Load:

By classifying and only applying the DAE to the noisy segments, the computational burden is reduced. This makes the process more efficient as the DAE does not need to process the entire signal, only the portions identified as problematic.

Potential Impact on Results

Using the DAE on the entire signal without prior classification might lead to the following:

Generalized Denoising:

The DAE might apply a generalized denoising effect across the entire signal. While this could still reduce noise, it might also inadvertently alter parts of the signal that were already clean, potentially leading to a loss of important ECG features.

Lower Precision:

The precision in removing noise may decrease because the DAE would need to distinguish between noise and signal within the entire dataset simultaneously, which is a more complex task compared to focusing solely on the noisy segments.

Potential Overfitting:

Without classification, the DAE might overfit to patterns that are not representative of noise, especially if the noise patterns are sparse compared to the overall dataset.

By first classifying the artifact noise in the ECG signals, I ensured that the DAE could operate more effectively and efficiently, preserving the clean parts of the signal while focusing its denoising capabilities where they were most needed. This step-wise approach not only improved the quality of the reconstructed signal but also maintained the integrity of the original ECG data, which is crucial for accurate analysis and diagnosis. Figure 4-4 demonstrates the proposed block diagram to extract characteristics in Table 4-1. Considering the frequency domain, artifact noise is known to be prevalent within the 0.45 - 10 Hz bandwidth. The "Band-power" value in Table 4-1 represents the percentage of signal power within this frequency range relative to the total signal power spanning from 0 to 62.5 Hz. As anticipated, the presence of artifact noise is reflected in an increased band-power (0.45-10 Hz), rising from 15.83% in the clean signal to 21.31% in the noisy signal. It is crucial to acknowledge that the occurrence of artifact noise can vary across different frequency ranges, contingent on the speed of body movement. The comprehensive insights provided by these attributes in Table 4-1 serve as a foundation for a nuanced understanding of the signal characteristics and the effectiveness of denoising techniques in mitigating the impact of artifacts on ECG data.

Parameter	Clean ECG (label4)	Noisy ECG (label77)	Filter Output	Reconstructed	Reconstructed raw ECG
Mean (µV)	-59.8197	-60.4043	-60.2214	-60.0818	-60.3823
Peak Value (µV)	1586	2024	1761	1624	2083
RMS (µV)	306.2112	441.8252	381.6869	312.7667	418.5652
STD (µV)	298.7792	437.7131	386.3333	299.7861	399.1458
Median (µV)	-56	-64	-64.4375	-56.901	-61.2153
Shape Factor	2.0316	1.7799	1.8895	1.9789	1.7968
Kurtosis	15.5691	8.8788	9.6195	12.7252	10.8192
Clearance Factor	15.6746	11.8628	14.0608	15.5307	13.0791
Band-Power 0.45 –10 Hz (%)	15.83	21.31	19.28	17.46	20.08

An innovative two-stage algorithm has been developed to address artifact noise in ECG signals, aiming to enhance signal quality without compromising underlying information.
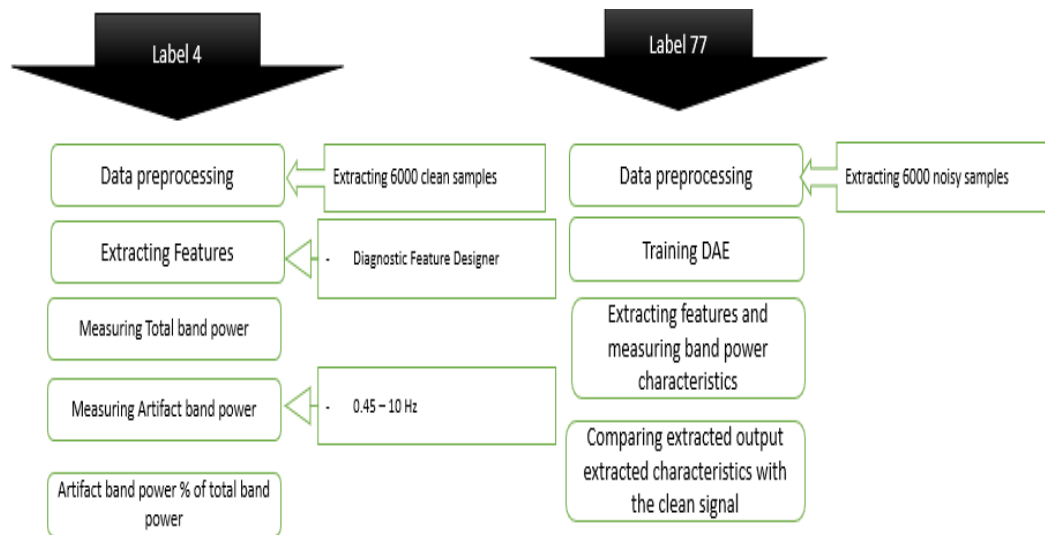
Figure 4-4. Proposed DAE block diagram employed to demonstrate characteristics of clean, noisy, filter output and final reconstructed ECG signals in Table 4.1.

The initial stage of the algorithm employs a Bior wavelet denoiser to effectively filter the signal. This step is crucial for reducing noise while preserving the essential features of the ECG waveform. However, some portions of the signal are deformed by artifact noise and cannot be fully denoised. In the subsequent stage, the proposed Denoising Autoencoder (DAE) is applied to further reconstruct the signal, enhancing the quality of the denoised output.

Table 4-2 Performance characteristics of proposed DAE model.

RMSE	Input SNR (dB)	Output SNR (dB)
0.0058	21.9	24.67

As it is demonstrated in Table 4-2, the performance evaluation of the denoising autoencoder yielded a RMSE of 0.0058, indicating a high level of accuracy in the reconstruction process. Additionally, the output noise level was measured at 24.67 dB, affirming the algorithm's proficiency in reducing unwanted artifacts.

Before application of the algorithm, the ECG signal, originally plagued by artifacts labeled as "77," exhibited a SNR of 21.9 dB. However, the proposed algorithm led to a significant improvement, increasing the SNR at the output by 2.77 dB. This enhancement underscores the effectiveness of the two-stage approach in reducing noise and enhancing the overall signal quality.

To visually represent the impact of the algorithm, Figure 4-5 provides PSD diagrams for the clean, noisy, and ultimately reconstructed ECG signals. The diagrams vividly illustrate that the majority of fluctuations initially occurred within the 0-30 Hz bandwidth. However, after the application of the Bior wavelet denoiser and the Denoising Autoencoder, a substantial portion of these fluctuation components has been successfully eliminated, as evidenced by Figure 4-5(b).

The proposed two-stage denoising and reconstructing algorithm demonstrates its efficacy in mitigating artifact noise in ECG signals. The combination of the Bior wavelet denoiser and the Denoising Autoencoder results in a notable improvement in signal quality, as indicated by quantitative measures such as RMSE and SNR, as well as through visual

representations of Power Spectral Density diagrams. This algorithm holds promise for applications where accurate ECG signal analysis is paramount.
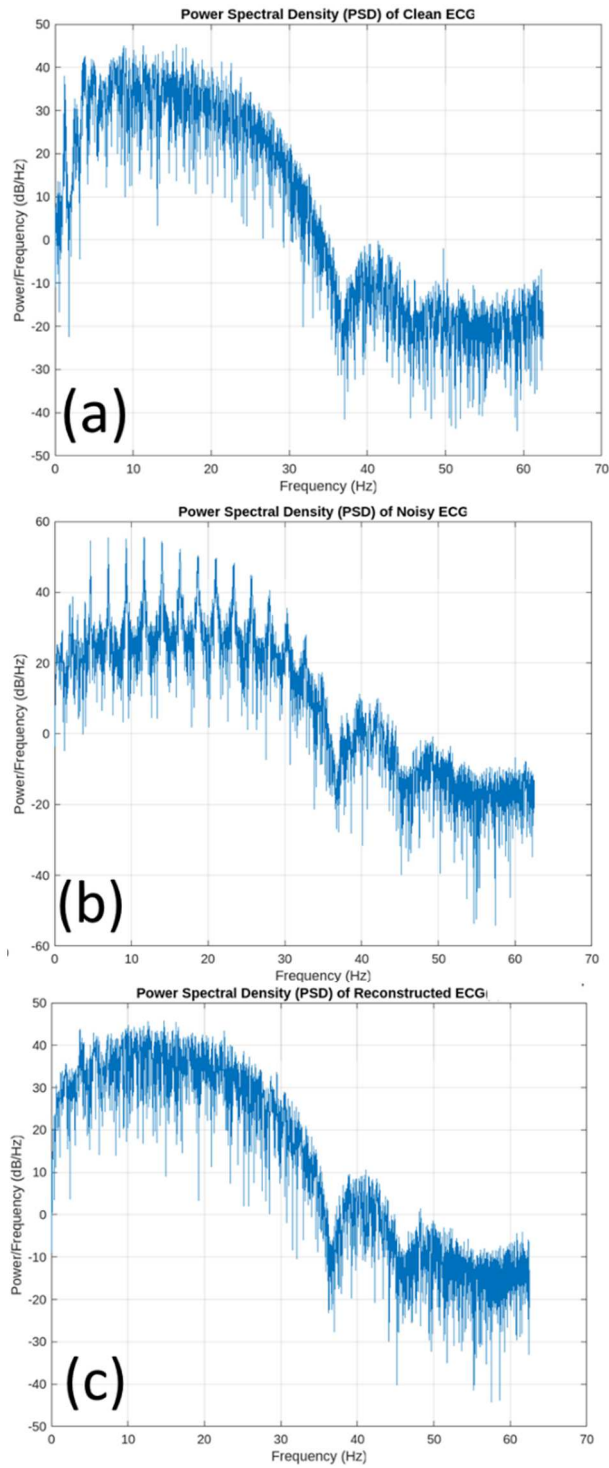

Figure 4-4. Power spectral density diagrams of (a). clean, b. noisy and c. filtered/reconstructed final ECG signal.

In contrast to the aforementioned studies in Section 1.1.1, Table 2-1, this work distinguishes itself by concentrating on the reduction of artifact noise, a type of interference identified through a machine learning classification system. Motion artifacts, in particular, introduce noise across a broader frequency spectrum, posing a unique set of challenges. In this context, the proposed two-stage algorithm has demonstrated superior performance in terms of SNR ratio (12.64%) improvement and RMSE (0.0058), underscoring its effectiveness in addressing the complexities associated with artifact noise. The two-stage algorithm not only enhances the SNR but also mitigates RMSE, showcasing its robustness in handling diverse noise sources that can be encountered in real-world signal processing scenarios. This distinction positions my approach as a promising solution for applications where artifact noise poses significant challenges in signal analysis and interpretation.

4.5 SUMMARY

In this chapter, a novel approach was introduced, presenting a fusion of DAE with wavelet denoising techniques to proficiently eliminate artifact noises from ECG signals. This innovative method harnesses Bior wavelet denoising to address high-amplitude noise within recorded ECG signals, particularly in the presence of artifacts. Following the application of Bior wavelet denoising, the filtered signal is reconstructed using the proposed denoising autoencoder.

The efficacy of this integrated technique has yielded promising results, as evidenced by a remarkably low RMSE value of 0.0058 and a substantial improvement in SNR by 12.64%. These outcomes signify a significant enhancement, highlighted by an average output SNR of 24.67 dB. Such improvements ensure the precise assessment of finer details within ECG signals, including ST-segment changes and T-wave abnormalities.

These encouraging findings pave the way for the potential application of the proposed technique as a robust artifact noise removal tool in vital sign monitoring devices. Beyond ECG signals, this approach holds promise for implementation in diverse vital sign monitoring contexts, such as EEG and PPG. The incorporation of this model into these

devices has the potential to greatly enhance the accuracy and reliability of vital sign measurements by effectively filtering out unwanted noises with wide-ranging frequency components.

As part of future research endeavors, the scope of the proposed method will be extended to EEG and PPG signals, acknowledging the diverse nature of noise in these signals. Comprehensive experiments in real-world settings will be conducted to evaluate the robustness of this approach and explore any potential limitations that may arise in practical scenarios. This expansion of the research agenda aims to further validate and refine the proposed method, ensuring its applicability across a broader spectrum of vital sign monitoring applications.

CHAPTER 5   CONCLUSION AND FUTURE WORK

This chapter serves as a comprehensive overview of the contributions discussed in preceding chapters and outlines potential avenues for future research within the scope of the dissertation. The primary focus of this thesis has been the exploration of innovative methods for the recognition and classification of samples containing artifact noises within ECG signals. In pursuit of this objective, a KNN model has been introduced and trained utilizing features extracted through the application of the wavelet scattering transform. Notably, feature extraction has been conducted not only on ECG signals but also on 3-axis accelerometer signals, contributing to a more holistic understanding and classification capability.

The thesis proposes a two-step methodology for denoising artifact-laden samples, leveraging a fine-KNN classification model. The denoising process involves the application of a Bior wavelet filter followed by the implementation of a DAE for signal reconstruction. This intricate approach aims to enhance the accuracy and reliability of the classification process by mitigating the impact of artifact noises in the signal.

Preliminary results have yielded promising outcomes, showcasing a high accuracy rate in the classification of samples. The effectiveness of the fine-KNN model, coupled with the denoising steps, underscores the robustness of the proposed methodology in handling artifacts and enhancing the overall signal classification process.

Moving forward, there exist several avenues for future work in this domain. Firstly, further exploration of different wavelet bases and filter configurations in conjunction with the wavelet scattering transform could be undertaken to optimize feature extraction for specific artifact types. Additionally, the fine-tuning of hyperparameters within the KNN model and the denoising components could potentially elevate the performance even further. The extension of the methodology to address real-time applications and scalability considerations is another compelling direction for future research.

The culmination of efforts presented in this thesis lays the groundwork for a sophisticated approach to recognizing and classifying samples with artifact noises in ECG signals. The

promising results underscore the potential applicability of the proposed methodology in real-world scenarios and motivate ongoing research endeavors to refine and extend the current framework.

5.1 MAIN CONTRIBUTIONS

Chapter 2 introduced the first significant contribution, unveiling a fine-KNN classification model trained with features derived from the wavelet scattering transform applied to 3-axis accelerometer signals. The exploration of time-domain and frequency-domain aspects of ECG signals enables the detection and analysis of motion artifacts in ECG samples. These signals, captured during various activities, bear resemblance to HAR systems. To assess the proposed model's efficacy, performance metrics such as PPV and test accuracy are employed. Comparative analysis with previous works underscores the model's high accuracy in recognizing artifact noise solely through captured 3-axis accelerometer signals. This versatility positions the proposed method as applicable to a spectrum of vital sign signals beyond ECG.

In Chapter 3, the second contribution builds upon the fine-KNN model by incorporating both ECG and 3-axis accelerometer signals. This hybrid approach harnesses a KNN machine learning model, leveraging wavelet scattering coefficients extracted from both accelerometer and ECG signals. The model's performance is rigorously evaluated, revealing promising results with high test accuracy and PPV, particularly in effectively handling samples marked with artifact noises (labeled as "77").

The third contribution, outlined in Chapter 4, introduced a robust two-step motion artifact denoising method. This innovative approach combines DAE with wavelet denoising techniques to efficiently eliminate artifact noises from ECG signals. The proposed methodology incorporates Bior wavelet denoising to address high-amplitude noise prevalent in ECG samples identified as having motion artifacts. Subsequently, the filtered

signal undergoes reconstruction using the proposed DAE. Performance evaluation showcases promising results, marked by a remarkably low RMSE value and a substantial enhancement in SNR. These outcomes signify a noteworthy improvement, ensuring the precise assessment of finer details within ECG signals, such as ST-segment changes and T-wave abnormalities. This robust denoising technique holds significant promise for advancing the accuracy and reliability of ECG signal analysis, especially in scenarios where motion artifacts pose challenges to signal interpretation.

5.2   FUTURE WORK

The motion artifact classification methods and the two-step denoising approach proposed in this thesis are pivotal for the precise assessment of intricate details within ECG signals. These methods specifically enable accurate analysis of ST-segment changes and T-wave abnormalities. The promising results suggest that the proposed method could serve as a robust tool for artifact noise removal in various vital sign monitoring devices, including EEG, PPG, and ECG. Integrating this model into such devices holds significant potential to enhance the accuracy and reliability of vital sign measurements by effectively filtering out unwanted noises with diverse frequency components.

Rationale for Using a Single Dataset
Data acquisition in this research involved capturing a single dataset as explained. Using one dataset allowed me to thoroughly analyze and fine-tune my methods without the complexities and variations that come with multiple datasets. This focused approach ensured that I could meticulously control and understand the variables and conditions affecting the ECG signals and the introduced motion artifacts.

Ensuring Robustness and Validity

To ensure that the limitations of using a single dataset did not affect the classification results, I validated my dataset against a larger and more diverse dataset from Physionet [87], as detailed in section 2.2. This comparative analysis demonstrated that the characteristics and noise patterns in my dataset were consistent with those found in the Physionet dataset, thereby affirming the validity and robustness of my results. The comparable performance between the two datasets provided confidence that my single dataset was representative and sufficient for the initial development and testing of my methods.

To build a more robust model in future work, I will capture additional datasets that include a wider variety of activities, such as punching and jumping. These activities are expected to introduce different types and intensities of motion artifacts in the ECG signal. By incorporating these new datasets, I aim to:

Enhance Reliability: Validate the model across a broader range of motion artifacts, ensuring that it performs well under diverse conditions.

Improve Performance: Fine-tune the model to handle more complex and varied noise patterns, leading to better artifact classification and signal reconstruction.

Increase Robustness: Ensure that the model can generalize well across different scenarios and types of physical activities, making it more adaptable for real-world applications.

Integration with Wearable ECG Monitoring Devices

All proposed methods are designed for wearable ECG monitoring devices. Running machine learning algorithms requires hardware resources, and the initial idea was to use mobile phones as the processing core. This approach allowed me to achieve high test accuracy while keeping processes and resource demands limited. In the future, capturing more diverse datasets will further improve model accuracy and robustness, making it more suitable for integration into various wearable devices. This expansion will ultimately enhance the reliability and performance of vital sign monitoring systems, ensuring they can effectively filter out unwanted noises and provide accurate measurements in real-time.Expanding Applications and Real-World Testing

Future research will aim to extend the application of the proposed method to EEG and PPG signals, considering the unique noise profiles encountered in these signals. Additionally, comprehensive experiments in real-world settings are planned to assess the robustness of the approach and identify potential limitations in practical scenarios. This exploration opens up numerous avenues for future work in this domain.

Exploring Different Activities

Another approach involves testing the system with various activities to increase robustness and determine which activities generate higher artifact noises. This will help in refining the classification methods to handle a wider range of scenarios.

Optimization and Adaptation

Exploring different wavelet bases and filter configurations in tandem with the wavelet scattering transform could optimize feature extraction for distinct types of artifacts, enhancing the method's adaptability and effectiveness. Additionally, fine-tuning the hyperparameters within the KNN model and the denoising components presents an opportunity to further improve performance.

Real-Time Applications and Scalability

Extending the methodology to real-time applications is a compelling direction for future research. Real-time applications pose unique challenges, requiring algorithm adaptations to ensure timely and accurate signal processing. Scalability considerations are also paramount as the proposed method advances towards broader implementation and usage. The combination of advanced motion artifact classification, two-step denoising, and the exploration of different configurations opens up new horizons for applying this methodology in vital sign monitoring. Continuous refinement through optimization, real-world experimentation, and addressing scalability concerns positions this research at the forefront of advancements in signal processing for healthcare applications.

BIBLIOGRAPHY

[1] J. Moss and S. Stern., "Non-invasive electrocardiology: Clinical aspects of holter monitoring", 1st edition, 1996, W.B. Saunders, Philadelphia, ISBN: 9-7020-1925-9.

[2] Michael Sampson, Anthony Mcgrath, "Understanding the ECG Part 1: Anatomy and physiology," British Journal of Cardiac Nursing, Nov 2015. http://dx.doi.org/10.12968/bjca.2015.10.11.548.

[3] Xiang An, George K. Stylios, "Comparison of motion artefact reduction methods and the implementation of adaptive motion artefact reduction in wearable electrocardiogram monitoring," 20(5), 1469, Sensors, Mar. 2020.

[4] Rahul Kher, "Signal processing techniques for removing noise from ECG signals," Journal of Biomedical Engineering and Research, 2019

[5] Leif Sornmo, Pablo Laguna, "Bioelectrical signal processing in cardiac and neurological applications," Elsevier, 1st Edition, eBook ISBN: 9780080527925, 2015.

[6] Shubhojeet Chatterjee, Rini Smita Thakur, Ram Narayan Yadav, "Review of noise removal techniques in ECG signals," IET Signal Processing, Vol. 14, Issue. 9, 2020.

[7] A. Alwan, "Global status report on noncommunicable diseases," World Health Org, Geneva, Switzerland, 2011.

[8] E. J. Benjamin et al., "Heart disease and stroke statistics," A report from American heart association, Circulation, vol. 135, 2017.

[9] R. M. John et al., "Ventricular arrhythmias and sudden cardiac death," Lancet, vol. 380, no. 9852, October, 2012.

[10] Y. Luo et al., "A hierarchical method for removal of baseline drift from biomedical signals: Application in ECG analysis," Sci. World J., vol. 2013, 2013.

[11] V. de Pinto, "Filters for the reduction of baseline wander and muscle artifact in ECG," J. Electrocardiol. Vol. 25, 1992.

[12] M. J. Rooijakkers et al, "Influence of electrode placement on signal quality for ambulatory pregnancy monitoring," Comput. Math. Methods. Med., vol., 2014.

[13] C. chandrakar and M. K. Kowar, "Denoising ECG signals using adaptive filter algorithm," Int. J. Soft Comput. Eng., vol. 2, no. 1, 2012.

[14] M. Z. U. Rahman, R. A. Shaik and D. V. R. K. Reddy, "Efficient and simplified adaptive noise cancelers for ECG sensor based remote health monitoring," IEEE Sensors J., vol. 12, no. 3, 2012.

[15] M. H. Moradi, M. A. Rad, and R. B. Khezerloo, "ECG signal enhancement using adaptive Kalman filter and signal averaging," Int. J. Cardiol., vol. 173, no. 3, 2014.

[16] G. U. Reddy, M. Muralidhar and S. Varadarajan, "ECG de-noising using improved thresholding based on wavelet transforms," Int. J. Comput. Sci. Netw. Secur., vol. 9, no. 9, September 2009.

[17] S. Liu, Y. Li, X. Hu, L. Liu and D. Hao, "A novel thresholding method in removing noises of electrocardiogram based on wavelet transform," J. Inf. Comput. Sci., vol. 10, no. 15, October 2013.

[18] O. El Bcharri, L. Rachid, K. Elmansouri, A. Abenaou, and W. Jenkal, "ECG signal performance de-noising assessment based on threshold tuning of dual-tree wavelet transform," Biomed. Eng. Online, vol. 16, no. 1, February 2017.

[19] N. E. Huang et al., "The empirical mode decomposition and the Hilbert spectrum for nonlinear and non-stationary time series analysis," Proc. Roy. Soc. London Ser. A Math. Phys. Eng. Sci, vol. 454, no. 1971, March 1998.

[20] B. Weng, M. Blanco-Velasco and K. E. Barner, "ECG denoising based on the empirical mode decomposition," Proc. Int. Conf. IEEE Eng. Med. Biol. Soc., 2006.

[21] M. A. Kabir and C. Shahnaz, "Denoising of ECG signals based on noise reduction algorithms in EMD and wavelet domains," Biomed. Signal Process. Control, vol. 7, no. 5, 2012.

[22] P. Xiong, H. Wang, M. Liu, F. Lin, Z. Hou, and X. Liu, "Denoising autoencoder for electrocardiogram signal enhancement," J. Med. Imaging Health Inform., vol. 5, no. 8, 2015.

[23] P. Xiong, H. Wang, M. Liu, F. Lin, Z. Hou, and X. Liu, "A stacked contractive denoising auto-encoder for ECG signal denoising," Physiol. Meas., vol. 37, no. 12, 2016.

[24] P. Xiong, H. Wang, M. Liu, S. Zhou, Z. Hou, and X. Liu, "ECG signal enhancement based on improved denoising auto-encoder," Eng. Appl. Artif. Intell., vol. 52, June 2016.

[25] A. A. Hamidi, B. Robertson, J. Ilow, "Robust ECG artifact noise classification method using wavelet scattering features in vital health applications," ICAIMA, Canada, 2023.

[26] N. Sivannarayana, D.C. Reddy, "Biorthogonal wavelet transforms for ECG parameters estimation," Medical Engineering & Physics, vol. 21, issue 3, April 1999.

[27] Bengio, Y, Courville, A. Vincent, "Representation learning: a review and new perspectives," Computer Science Machine Learning, vol. 35, 2014.

[28] L. Deng, M. Seltzer, D. Yu, A. Acero, A. Mohamed, and G. Hinton, "Binary coding of speech spectrograms using a deep auto-encoder," in Proc. Interspeech, vol. 2010.

[29] Li Y, Wang L. Human Activity Recognition Based on Residual Network and BiLSTM. Sensors (Basel). 2022 Jan 14;22(2):635. doi: 10.3390/s22020635. PMID: 35062604; PMCID: PMC8778132.

[30] William F. Fadel, Jack K. Urbanek, Steven R. Albertson, "Differentiating Between Walking and Stair Climbing Using Raw Accelerometry Data," Statistics in Biosciences, 11:334-354, 2019.

[31] D.K. Vishwakarma, Prachi Rawat, Rajiv Kapoor, "Human activity recognition using Gabor wavelet transform and Ridgelet transform," Procedia Computer Science, Vol 57, 2015

[32] Vrigkas M, Nikou C, Kakadiaris IA, "A review of human activity recognition methods," Front. Robot. AI 2:28, 2015.

[33] Gabriel Michau, Getan Frusque, Olga Fink, "Fully learnable deep wavelet transform for supervised monitoring of high-frequency time series," Proceedings of the National Academy of Sciences, 119(8): e 2106598119, Feb 2022.

[34] Mallat, S. "Group Invariant Scattering." Communications in Pure and Applied Mathematics. Vol. 65, Number 10, 2012.

[35] B Runa, J., and S. Mallat. "Invariant Scattering Convolution Networks." IEEE Transactions on Pattern Analysis and Machine Intelligence. Vol. 35, Number 8, 2013.

[36] A ndén, J., and S. Mallat. "Deep Scattering Spectrum." IEEE Transactions on Signal Processing. Vol. 62, Number 16, 2014.

[37] M allat, S. "Understanding deep convolutional networks." Philosophical Transactions of the Royal Society A. Volume 374: 20150203, 2016, dx.doi.org/10.1098/rsta.2015.0203.

[38] Lostanlen, V. Scattering.m, Github. (2022). A MATLAB toolbox for wavelet scattering. Retrieved May 30, 2024, from https://github.com/lostanlen/scattering.m.

[39] Mathworks .(2024). Wavelet-Scattering. Retrieved May 30, 2024, from https://ch.mathworks.com/help/wavelet/ug/wavelet-scattering.html

[40] ScatNet. (2013). Retrieved May 30, 2024, from https://www.di.ens.fr/data/software/scatnet/.

[41] Kymatio. (2021). Wavelet scattering in Python – v0.3.0 Erdre. Retrieved May 30, 2024, from https://www.kymat.io/.

[42] Mathworks. (2024), Feature selection and feature transformation. Retrieved May 30, 2024, from https://mathworks.com/help/stats/feature-selection-and-feature-transformation.html.

[43] Mia Hubert, Sanne Engelen, "Robust PCA and classification in biosciences," Bioinformatics, Vol. 20, Issue 11, 2004.

[44] S. Mallat, "Classification with scattering operators," in Computer Vision and Pattern Recognition, USA, June 2011.

[45] Attalah L, "Sensor positioning for activity recognition using wearable accelerometers," IEEE Trans Biomed Circuits Sys, 320–329, 2011.

[46] Siirtola P, Röning J, "Recognizing human activities user-independently on smartphones based on accelerometer data," IJIMAI 1(5):38–45, 2012

[47] Debache I, Jeantet L, Chevallier D, Bergouignan A, Sueur C, "A lean and performant hierarchical model for human activity recognition using body-mounted sensors," Sensors 20(11):3090, 2020.

[48] Hassan MM, Uddin MZ, Mohamed A, Almogren A, "A robust human activity recognition system using smartphone sensors and deep learning," Futur Gener Comput Syst 81:307–313, 2018.

[49] Bangwen Zhou, Cheng Wang, Zhan Huan, Zhixin Li, "A novel segmentation scheme with multi-probability threshold for human activity recognition using wearable sensors," Sensors, 22(19), 7446, 2022.

[50] Amy L. Magnus, Mark. E. Oxley, "Theory of confusionm" Proc. SPIE 4479, Applications of Science of Neural Networks, Fuzzy Systems, and Evolutionary Computation IV, 2001.

[51] Shaibal Barua, Shahina Begum, "A review on machine learning algorithms in handling EEG artifacts," Conference: SAIS Workshop, Stockholm, Sweden, 2014.

[52] Shalini Stali, Vandana Roy, Prashant Kumar Shukla, "A machine learning-based big EEG data artifact detection and wavelet-based removal: an empirical approach," Hindawi, Mathematical Problems in Engineering, Vol. 2021, 94808, 2021.

[53] Turkowski K, Gabriel S, 'Filters for common resampling tasks," Academic Press, Waltham, 1990.

[54] Richard G. Lyons, "Efficient resampling implementations," Streamlining digital signal processing: a tricks of the trade guidebook, Wiley-IEEE Press, 2012.

[55] Dr. Erol Kalkan, P.E. (2023). Time-domain Sinc Interpolation (Resampling)(https://www.mathworks.com/matlabcentral/fileexchange/59027-time-domain-sinc-interpolation-resampling), MATLAB Central File Exchange. Retrieved June 27, 2023.

[56] Shaibal Barua, Shahina Begum, "A review on machine learning algorithms in handling EEG artifacts," Conference: SAIS Workshop, Stockholm, Sweden, 2014.

[57] Shalini Stali, Vandana Roy, Prashant Kumar Shukla, "A machine learning-based big EEG data artifact detection and wavelet-based removal: an empirical approach," Hindawi

[58] Pramendra Kumar, Vijay Kumar Sharma, "Detection and classification of ECG noises using decomposition on mixed codebook for quality analysis," Healthcare Technology Letters, Vol 7. Issue 1, 2020.

[59] Dukyong Yoo, Hong Seok Lim, "Deep learning-based electrocardiogram signal noise detection and screening model," Healthcare Informatics Research, 25(3), 201-211, 2019.

[60] Pramendra Kumar, Vijay Kumar Sharma, "Detection and classification of ECG noises using decomposition on mixed codebook for quality analysis," Healthcare Technology Letters, Vol 7. Issue 1, 2020.

[61] Tanatorn Tanantong, "A KNN approach for ECG signal quality classification," IJIEE, Vol. 6, No.5, July 2016.

[62] E. J. Benjamin et al., "Heart disease and stroke statistics," A report from American heart association, Circulation, vol. 135, 2017.

[63] Tereshchenko LG, Waks JW, Kabir M, Ghafoori E, Shvilkin A, Josephson ME. Analysis of speed, curvature, planarity and frequency characteristics of heart vector movement to evaluate the electrophysiological substrate associated with ventricular tachycardia. Comput Biol Med. 2015.

[64] Larisa G. Tereshchenko, MD and MARK E. Josephson, MD, "Frequency content and characteristics of ventricular conduction," J. Electrocardiol. , 48(6): 933-937, 2015.

[65] P.M Agante, J.P. Marques de Sa, "ECG noise filtering using wavelets with soft-thresholding methods," Computers in Cardiology 1999, Vol. 26, Sep 1999.

[66] A. Gogna, A. Majumdar, and R. Ward, "Semi-supervised stacked label consistent autoencoder for reconstruction and analysis of biomedical sginals," IEEE Trans. Biomed. Eng., vol. 64, no. 9, September 2017.

[67] X. Lu, Y. Tsao,, S. Mtsuda, and C. Hori, "Speech enhancement based on deep denoising autoencoder," in Proc. Interspeech, vol., 2013.

[68] Y. H. Lai, F. Chen, S. -S, Wang, and C. -H. Lee, "A deep denoising autoencoder approach to improving the intelligibility of vocoded speech in cochlear implant simulation," IEEE Trans. Biomed. Eng., vol. 64, no. 7, 2017.

[69] L. Gondara, "Medical image denoising using convolutional denoising autoencoders," in Proc. IEEE 16th Int. Conf. Data Mining Workshops (ICDMW), 2016.

[70] Leif Sornmo, Pablo Laguna, "Bioelectrical signal processing in cardiac and neurological applications," Elsevier, 1st Edition, eBook ISBN: 9780080527925, 2015.

[71] Shubhojeet Chatterjee, Rini Smita Thakur, Ram Narayan Yadav, "Review of noise removal techniques in ECG signals," IET Signal Processing, Vol. 14, Issue. 9, 2020.

[72] Haicai Lin, Ruixia Liu, Zhaoyang Liu, "ECG signal denoising method based on Disentangled Autoencoder," Advanced Technologies of Artificial Intelligence in Signal Processing, Vol. 12, Issue. 7, 2023.

[73] Szu-Wei Fu, Kuo-Hsuan Hung,Yu Tsao, "Noise reduction in ECG signals using fully convolutional denoising autoencoders," IEEE Access, 2019.

[74] Md Samiul, Shifat Hossain, Nashrah Afroze, "Understanding the nonlinear behavior of EEG with advanced machine learning in artifact elimination," Vol. 8, Num, 1, Biomedical Physics & Engineering Express, IOP Science, Dec. 2021.

[75] [11] Xiao Jiang, Gui-Bin Bian, Zean Tian, "Removal of artifacts from EEG signals: A review," 19(5), 987, Sensors, 2019.

[76] T. M. Cover and P. E. Hart, "Nearest neighbor pattern classification," IEEE Trans. On Information Theory, Vol. 13, no. 1, pp. 21-27, 1967.

[77] Murad A, Pyun J-Y. Deep Recurrent Neural Networks for Human Activity Recognition. Sensors. https://doi.org/10.3390/s17112556

[78] [16] Zhao, Y., Yang, R., Chevalier, G., Xu, X., & Zhang, Z. (2018). Deep residual bidir-LSTM for human activity recognition using wearable sensors. Mathematical Problems in Engineering, 2018.

[79] M. Sekine, T. Tamura, T. Togawa and Y. Fukui, "Classification of waist-acceleration signals in a continuous walking record," Med. Eng. Phys., vol. 22, 2000.

[80] T. Tamura, M. Sekine, M. Ogawa, T. Togawa et al., "Classification of acceleration waveforms during walking by wavelet transform," Meth. Inform. Med., vol. 36, 1997.

[81] M. N. Nyan, F. E. Tay, K. H. Seah and Y. Y. Sitoh, "Classification of gait patterns in the time-frequency domain," J. Biomech., vol. 39, 2006.

[82] Mathworks. (2024). Classification learner app. Retrieved May 30, 2024, from https://www.mathworks.com/help/stats/classification-learner-app.html

[83] Mathworks. (2024). Autoencoder. Retrieved May 30, 2024, from https://se.mathworks.com/discovery/autoencoder.html

[84] Mathworks. (2024). Wavelet signal denoiser app. Retrieved May 30, 2024, from https://se.mathworks.com/help/wavelet/ref/waveletsignaldenoiser-app.html

[85] Mathworks. (2024). Data cleaner app. Retrieved May 30, 2024, from https://se.mathworks.com/help/matlab/ref/datacleaner-app.html

[86] A. A. Hamidi, B. Robertson, J. Ilow, "A novel approach for ECG artifact detection using fine-KNN classification and wavelet scattering features in vital health applications," Procedia Computer Science, Vol. 224, 2023.

[87] Physionet. Marta Karas, Jacek Urbanek, Cirprian Crainiceanu, Jaroslaw Harezlak, William Fadel, (2021). Labeled raw accelerometry data captured during walking, stair climbing and driving. Retrieved May 30, 2024, from https://physionet.org/content/accelerometry-walk-climb-drive/1.0.0/

APPENDIX A – WAVELET SCATTERING TRANSFORM

The wavelet scattering function is composed of both a mother wavelet and a father wavelet. In this specific application, it is opted for the Morlet wavelet, defined by equation 2.1, to serve as the mother wavelet. The choice of the Morlet wavelet was driven by its well-established properties in signal processing and its effectiveness in capturing both temporal and frequency information in a signal. The Morlet wavelet is a complex wavelet that combines sinusoidal oscillations with a Gaussian window. This characteristic makes it particularly suitable for applications like feature extraction in ECG signals, where capturing both time and frequency aspects is crucial. The oscillatory nature of the Morlet wavelet allows it to efficiently represent periodic patterns in the signal, while the Gaussian window contributes to its ability to localize features in both time and frequency domains. By incorporating the Morlet wavelet into the wavelet scattering function, the resulting feature extraction process gains the advantages of a multi-scale representation. The Morlet wavelet's flexibility in handling different scales contributes to a more comprehensive analysis of the signal, making it robust against noise and enhancing the discriminatory power of the extracted features. It is worth noting that the choice of the mother wavelet can significantly impact the performance of the wavelet scattering transform. Different wavelets may be better suited for specific types of signals or noise characteristics. Therefore, the selection of the Morlet wavelet in this context is a thoughtful decision, aligning with its strengths in preserving signal features and mitigating the effects of noise. The incorporation of the Morlet wavelet as the mother wavelet in the wavelet scattering function enhances the feature extraction process, especially in applications dealing with ECG signals. This choice reflects a strategic consideration of the wavelet's characteristics, emphasizing its ability to capture intricate patterns in both time and frequency domains, ultimately contributing to a robust and informative representation of the underlying signal.

$$\psi(\mu) \ = \ C_1(e^{i\omega t} - C_2)e^{\left(-|\mu|\frac{2}{2\sigma^2}\right)} \tag{2.1}$$

In the context of wavelet analysis, where ω represents frequency, σ is a measure of support, μ denotes scale, ψ is the wavelet function, and C_1/C_2 are constants, obtaining a locally

translation-invariant descriptor can be achieved by employing a time average, as illustrated in equation 2.2. The variable ϕ corresponds to the low-pass filter, while x represents the signal under analysis. The application of equation 2.2 serves to eliminate high-frequency components, which can later be recovered through the wavelet modulus operation. The $\phi(t)$ component of the equation acts as the low-pass filter, facilitating the derivation of locally translation-invariant descriptions of the signal x at a predefined scale of t. It is noteworthy that each family of wavelets is denoted by λm, and these wavelets exhibit an octave frequency resolution of Qm. To further enhance the analysis, high-pass filter banks can be constructed by dilating the wavelet function ψ. This dilation process allows for the creation of filter banks that capture varying frequency components, contributing to a more comprehensive representation of the signal x. The resulting locally translation-invariant descriptors, coupled with the octave frequency resolution provided by the wavelet families, empower the analysis of signals in diverse scales and frequency bands. The interplay of wavelet functions, low-pass filters, and high-pass filter banks, along with the incorporation of locally translation-invariant descriptors, forms a robust framework for the analysis and representation of signals, offering adaptability to different scales and frequency resolutions.

$$|W_1|x = x * \phi \,|x * \psi\lambda_1 \,| \tag{2.2}$$

In the context of wavelet scattering transform, the first order of scattering coefficients is characterized by equation 1.3. This equation serves the purpose of quantifying the average signal amplitude within the frequency interval defined by $\psi\lambda1$. The first-order scattering coefficients play a pivotal role in providing a fundamental representation of the signal's characteristics. Specifically, they capture essential information about the signal's amplitude distribution within the range spanned by the mother wavelet function $\psi\lambda1$. This measurement is crucial for discerning patterns and features in the signal at a particular frequency scale, laying the groundwork for subsequent stages of the scattering transform. It is important to note that the choice of the wavelet basis function ψ and its associated scale parameter $\lambda1$ significantly influences the characteristics of the first-order scattering coefficients. The flexibility in selecting different wavelets enables adaptability to diverse signal structures and facilitates the extraction of relevant features across various frequency

bands. As we delvinge into the realm of wavelet scattering, the comprehensive nature of the first-order coefficients becomes apparent. Beyond merely measuring average signal amplitudes, they contribute to a richer understanding of the signal's frequency content and distribution. This nuanced representation proves advantageous, especially when confronted with signals embedded in noisy environments or exhibiting complex patterns. Furthermore, the first-order scattering coefficients lay the foundation for higher-order coefficients, fostering a hierarchical feature extraction approach. The subsequent orders build upon the initial measurements, capturing increasingly intricate details of the signal's behavior across multiple scales.

$$S_1 x(t, \lambda_1) = |x * \psi\lambda_1| * \phi \tag{2.3}$$

To compute the second-order scattering coefficients, it is necessary to iterate through the previously outlined steps for each term |x * ψλ1|, as defined in equation 2.4. This involves an extension of the initial wavelet transform process, where the signal x is convolved with the wavelet function ψ at a particular scale λ1. The resulting modulus of the convolution, denoted as |x * ψλ1|, serves as the basis for further computations. Expanding on this, the second-order scattering coefficients involve a cascaded application of the wavelet transform to the aforementioned modulus |x * ψλ1|. For each scale λ2, this process is repeated, leading to an enhanced representation that captures intricate details at multiple scales. The hierarchical nature of the second-order scattering coefficients allows for a more nuanced understanding of the signal, particularly beneficial when dealing with complex data such as ECG signals. Moreover, the repeated application of the wavelet transform at different scales contributes to the robustness of the feature extraction process. It enables the identification and preservation of significant signal components while mitigating the impact of noise, a crucial aspect when working with real-world data that often contains various artifacts. To derive the second-order scattering coefficients, the methodology involves a systematic application of the wavelet transform to the modulus of the signal convolved with the wavelet function at each scale. This hierarchical approach enhances the feature extraction process, providing a more comprehensive representation of the signal's characteristics. The iterative nature of the computation ensures a thorough exploration of

multiple scales, contributing to the effectiveness of the scattering transform in capturing and discriminating features in the presence of noise.

$$S_2 x(t, \lambda_1) = |x * \psi\lambda_1| * |\psi\lambda_2| * \phi \qquad (2.4)$$

S0x, S1x, and S2x denote the 0th order (corresponding to the low pass filter or time average), 1st order, and 2nd order scattering coefficients, respectively.

Moreover, the application of modulus nonlinearities enhances the stability of the transform, making it less sensitive to amplitude variations and noise. This feature is particularly valuable when dealing with real-world time series data that often exhibit fluctuations and interference. The incorporation of lowpass filters aids in capturing the low-frequency components of the signal, ensuring a comprehensive representation that includes both high and low-frequency information. In practical terms, the wavelet scattering transform proves advantageous for processing time series data, such as ECG, where robust feature extraction is essential for accurate analysis. Its shift-invariance and stability against deformations make it well-suited for scenarios where signals may undergo temporal distortions or variations. Furthermore, the low-variance features extracted by the transform serve as valuable inputs for machine learning and deep learning models, facilitating tasks such as classification and anomaly detection. The wavelet scattering transform, with its unique oefficientn of wavelet cascades, modulus nonlinearities, and lowpass filters, stands out as a powerful tool for extracting robust features from time series data. Its applicability to various domains, including healthcare for ECG analysis, underscores its versatility and effectiveness in capturing intricate signal characteristics.

The invariance scale in wavelet scattering networks has the potential to be notably large, primarily influenced by the average operation determined by the low-pass filter. This scale of invariance is a critical parameter, as the scattering wavelet network exhibits translation invariance up to this specific scale. This property makes it particularly robust in capturing patterns and features that may undergo translations within a certain range.The wavelet scattering decomposition further extends its utility by effectively capturing variations in both duration and amplitude within accelerometer signals. This is crucial in applications such as signal processing for accelerometers, where changes in both temporal and intensity aspects of the signal carry valuable information.

The process of obtaining higher-order wavelet scattering coefficients (m ≥ 2) involves iterating the previously described procedure, as outlined in Equation 1.5. This iterative approach enables the extraction of increasingly complex and nuanced features from the signal. To elaborate further, each order of scattering coefficients provides unique insights into the signal's characteristics at different scales. The 0th order captures the low-frequency components or overall trends, the 1st order focuses on finer details and transitions, while the 2nd order delves even deeper into the signal's intricacies. The iterative application of the scattering transform enhances the feature extraction process, allowing for a more comprehensive representation of the signal's hierarchical structure. Additionally, the use of wavelet scattering is particularly advantageous when dealing with signals that exhibit noise or artifacts. The multi-scale nature of the transform aids in discerning genuine signal patterns from undesired interference, contributing to the robustness of the extracted features. Equation 2.5 serves as a guide for extending the feature extraction process to higher orders, emphasizing the adaptability and versatility of the wavelet scattering transform in capturing the diverse and complex characteristics present in signals. This comprehensive approach to feature extraction is beneficial in applications such as signal processing, where a nuanced understanding of the signal's composition is crucial for subsequent analysis and classification tasks.

$$S_m x(t, \lambda_1, \dots, \lambda_m) = |x * \psi \lambda_1| * |\psi \lambda_2| \dots * |\psi \lambda_m| * \phi \tag{2.5}$$

APPENDIX B – WAVELET SCATTERING IN MATLAB

The waveletScattering function is utilized to construct a Wavelet Scattering Transform network (sn1) with specific parameters tailored for robust signal analysis. The key parameters include:

• Signal Length: Specifies the length of the input signal (X1) with 36462 samples.

• Invariance Scale: Sets the invariance scale to 40 seconds, determining the analysis window size and temporal resolution of scattering coefficients.

• Sampling Frequency: Defines the sampling frequency of the input signal (X1) as 104 Hz.

• Q1 and Q2: Represent the number of wavelet filters at the first and second layers of the scattering transform, respectively. In this instance, Q1=8 and Q2=1, indicating two filter banks—zeroth and first order filter banks.

Following the construction of the Wavelet Scattering Transform network, the featureMatrix function is employed to compute scattering coefficients for each path through the scattering tree. The input signal (X1) with a signal length of 36000 samples produces the XS1 matrix. This resulting matrix is of size 261x36, where 261 denotes the number of paths through the scattering tree, and 36 signifies the number of coefficients at each scale.

The mathematical computation of the scattering coefficients unfolds through several steps:

1. Convolution with Wavelet Filters: The input signal undergoes convolution with a set of wavelet filters at the first layer, yielding low-pass and high-pass filtered signals.

2. Downsampling: The low-pass filtered signals are downsampled by a factor of 2, and the high-pass filtered signals undergo another set of wavelet filters at the second layer, generating 1st-order scattering coefficients.

3. Second-Order Scattering Coefficients: The 1st-order scattering coefficients undergo downsampling by a factor of 2 and pass through a modulus operation to compute second-order scattering coefficients. It is noted that only zeroth and first order scattering coefficients are present in this specific case.

4. Path Iteration: The entire process is repeated for each possible path through the scattering tree, resulting in a set of 261 paths for the network.

5. Magnitude Computation: The magnitude of the resulting scattering coefficients is computed and stored in the XS1 matrix.

In summary, the wavelet scattering technique, coupled with the described mathematical computations, provides a comprehensive and robust feature extraction method for signals, especially in scenarios involving noisy data such as ECG signals. The resulting scattering coefficients, stored in the XS1 matrix, capture essential information at different scales, contributing to effective signal analysis and subsequent applications, such as classification using a KNN classifier.

Number of Coefficients

To calculate the total number of coefficients in the waveletScattering transform, MATLAB employs a formula based on the provided parameters. The formula is expressed as follows:

$$ncf = 2 + 2 \times (Q_1 \ x \ Q_2 + Q_2^2 \ ) \times J \times \log_2(\text{SignalLength} \times \text{SamplingFrequency} / \text{InvarianceScale})$$

where ncf represents the number of coefficients, and the variables are defined as follows:

• Q1 and Q2: Quality factors of the two wavelet filter banks used.

• J: Wavelet scales used in the transform (40 seconds windows).

• SignalLength: Length of the input signal in samples.

• SamplingFrequency: Sampling frequency of the input signal in Hz.

• InvarianceScale: Invariance scale of the scattering coefficients in seconds.

Substituting the provided values into the formula, I obtain:

$ncf = 2 + 2 \times (1 \times 8 + 8 \times 8) \times 40 \times \log2(36462 \times 104 / 40)$

$ncf = 36$

Scattering Paths

The formula to calculate the number of unique scattering paths involves the number of possible combinations of scattering orders, filters, and delays that can be applied to the input signal. The formula for the number of unique scattering paths for a given signal length N, invariance scale T, and a filter bank of Q filters is:

$M = Q \times (Q - 1)^{\log_2 N/T}$

Plugging in the values from the provided MATLAB algorithm, I get:

$M = 8 \times (8\text{-}1)^{(\log2(36462/40))} = 261.0171$

Therefore, MATLAB calculates the number of unique scattering paths to be 261.

APPENDIX C – MACHINE LEARNING

KNN Classifier

The Euclidean distance function is a fundamental metric used to quantify the distance between two points in a two-dimensional plane. For two points with coordinates (x, y) and (a, b), the Euclidean distance (dist) is calculated as follows:

$$dist\big((x,y),(a,b)\big) = \sqrt{(x-a)^2 + (y-b)^2}$$ (2.6)

In the context of the K-nearest neighbors (KNN) algorithm, this distance measure plays a crucial role. The algorithm identifies the K-nearest neighbors of a given data point, where K is a predefined value. Subsequently, the class assignment for the data point is determined by selecting the class with the highest count among the K neighbors. Mathematically, this can be expressed as:

$$P\,(y = j \mid X = x) = \frac{1}{K}\sum_{j \in A} l\,(y^{(i)} = j)$$ (2.7)

S $P(y = j \mid X = x)$ represents the probability of the data point belonging to class j, a denotes the set of K-nearest neighbors, and I is the indicator function.

In the specific case of the fine-KNN classifier, only one neighbor is considered for distinguishing data points. The Euclidean distance for fine KNN is expressed by the following equation:

$$d = \sqrt{\sum_{k=1}^{n}(X_{1K} - X_{2K})^2}$$ (2.8)

In this equation, n represents the number of values in each sample vector, and X_1 and X_2 denote input samples. The fine-KNN classifier thus utilizes a simplified distance metric, considering the individual components of the sample vectors. It is worth noting that the choice of distance metric, such as the Euclidean distance, and the value of K are crucial parameters in the performance of the KNN algorithm. Fine-tuning these parameters is often necessary to achieve optimal classification results in diverse applications.

The KNN algorithm stands out for its commendable performance in effectively classifying noises during model training, particularly in the realm of ECG and accelerometer signal processing. This efficacy is notably evident in scenarios involving activities that introduce noise into the ECG signal, such as clapping. The success of KNN in these applications can be attributed to several inherent characteristics that enhance its adaptability and robustness.

Localized Decision Boundaries:

KNN operates on the principle of proximity in feature space. This proves advantageous when confronted with intricate and complex decision boundaries. The algorithm excels in creating localized decision boundaries based on the nearest neighbors. In the context of artifact noise classification, where patterns may exhibit variations across different sections of the feature space, KNN's ability to adapt to local patterns enhances its performance.

Non-Parametric Nature:

KNN is a non-parametric algorithm, implying that it refrains from making assumptions about the underlying data distribution. This characteristic lends itself well to applications involving diverse and dynamic patterns, a common scenario in artifact noise classification. The algorithm's flexibility enables it to handle varying data distributions without imposing rigid assumptions.

Feature Interactions:

In scenarios where both ECG and accelerometer signals are involved, the interactions between features can be intricate. KNN excels in capturing complex feature interactions without imposing strict assumptions about the relationships between features. This adaptability is crucial in applications where the relationships between different signal components play a significant role in accurate classification [61].

The collective characteristics of KNN position it as an invaluable tool, particularly well-suited for tasks that demand robust noise classification within diverse and dynamic signal

datasets [76]. In the context of this work, a Fine-KNN classifier is employed, utilizing the Euclidean distance function, to effectively classify accelerometer signals.

KNN, as a versatile classification algorithm, is known for its simplicity and effectiveness. It operates based on the principle of proximity, classifying a data point by considering the classes of its nearest neighbors.

PCA in MATLAB

MATLAB employs the singular value decomposition method to calculate principal component coefficients, a crucial step in PCA. PCA is widely utilized for dimensionality reduction and feature extraction. Given a data matrix X with n observations and p variables, the SVD of X is represented as X=USV, where U and V are orthogonal matrices, and S is a diagonal matrix containing the singular values of X.

The principal component coefficients, often termed loadings, are simply the elements of the V matrix. It is noteworthy that the principal component coefficients matrix is always a $p \times p$ squared matrix. This is because each principal component is a linear combination of all p variables in the data matrix. Consequently, the coefficients for each principal component must be stored in a $p \times 1$ vector. Given there are p principal components in total, the coefficients matrix will have dimensions $p \times p$. Moreover, since each principal component is a linear combination of all p variables, the coefficients matrix must store the coefficients for all p variables for each of the p principal components, resulting in a $p \times p$ squared matrix.

The transformation of data through centering, rotating, and scaling, as informed by PCA, can lead to improved convergence times and result in higher-quality outcomes. While theoretically, PCA may not alter the fundamental nature of the data, in practice, it accelerates training rates, simplifies required neural structures, and yields systems that more accurately characterize the "intermediate structure" of the data, avoiding the need to account for multiple scales. It is important to note that PCA is an algorithm that does not consider the response variable or prediction target. It treats features with large variances as

important, but these features may not necessarily be directly linked to the prediction target. As such, careful consideration is required when interpreting the significance of features identified by PCA in relation to the overall predictive goals of a model.

The principal component analysis process, as implemented in MATLAB, can be comprehensively divided into six distinct steps:

1. **Dataset Preparation:** Begin with a dataset comprising d+1 dimensions, where d represents the input features (X_train), and 1 denotes the corresponding labels (y_train). In this step, the labels are disregarded, resulting in a reduced d-dimensional dataset. The modified dataset (X_train) is then employed to identify principal components.
2. **Mean Computation:** Treat the modified dataset as a matrix A and compute the mean of each dimension across the entire dataset. This yields a vector of mean values corresponding to the d dimensions of the dataset.
3. **Covariance Matrix Calculation:** Utilizing Equation 1.3, calculate the covariance matrix of A. The resulting square matrix is of dimensions d * d. The covariance matrix is computed by determining the covariance between two variables, X and Y, employing the formula:

$$cov(X, Y) = \frac{1}{n-1}\sum_{i=1}^{n}(Xi - \bar{x})(Yi - \bar{y}) \tag{2.9}$$

4. **Eigenvalue and Eigenvector Extraction:**
   - Proceed to extract eigenvalues and corresponding eigenvectors from the covariance matrix. For a square matrix A, consider a vector v and scalar λ satisfying Av=λv, where λ is the eigenvalue associated with eigenvector v. The eigenvalues are determined by solving the characteristic equation:

$$\det(a - \lambda l) = 0 \tag{2.10}$$

   - Subsequently, sort the eigenvectors in descending order based on their eigenvalues. Form a d * k dimensional matrix W, selecting the eigenvectors with the largest eigenvalues. The choice of eigenvectors with higher eigenvalues captures the most significant information about the data distribution.
5. **Dimensionality Reduction:** The selected matrix W is then used to transform the original dataset samples into a new subspace. The transformation is achieved via the equation y=W^T· x, where W^T denotes the transpose of matrix W.
6. **Final Transformation:** Complete the PCA process by transforming the samples into the new subspace using the computed matrix W. The transformed dataset y

reflects the essential characteristics of the original data in a reduced-dimensional space.

By meticulously following these six steps, MATLAB's PCA implementation provides a powerful tool for dimensionality reduction and feature extraction, facilitating efficient data representation and analysis. The process ensures that the most informative features are retained while discarding less significant information, leading to enhanced computational efficiency and improved interpretability of the dataset.

APPENDIX D – DENOISING AUTOENCODERS

The denoising autoencoder operates through two distinct stages: encoding and decoding. The encoder performs a nonlinear transformation, mapping an input x to a hidden representation z. Subsequently, the decoder executes another nonlinear transformation, mapping the hidden representation z back to the reconstructed data $\hat{x}$. This multi-stage process enables effective data recovery and denoising, contributing to the versatility of autoencoders in addressing signal processing challenges, including those posed by motion artifacts in ECG signals.

Encoder:

$$z = f(W_x + b) \tag{4.1}$$

Decoder:

$$\hat{x} = g(\widehat{W}_z + \hat{b}) \tag{4.2}$$

In the given context, the symbols W and b denote the weight and bias matrices of the encoder, respectively, while $\widehat{W}$ and $\hat{b}$ represent the corresponding matrices for the decoder. These matrices play a pivotal role in autoencoder architectures, which are neural network models employed for unsupervised learning tasks such as feature learning and data compression. Furthermore, the activation functions f and g, applied within the network, introduce non-linearities critical for capturing complex relationships in the data.

The choice of activation functions, f and g, is a crucial aspect in the design of the autoencoder. Commonly used activation functions include the sigmoid, hyperbolic tangent, and rectified linear functions, each offering unique characteristics suitable for specific types of data and learning objectives.

The objective function that governs the training process of the autoencoder is defined as follows:

$$L(\theta) = \sum_i ||x - \hat{x}||^2 \tag{4.3}$$

$$\theta = \{W, b, \widehat{W}, \hat{b}\} \tag{4.4}$$

It is worth noting that the success of an autoencoder relies heavily on the careful tuning of these parameters and the choice of the appropriate activation functions. Through iterative optimization, the autoencoder learns a compact and informative representation of the input data, facilitating tasks such as dimensionality reduction and denoising. The specific configuration and hyperparameters selected during training significantly influence the effectiveness of the autoencoder in capturing meaningful features and patterns from the input data. In this way, the autoencoder serves as a powerful tool for unsupervised learning, particularly in scenarios where obtaining labeled data may be challenging or expensive.

The DAE, pioneered in [24], represents an evolution of the conventional autoencoder (AE), introducing a stochastic element to enhance its capabilities. Unlike the AE, which focuses on deterministic transformations, the DAE is designed to handle noisy or corrupted input data, aiming to reconstruct a clean version of the original input.

In the framework of the DAE, the process begins with an initial input, denoted as x, which undergoes a stochastic transformation, resulting in a corrupted counterpart $\tilde{x}$. This stochastic transformation is expressed as $\tilde{x} \sim q(\tilde{x}|x)$, indicating that $\tilde{x}$ is generated based on a probabilistic distribution q conditioned on the original input x. This corrupted representation $\tilde{x}$ captures the effects of noise or corruption introduced to the input.
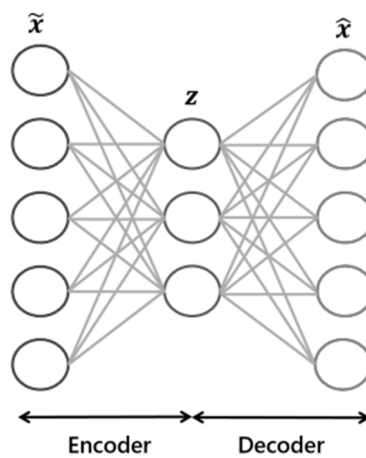

Figure 5-1. The structure of denoising autoencoder [73].

Moving forward, the DAE takes this corrupted representation $\tilde{x}$ as input data and endeavors to map it to a corresponding hidden representation z. The ultimate goal is to successfully reconstruct the original input ($\tilde{x}$) from its corrupted version, completing the denoising process.

This denoising capability is particularly valuable in various applications, such as image processing, speech recognition, and data compression, where input data may be susceptible to noise or corruption. The stochastic nature of the DAE allows it to learn robust representations by considering different possible corrupted versions of the input during training.

Figure 4-3 provides a visual depiction of the denoising process in the DAE. The incorporation of stochasticity not only enhances the model's ability to handle noisy input but also contributes to its adaptability and generalization to diverse and unpredictable data scenarios.The Denoising Autoencoder, with its stochastic approach to handling corrupted input, presents a powerful tool for reconstructing clean representations of data in the presence of noise. This makes it a valuable asset in scenarios where robust and accurate data reconstruction is essential. The stochastic transformation and subsequent reconstruction contribute to the model's versatility and effectiveness in real-world, noisy data environments.

The robust nonlinear mapping capabilities of both Autoencoder (AE) and Denoising Autoencoder (DAE) models have led to their increased popularity in diverse applications, ranging from data compression [[28], [66]] to noise reduction in critical domains like speech signals [[67], [68]] and medical images [70].

In this chapter, a comprehensive set of quantitative performance metrics is employed to rigorously evaluate the efficacy of my models. These metrics include the Root Mean Square Error (RMSE), Power Spectral Density (PSD) diagrams, and Signal-to-Noise Ratio Improvement (SNR$_{imp}$).

The RMSE serves as a pivotal indicator, quantifying the variance between the predicted output of the model and the actual output. A lower RMSE value signifies a reduced disparity, indicating superior performance. Mathematically, RMSE is defined as:

$$RMSE = \sqrt{\frac{1}{N} \times \sum_{n=1}^{N}(x_i - \hat{x}_i)^2} \tag{5.5}$$

Here, x represents the value at sampling point i in the original ECG signal, and $\hat{x}$ signifies the value at the corresponding point in the predicted output.

SNRimp is a crucial metric that measures the disparity between the SNR subsequent to noise reduction and the initial input signal SNR. A higher SNR_{imp} value indicates superior denoising performance. It is calculated as the difference between the output SNR (SNR$_{out}$) and the input SNR (SNR$_{in}$):

$$SNR_{imp} = SNR_{out} - SNR_{in} \tag{4.6}$$

The input SNR (SNR$_{in}$) and output SNR (SNR$_{out}$) are defined by the following expressions:

$$SNR_{in} = 10 \times log_{10}\left(\frac{\sum_{n=1}^{N} x_i^2}{\sum_{n=1}^{N}(\tilde{x}_i - x_i)^2}\right) \tag{4.7}$$

$$SNR_{in} = 10 \times log_{10}\left(\frac{\sum_{n=1}^{N} x_i^2}{\sum_{n=1}^{N}(\hat{x}_i - x_i)^2}\right) \tag{4.8}$$

Here, $\tilde{x}$ represents the value at sampling point i in the noisy ECG signal, and $\hat{x}$ corresponds to the value at the same sampling point in the denoised waveform. N represents the length of the ECG signal. In these equations, the detailed representations of original, noisy, and denoised ECG signals provide a comprehensive framework for evaluating the performance of AE and DAE models in noise reduction applications. The inclusion of multiple metrics ensures a thorough assessment of the models' capabilities in handling complex signal processing tasks.

APPENDIX E – RESAMPLING

Resampling methods serve as a valuable approach for aligning the sampling frequencies of two signals, particularly when dealing with signals of disparate rates that need to be synchronized for further analysis or processing. These techniques enable the adjustment of the sampling rate of a signal while maintaining its content and inherent characteristics [53]. As delving into the consideration of employing resampling methods for sampling frequency matching, several factors come into play:

1- Difference in Sampling Rates:

Resampling proves instrumental in aligning two signals with distinct sampling rates, facilitating their comparison or combination. This is particularly pertinent in this scenario, where the combination of ECG and accelerometer signals is essential for training my model.

2- Signal Characteristics:

Resampling methods are designed to preserve the essential features of a signal, such as its frequency content, during the alteration of the sampling rate. However, it is crucial to acknowledge that resampling is not without its trade-offs [53]. The process introduces interpolation or decimation errors that can impact signal quality. The severity of these errors depends on the specific resampling algorithm employed and the properties of the original signal.

3- Computational Complexity:
- Resampling algorithms can exhibit computational intensity, especially when dealing with large signals or real-time applications [54]. Certain methods, like polyphase resampling [26] or sinc interpolation [55], involve intricate calculations and may necessitate substantial processing power. In this approach, a combination of up-sampling, filtering, and down-sampling using MATLAB DSP tools is employed. The procedure involves the following steps:

- Up-sampling: This involves increasing the sampling rate by inserting zeros between the original samples. MATLAB utilizes the 'upfirdn' function, combining up-sampling and filtering in a single step.

- Antialiasing Low-Pass Filter: After up-sampling, an antialiasing low-pass filter is applied to the signal. This filter eliminates high-frequency components (above the Nyquist frequency) introduced during up-sampling, preventing aliasing—distortion occurring when high-frequency components fold back into the desired frequency [53].

- Down-sampling: This process reduces the sampling rate by discarding some samples from the up-sampled and filtered signal. Down-sampling occurs after the antialiasing filtering stage, with the down-sampling factor determining the number of retained samples from the up-sampled signal.

The careful consideration of these factors and the implementation of a well-defined resampling strategy, as outlined in this approach, are crucial for maintaining signal integrity and facilitating the integration of heterogeneous signals for subsequent analysis and model training.

In conclusion, the use of FIR filters in MATLAB, combined with the meticulous manipulation of sampling rates through up-sampling, antialiasing filtering, and down-sampling, underscores a powerful strategy for altering sampling rates while preserving signal integrity. This approach finds utility in diverse fields, ensuring accurate signal representation and mitigating aliasing effects for more robust signal processing applications.